NAVAL POSTGRADUATE SCHOOL
MONTEREY, CALIFORNIA

THESIS

DETECTION AND IDENTIFICATION OF CYCLOSTATIONARY SIGNALS

by

Evandro Luiz da Costa

March, 1996

Thesis Co-Advisors: Ralph Hippenstiel
Roberto Cristi

Approved for public release; distribution is unlimited.

REPORT DOCUMENTATION PAGE

Form Approved OMB No. 0704-0188

1. AGENCY USE ONLY *(Leave blank)*	2. REPORT DATE March 1996	3. REPORT TYPE AND DATES COVERED Master's Thesis

4. TITLE AND SUBTITLE
DETECTION AND IDENTIFICATION OF CYCLOSTATIONARY SIGNALS

5. FUNDING NUMBERS

6. AUTHOR(S)
Da Costa, Evandro L.

7. PERFORMING ORGANIZATION NAME(S) AND ADDRESS(ES)
Naval Postgraduate School
Monterey CA 93943-5000

8. PERFORMING ORGANIZATION REPORT NUMBER

9. SPONSORING/MONITORING AGENCY NAME(S) AND ADDRESS(ES)

10. SPONSORING/MONITORING AGENCY REPORT NUMBER

11. SUPPLEMENTARY NOTES
The views expressed in this thesis are those of the author and do not reflect the official policy or position of the Department of Defense or the U.S. Government.

12a. DISTRIBUTION/AVAILABILITY STATEMENT
Approved for public release; distribution is unlimited.

12b. DISTRIBUTION CODE

13. ABSTRACT *(maximum 200 words)*

Propeller noise can be modeled as an amplitude modulated (AM) signal. Cyclic Spectral Analysis has been used successfully to detect the presence of analog and digitally modulated signals in communication systems. It can also identify the type of modulation. Programs for Signal Processing based on compiled languages such as FORTRAN or C are not user friendly, and MATLAB based programs have become the *de facto* language and tools for signal processing engineers worldwide.

This thesis describes the implementation in MATLAB of two fast methods of computing the Spectral Correlation Density (SCD) Function estimate, the FFT Accumulation Method (FAM) and the Strip Spectral Correlation Algorithm (SSCA), to perform Cyclic Analysis. Both methods are based on the Fast Fourier Transform (FFT) algorithm. The results are presented and areas of possible enhancement for propeller noise detection and identification are discussed.

14. SUBJECT TERMS
Cyclic Spectral Analysis, FFT Accumulation Method, Strip Spectral Correlation Algorithm.

15. NUMBER OF PAGES
126

16. PRICE CODE

17. SECURITY CLASSIFICATION OF REPORT	18. SECURITY CLASSIFICATION OF THIS PAGE	19. SECURITY CLASSIFICATION OF ABSTRACT	20. LIMITATION OF ABSTRACT
Unclassified	Unclassified	Unclassified	UL

NSN 7540-01-280-5500

Standard Form 298 (Rev. 2-89)
Prescribed by ANSI Std. 239-18 298-102

DISCLAIMER NOTICE

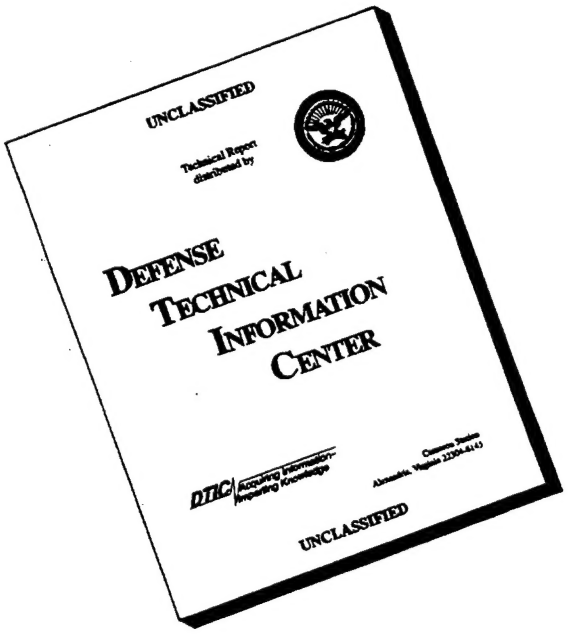

THIS DOCUMENT IS BEST QUALITY AVAILABLE. THE COPY FURNISHED TO DTIC CONTAINED A SIGNIFICANT NUMBER OF PAGES WHICH DO NOT REPRODUCE LEGIBLY.

Approved for public release; distribution is unlimited.

DETECTION AND IDENTIFICATION OF CYCLOSTATIONARY SIGNALS

Evandro Luiz da Costa
Lieutenant Commander, Brazilian Navy
B.S., Instituto Militar de Engenharia, 1980

Submitted in partial fulfillment
of the requirements for the degree of

MASTER OF SCIENCE IN ELECTRICAL ENGINEERING
AND
MASTER OF SCIENCE IN ENGINEERING ACOUSTICS

from the

NAVAL POSTGRADUATE SCHOOL
March, 1996

Author: _____
Evandro L. da Costa

Approved by: _____
Ralph Hippenstiel, Thesis Co-Advisor

_____
Roberto Cristi, Thesis Co-Advisor

_____
Herschel H. Loomis, Jr., Chairman
Department of Electrical and Computer Engineering

_____
Anthony A. Atchley, Chairman
Engineering Acoustics Academic Committee

ABSTRACT

Propeller noise can be modeled as an amplitude modulated (AM) signal. Cyclic Spectral Analysis has been used successfully to detect the presence of analog and digitally modulated signals in communication systems. It can also identify the type of modulation. Programs for Signal Processing based on compiled languages such as FORTRAN or C are not user friendly, and MATLAB based programs have become the *de facto* language and tools for signal processing engineers worldwide.

This thesis describes the implementation in MATLAB of two fast methods of computing the Spectral Correlation Density (SCD) Function estimate, the FFT Accumulation Method (FAM) and the Strip Spectral Correlation Algorithm (SSCA), to perform Cyclic Analysis. Both methods are based on the Fast Fourier Transform (FFT) algorithm. The results are presented and areas of possible enhancement for propeller noise detection and identification are discussed.

TABLE OF CONTENTS

I. INTRODUCTION

A. MOTIVATION

Propeller related acoustic signatures typically exhibit modulation characteristics. These modulation characteristics originate from the cavitation process that takes place in the water due to the cyclic movement of the propeller.

The cavitation process is basically the collapse of air and vapor bubbles due to variations in the static pressure. These variations in static pressure are a consequence of the passage of the propeller blades through the water. This movement, cyclic in nature, causes amplitude modulation in the static pressure, and as a consequence an amplitude-modulated (AM) signal can be detected in a receiver.

Cyclostationary processing techniques have been used to detect and identify analog and digital communication signals very successfully. These techniques have the advantage of using a more realistic model for the signal than the stationary model used in most of the more conventional signal processing techniques.

B. BACKGROUND

The basic elements of cyclic spectral analysis are the time-variant cyclic periodogram and the time-variant cyclic correlogram. These two functions form a Fourier transform pair. This fact is known as the *cyclic Wiener relation* or the *cyclic Wiener-Khinchin relation* [Ref. 1: p. 49.]

In order to estimate the cyclic spectrum of a signal of interest, both the time-smoothed cyclic periodogram and the frequency-smoothed cyclic periodogram can be used, giving rise to two classes of computational algorithms: the time-smoothing algorithms and the frequency-smoothing algorithms.

Although both classes of algorithms produce similar approximations to the cyclic spectrum, time-smoothing algorithms are considered to be more computationally efficient for general cyclic spectral analysis [Ref. 2: p.38]. Taking advantage of the efficiency, two computationally fast algorithms based on the time-smoothed cyclic periodogram were developed by Roberts et al. [Ref. 2]: the FFT Accumulation Method (FAM) and the Strip Spectral Correlation Algorithm (SSCA).

C. THESIS GOALS

The purpose of this thesis is to implement the FFT Accumulation Method as well as the Strip Spectral Correlation Method in MATLAB [Ref. 3]. These two methods are already implemented in C [Ref. 4]. MATLAB is a more user-friendly and widely-used language that makes simulations and evaluations accessible for students and researchers. These cyclic spectral analysis programs written in MATLAB can easily be modified and are transportable across operating systems (i. e., UNIX, PC systems, MAC systems, VMS, etc).

Both programs are used to compute the spectral correlation density (SCD) function estimate for a number of analog and digital modulated signals, such as

AM, PAM, ASK, and BPSK. The simulation results are then compared to the theoretical ones. After that the attention is focused on the AM signals for which a number of different signal-to-noise ratios (SNR) are processed using both methods. The results are presented and discussed for two types of modulation messages: a periodic message (a tone) and a random message (white noise).

Results are presented by showing a three-dimensional plot of the cyclic spectrum surface, a contour plot, a plot of the power spectral density (PSD) obtained by setting the value of the cyclic frequency equal to zero, and some additional two-dimensional plots for cyclic frequencies of interest.

II. NOISE IN THE OCEAN

Ross [Ref.5] defines noise as unwanted sound. The noise presence interferes with the signals that are of interest. If one is interested in detecting the presence of a particular class of surface ships, the sound generated by a near by submarine can be interpreted as noise. The reverse situation also leads to a similar statement. Therefore, the concept of noise has no absolute definition. It is a relative concept, and its characterization depends on the signal of interest in a particular situation.

In this thesis, as we are interested in the detection and possible identification of the noise radiated by propeller, underwater noise is defined as any sound that interferes with our ability to detect and identify those signals.

As reported by Ross [Ref. 5: p. 1], underwater noise is defined as sound in the water that limits the military effectiveness of naval detection and identification systems. Noise is unavoidable and sources that radiate as much as one watt of acoustics power can be detected at relatively long ranges by modern passive sonars.

A. TYPES OF UNDERWATER NOISE

There are several different sources of underwater noise that are grouped and classified in different ways according to the reference used. The main sources of underwater noise can be divided in ambient noise, self noise, and

radiated noise. Ambient noise and self-noise together constitute what is called the background noise which interferes with the operation of a sonar system.

1. Ambient Noise

Ambient noise is the prevailing, sustained unwanted background of sound at some location in the ocean. It excludes momentary, occasional sounds, such as the noise of a close-by passage of a ship or of an occasional rain squall. It is the background of noise, typical of the location and depth where a measuring hydrophone is located, against which a "signal," such as the sound of a submarine or the echo from a target, must be detected [Ref. 6: p. 1-1]. It comprises all noises associated with the medium in which a sonar operates that would exist in the medium if the sonar platform or vehicle itself were not present.

The spectrum and characteristics of this kind of noise are complicated and depend upon location, position of the receiver, direction, and weather conditions. In its most general form, the ambient noise spectrum has some frequency bands where tonal components occur, and others where the spectrum is continuous and negatively sloping ("pink" noise), separated by portions where the spectrum is flat ("white" noise) or even reversed in slope [Ref. 6: p. 2-1]. This observation indicates that different sources of noise must exist and be prevalent in different regions of the spectrum.

Urick [Ref. 6] divides the overall frequency range into five frequency bands: the ultra-low band ($<1Hz$), the infrasonic band ($1\ to\ 20Hz$), the low sonic

band ($20\ to\ 200Hz$), the high sonic band ($200\ to\ 50{,}000Hz$), and the ultrasonic ($>50kHz$).

Almost nothing is known about the noise in the ultra-low band, since just a few measurements are reported. The infrasonic band contains the strong blade-rate fundamental frequency of propeller-driven vessels, plus one or two of its harmonics. It is of great interest to low frequency passive sonars. The low sonic band is characterized by the noise of distant shipping in areas where distant ships are prevalent. In areas remote from shipping lanes, the noise in this band is mainly dependent on wind speed [Ref. 6]. According to Ross [Ref. 5: p. 280], ship-generated noise is the dominant source of ambient noise in the spectral region between 20 and 200 Hz in most deep-water, open ocean areas and in highly traveled seas such as the Baltic and Mediterranean. The noise in the high sonic band is very dependent on the sea state and the wind speed. Thermal noise begins to dominate the noise background in the ultrasonic band.

2. Self Noise

Self noise is the noise associated with a platform and its sonar hydrophones. It includes the electronic noise generated by its preamplifiers, as observed by the sonar hydrophone array [Ref. 5: p. 4]. It can reach the receiver by transmission through the mechanical structure and by transmission through the water either directly from the source or by reflection from the sea surface.

Self noise usually tends to increase as the speed of the platform

increases. At low frequencies and slow speeds, machinery noise dominates, whereas at high frequencies propeller and flow noise become important. Actually, as the speed is increased, these latter sources of noise assume more importance at all frequencies.

At very low speeds, self noise is usually less important than ambient noise. At higher speeds the self noise can become the limiting factor [Ref. 7: p. 413].

3. Radiated Noise

Radiated noise is that sound radiated into the water which can be used by some receiver to detect the presence of the emitter at a considerable distance. It is very important for passive sonars, which are designed to exploit the peculiarities of this form of noise and to distinguish it from the background of self-noise and ambient noise in which it is normally observed [Ref. 8: p.328].

A detailed discussion of the mechanisms involved in the radiation of sound through the ocean can be found in several references such as Ross [Ref. 5], Kinsler et al. [Ref. 7], and Urick [Ref. 8].

B. RADIATED NOISE FROM SHIPS, SUBMARINES, AND TORPEDOES

The sources of noise on ships, submarines, and torpedoes can be grouped into three major classes: machinery noise, propeller noise, and

hydrodynamic noise.

Machinery noise comprises that part of the total noise of the vessel caused by the ship's machinery. It originates as mechanical vibration of the many and diverse parts of a moving vessel. This vibration is coupled to the sea via the hull of the vessel.

Machinery vibration can originate from five different sources. The first source of machinery noise are rotating unbalanced parts, such as out-of-round shafts or motor armatures. The second one are repetitive discontinuities, such as gear teeth, armature slots, and turbine blades. Reciprocating parts, such as the explosions in cylinders of reciprocating engines, are the third source of machinery vibration. The fourth are cavitation and turbulence in the fluid flow in pumps, pipes, valves, and condenser discharges. And mechanical friction, as in bearings and journals, is the fifth source of machinery noise.

The first three sources of machinery vibration produce a line-component spectrum in which the noise is dominated by tonal components at the fundamental frequency and harmonics of the vibration-producing process; the other two give rise to noise having a continuous spectrum containing superimposed line components from structural members that are excited into resonant vibration. The machinery noise of a vessel may therefore be visualized as possessing a low-level continuous spectrum containing strong line components that originate in one or more of the repetitive vibration-producing

processes listed above.

Even though the propeller is a part of the propulsion machinery of a vessel, the noise it generates has both a different origin and a different frequency spectrum from machinery noise. Machinery noise originates inside the vessel and reaches the water by various processes of transmission and conduction through the hull. Propeller noise, on the other hand, originates outside the hull as a consequence of the propeller action and by virtue of the vessel's movement through the water.

The source of propeller noise is principally the cavitation induced by the rotating propellers [Ref. 8: p. 334]. Because cavitation noise consists of a large number of random small bursts caused by bubble collapse, it has a continuous spectrum, covering a wide frequency range.

Hydrodynamic noise originates in the irregular and fluctuating flow of fluid moving by the vessel. The noise created by the turbulent boundary layer is sometimes called "flow noise." Under normal circumstances, hydrodynamic noise is likely to be only a minor contributor to radiated noise, and is apt to be masked by machinery and propeller noises.

C. PROPELLER NOISE

Ross [Ref. 5: p. 253] describes cavitation of marine propeller as the most prevalent source of underwater sound in the oceans. Furthermore, when it

occurs, propeller cavitation is usually the dominant noise source for any single marine vehicle. Submarines and torpedoes often operate deep enough to avoid cavitation. Surface ships, on the other hand, generally have well-developed propeller cavitation, with the result that their entire radiated spectra from as low as 5 Hz to as high as 100 kHz are controlled by this source [Ref. 5: p. 253].

Cavitation is essentially the rupture of bubbles in a liquid caused by reduction of local static pressure. It differs from boiling because the first is caused by a reduction of local static pressure while the second is due to an increase of temperature. Because of the pulse nature of the individual collapses and the random sequence of occurrence, the resultant spectrum covers a wide frequency range. Also, the pulsations of the aggregate volume of cavitation radiate strong tonals at frequencies below 70 Hz [Ref. 5: p. 270].

Of the various types of cavitation, blade-surface cavitation on the suction surface is the one that produces the highest noise levels. A more detailed explanation on the different types of cavitation, particularly on the blade-surface cavitation noise is found on Ross [Ref. 5: pp. 253-260].

Radiated spectra of surface ships are dominated by propeller cavitation noise except when the ships are operating at very slow speeds [Ref. 5: p. 272]. Some characteristics of surface ship noise that confirm the dominance of propeller cavitation are strong modulation of the broadband spectrum at shaft and blade frequencies and the radiation of low-frequency tonals at harmonics of

these frequencies.

Propeller noise has been known for many years to be amplitude-modulated and to contain "propeller beats," or periodic increases of amplitude, occurring at the rotation speed of the propeller shaft, or at the propeller blade frequency, which is equal to the shaft frequency multiplied by the number of blades. The modulation at the shaft rotational frequency is due to slight physical differences between blades, that causes one blade to cavitate more than the others. It is this shaft-rate modulation that can be detected by the human ear and which enables an experienced sonar operator to determine the propeller rotational rate (rpm) and often classify the target [Ref. 5: p. 269]. Propeller beats have long been used by listening observers for target identification and for estimating target speed [Ref. 8: p. 338].

Propeller noise, with its origin in the flow of water about the propeller, creates tonal components in addition to the continuous spectrum of cavitation noise. Low-frequency spectra of cavitating ship propellers are usually dominated by tonal components at harmonics of the rotational frequency. More often, at the low-frequency end of the spectrum, propeller noise contains discrete spectral "blade-rate" components occurring at multiples of the rate at which any irregularity in the flow pattern into or about the propeller is intercepted by the propeller blades. The frequency of the blade-rate series of line components is given by

$$f_m = mns\,, \tag{1}$$

where f_m is the frequency, in Hertz, of the m^{th} harmonic of the blade-rate series of lines, n is the number of blades on the propeller, and s is the propeller rotation speed in number of turns per second.

Shaft and blade modulation frequencies for merchant ships are now significantly higher than they were during WWII. Forty years ago most merchant ships had three- or four-bladed propellers and operated at from 60 to 100 rpm. Shaft modulation frequencies were generally between 1.0 and 1.6 Hz and blade frequencies were from 3.5 to 6.5 Hz. Today, typical merchant propellers have four, five or six blades and operate at from 75 to 135 rpm; shaft frequencies range from 1.3 to 2.2 Hz, and blade frequencies are typically 6 to 12 Hz [Ref. 5: p. 279].

III. CYCLOSTATIONARY PROCESSING

The majority of the current signal processing techniques for intercepting or analyzing manmade signals in a noise contaminated environment typically utilize probabilistic models based on stationary statistics. In other words, they describe the signal on the average, and they have to restrict themselves to a small time interval in order for this approximation to hold. That limits the amount of data that can be used to derive the features in the signal and the resulting information.

Most manmade signals, as are typically encountered in communication, radar, and sonar systems have some parameters that vary with time. Examples include sinusoidal carriers in amplitude, phase and frequency modulation systems, periodic keying of the amplitude, phase, or frequency in digital modulation systems, periodic scanning in some radar systems, and amplitude modulation in propeller noise. This requires that the random signal be modeled as cyclostationary, in which case the statistical parameters vary in time with single or multiple periodicity.

Much of the background material in this chapter was taken from Gardner [Ref. 1].

A. CYCLOSTATIONARITY

According to Gardner [Ref. 1], the essence of cyclostationarity is the fact that sinewaves can be generated from random data by applying certain

nonlinear transformations. As a consequence, a continuous signal $x(t)$ is cyclostationary of order n (in the wide-sense) if and only if we can find some n^{th} order nonlinear transformation of the signal, $y(t) = f(x(t))$, that will generate finite-amplitude additive sine-wave components, which produce spectral lines. In the same sense, a discrete-time signal $x[m]$ is cyclostationary of order n (in the wide-sense) if and only if we can find some n^{th} order nonlinear transformation of the signal, $y[m] = f[x[m]]$, that will generate finite-amplitude additive sine-wave components, which will produce spectral lines [Ref. 1: p. 2].

A continuous signal $y(t)$ contains a finite-amplitude additive sine-wave component with frequency α , $\alpha \neq 0$, if the Fourier coefficient

$$M_y^{\alpha} = \left\langle y(t)\, e^{-i2\pi\alpha t} \right\rangle \tag{2}$$

is not zero. In the same way, a discrete-time signal $y[m]$ contains a finite-amplitude additive sine-wave component with frequency α , $\alpha \neq 0$, if the Fourier coefficient

$$M_y^{\alpha} = \left\langle y[m]\, e^{-i2\pi\frac{\alpha}{f_s}m} \right\rangle \tag{3}$$

is not zero. Here, f_s denotes the sampling frequency and i is the square root of minus one.

The operation $\langle\cdot\rangle$ is the time-averaging operation defined as

$$\langle \cdot \rangle = \lim_{T \to \infty} \frac{1}{T} \int_{-T/2}^{T/2} (\cdot)\, dt \tag{4}$$

for analog signals, and as

$$\langle \cdot \rangle = \lim_{N \to \infty} \frac{1}{2N+1} \sum_{m=-N}^{N} (\cdot) \tag{5}$$

for discrete-time signals.

For second-order cyclostationarity, the nonlinear transformation for a continuous signal $x(t)$ (i. e., $y(t) = f(x(t))$ is given by

$$y_\tau(t) = x(t + \tau/2)\, x^*(t - \tau/2)\,, \tag{6}$$

while for a discrete-time signal $x[m]$ (i. e., $y[m] = f[x[m]]$) it is given by

$$y_\ell[m] = x[m]\, x^*[m - \ell]\,, \tag{7}$$

where the symbol $*$ stands for complex conjugation.

B. THE CYCLIC AUTOCORRELATION FUNCTION (ACF)

The Fourier coefficient M_y^α for second-order cyclostationarity is given by

$$M_y^\alpha = \langle\, x(t + \tau/2)\, x^*(t - \tau/2)\, e^{-i2\pi\alpha t} \,\rangle\,. \tag{8}$$

This quantity is the fundamental parameter of second-order periodicity in continuous time and is called the cyclic autocorrelation function (ACF), $R_x^\alpha(\tau)$, of $x(t)$.

For discrete-time signals, the ACF is defined as

$$R_x^{\alpha}[\ell] = \left\langle x[n]x^*[n-\ell]e^{-i2\pi\alpha n} \right\rangle e^{i\pi\alpha\ell}, \tag{9}$$

since delays other than sampling increments are not allowed.

The ACF can be interpreted as measuring the amount of correlation between different frequency-shifted versions of a given signal, as shown in detail in Appendix A for an AM signal.

Therefore, a signal exhibits second-order cyclostationarity in the wide-sense when its cyclic autocorrelation function, $R_x^{\alpha}(\tau)$ for a continuous time signal or $R_x^{\alpha}[\ell]$ for a discrete-time signal, is different from zero for some nonzero frequency α. The frequency α is called cycle frequency or cyclic frequency, and the discrete set of cycle frequencies α for which $R_x^{\alpha}(\tau) \neq 0$ or $R_x^{\alpha}[\ell] \neq 0$ is called the cycle spectrum or cyclic spectrum.

If a signal is cyclostationary, the cycle spectrum contains only harmonics (integer multiples) of the fundamental cycle frequency. Neverthless, if the signal has more than one fundamental cycle frequency, then the cycle spectrum contains harmonics of each of those frequencies. In this situation the signal is said to be polycyclostationary.

C. THE SPECTRAL CORRELATION DENSITY FUNCTION (SCD)

Signals usually have distinctive features in the frequency domain that are not easily seen in the time domain. Those features are generally used for detecting the presence of those signals. For instance, is very hard to detect the

presence of a sinusoidal signal, when embedded in noise, by just looking at its time-domain representation. The same signal can easily be detected in the frequency domain, provided the integration time can be made sufficiently long.

For the same reason, it is beneficial to determine in the frequency domain the amount of correlation between frequency-shifted versions of $x(t)$. The spectral correlation density function (SCD) is defined as the Fourier Transform of the cyclic autocorrelation function (ACF), to allow the localization in the frequency domain of the amount of time-correlation between frequency-shifted versions of the signal $x(t)$. The SCD is given by

$$S_x^\alpha(f) = \int_{-\infty}^{\infty} R_x^\alpha(\tau)\, e^{-i2\pi f\tau}\, d\tau, \tag{10}$$

for a continuous signal $x(t)$, and by

$$S_x^\alpha(f) = \sum_{\ell=-\infty}^{\infty} R_x^\alpha[\ell]\, e^{-i2\pi f\ell}, \tag{11}$$

for a discrete-time signal $x[n]$.

To determine the correlation in the frequency domain, we simply pass both of the two frequency translates $u(t) = x(t)e^{-i\pi\alpha t}$ and $v(t) = x(t)e^{i\pi\alpha t}$ through the same set of bandpass filters and then measure the temporal correlation of the filtered signals, as shown in Figure 1 (The signal $u(t)$ represents a downshift in frequency by $\alpha/2$ while $v(t)$ represents an upshift in frequency by $\alpha/2$ of the signal $x(t)$). In the limit when the bandwidth B of these narrowband components

approaches zero, we obtain

$$S_x^\alpha(f) = \lim_{B\to 0} \frac{1}{B} \left\langle \left[h_B^f(t) \otimes u(t)\right] \left[h_B^f(t) \otimes v(t)\right]^* \right\rangle, \tag{12}$$

where the symbol $\otimes$ stands for convolution, and $h_B^f(t)$ is the impulse response of the bandpass filters.

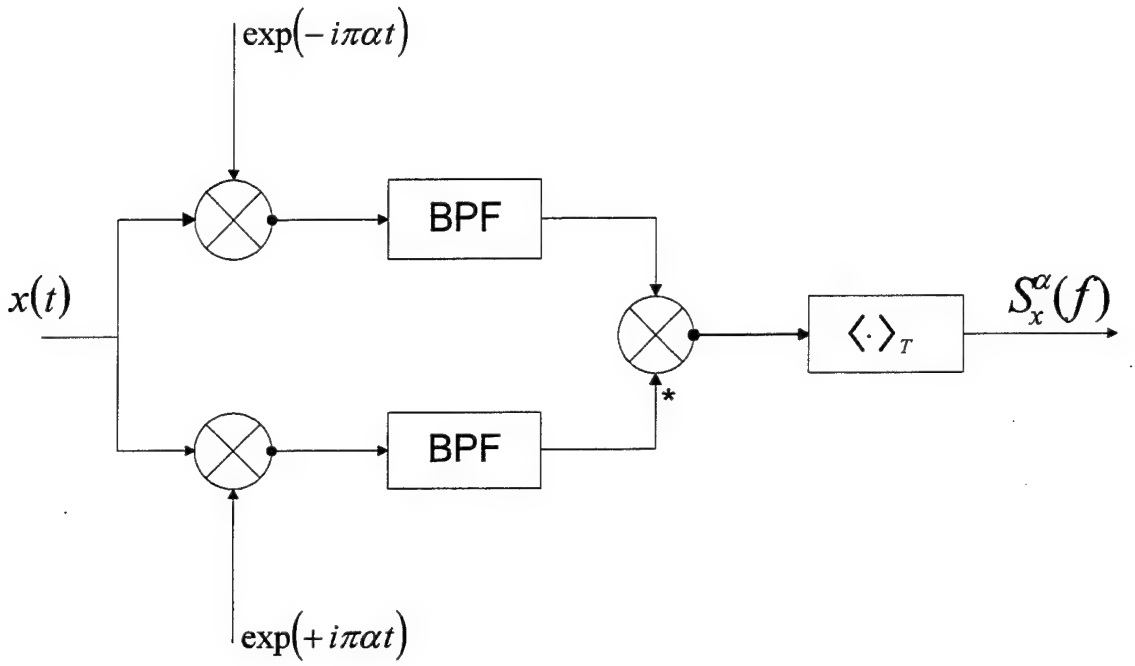

Figure 1 Spectral Correlation Analyzer (after Gardner [Ref. 1])

Strictly speaking, the SCD is not a valid density function in the usual sense, since it is not nonnegative and, in fact, not even real-valued. However, because of the similar properties that the SCD does share with the PSD, the term density is retained.

The SCD is also called the cyclic spectral density. Observe that although the argument f of the SCD is continuous, as it always will be for a random signal, the argument α is discrete, as it always will be since it represents the harmonic frequencies of periodicities underlying the random time-series.

A detailed example of the computation of the SCD for an amplitude-modulated (AM) signal is given in Appendix A.

IV. ESTIMATION OF THE SPECTRAL CORRELATION DENSITY FUNCTION

Cyclic spectral analysis is used to detect the presence of a signal via the spectral correlation density (SCD) function. To accomplish this goal a series of codes that estimates the SCD function were developed in MATLAB language. Those codes are implementations of two FFT based time smoothing algorithms called the FFT Accumulation Method (FAM) and the Strip Spectral Correlation Algorithm (SSCA). The majority of the background material in this chapter was taken from Roberts et al. [Ref. 2].

As reported by Roberts et al. [Ref. 2], cyclic spectral analysis algorithms generally fall into two classes: those that average in frequency (frequency smoothing) and those that average in time (time smoothing). Although both classes of algorithms produce similar approximations to the cyclic spectrum, time smoothing algorithms are considered to be more computationally efficient for general cyclic spectral analysis.

Both methods are based on modifications of the time smoothed cyclic cross periodogram, defined as:

$$S_{xy_T}^{\alpha}(n,f)_{\Delta t} = \frac{1}{T}\left\langle X_T\left(n, f+\frac{\alpha}{2}\right) Y_T^*\left(n, f-\frac{\alpha}{2}\right)\right\rangle_{\Delta t}, \tag{13}$$

where Δt represents the data time span, and $X_T\left(n, f+\frac{\alpha}{2}\right)$ and $Y_T\left(n, f-\frac{\alpha}{2}\right)$ are the complex envelopes of narrow-band, bandpass components of the signals

$x(n)$ and $y(n)$, respectively. The complex envelopes are also called the complex demodulates of the signals. These complex demodulates are computed in the following way:

$$X_T(n,f) = \sum_{r=-N'/2}^{N'/2} a(r)\, x(n-r)\, e^{-i2\pi f(n-r)T_s} \tag{14}$$

and

$$Y_T(n,f) = \sum_{r=-N'/2}^{N'/2} a(r)\, y(n-r)\, e^{-i2\pi f(n-r)T_s}, \tag{15}$$

where $a(r)$ is a data tapering window of length $T = N'T_s$ seconds, with T_s being the sampling period. The Fourier transform of $a(r)$ plays the role of a spectral window. The particular shape of window, especially the spectral window, is of considerable importance. Windows other than the rectangle have a tapering effect on the data they multiply, since data occurring away from the aperture center are attenuated relative to the data at the aperture center. A data tapering window whose Fourier transform has low skirts and low sidelobes is desirable to reduce cycle leakage. A Hamming window is used for the input bandpass filters.

Figure 2 shows a basic implementation of the discrete time smoothed cyclic cross periodogram, where the symbol $*$ stands for complex conjugation. The complex demodulate frequencies f_1 and f_2 are related to the spectrum frequency f and the cyclic frequency α of the point estimate by the following

two equations:

$$f = \frac{f_1 + f_2}{2}, \tag{16}$$

and

$$\alpha = f_1 - f_2 . \tag{17}$$

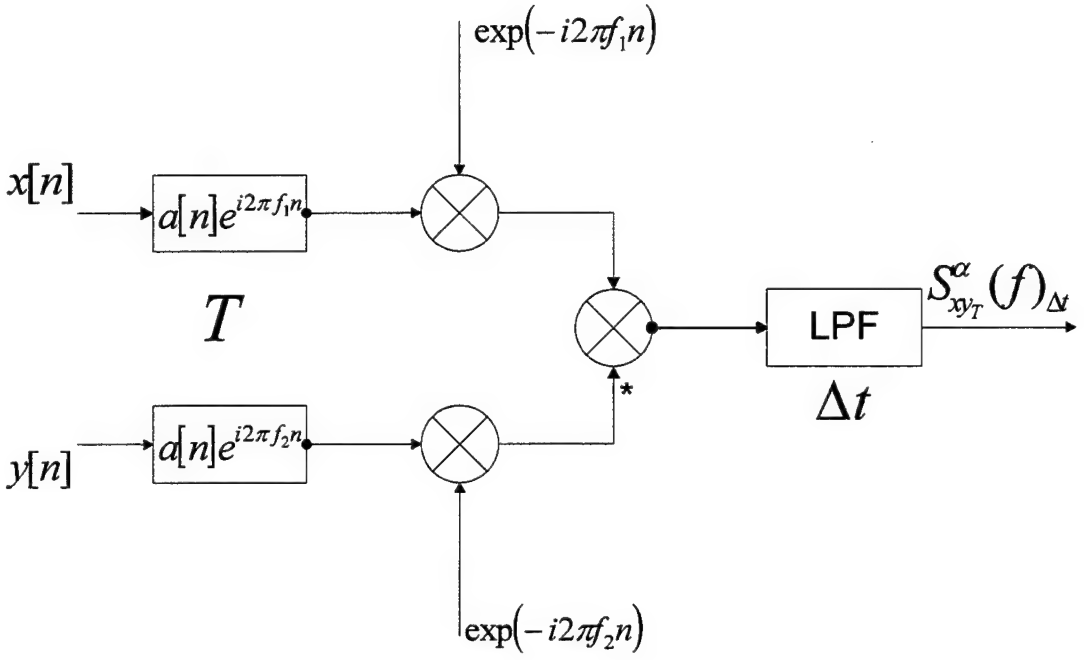

Figure 2 Discrete Time Smoothed Cyclic Cross Periodogram (after Roberts et al. [Ref. 2]).

A. FFT ACCUMULATION METHOD (FAM)

In this method, the complex demodulates are estimated efficiently by means of a sliding N'-point FFT, followed by a downshift in frequency to

baseband. In order to allow for an even more efficient estimation, the N'-point FFT is hopped over the data in blocks of L samples (channelization). This means that L data points are skipped between successive computations of the N'-point FFT. The value of L was chosen to be equal to $N'/4$ since, according to Reference 2, p.462, it allows for a good compromise between maintaining computational efficiency and minimizing cycle leakage and cycle aliasing. The value of N' is determined according to the desired resolution in frequency (Δf) used in the algorithm, and is given by

$$N' = \frac{f_s}{\Delta f}. \tag{18}$$

N' is chosen to be the power of 2 equal to or larger than the number given by Eq. 18 to take advantage of the Fast Fourier Transform (FFT) algorithm without making use of zero-padding.

After the complex demodulates are computed and the product sequences between each one of them and the complex conjugate of the others are formed, the time smoothing is accomplished by means of a P-point FFT. The value of P is determined according to the desired resolution in cyclic frequency ($\Delta\alpha$), and is given by

$$P = \frac{f_s}{L\,\Delta\alpha}. \tag{19}$$

Again, P is chosen to be the power of 2 equal to or larger than the

number given by Eq. 19 to take advantage of the FFT algorithm avoiding zero-padding.

Figure 3 illustrates the generation of the complex demodulates while Figure 4 shows the implementation of the FAM method.

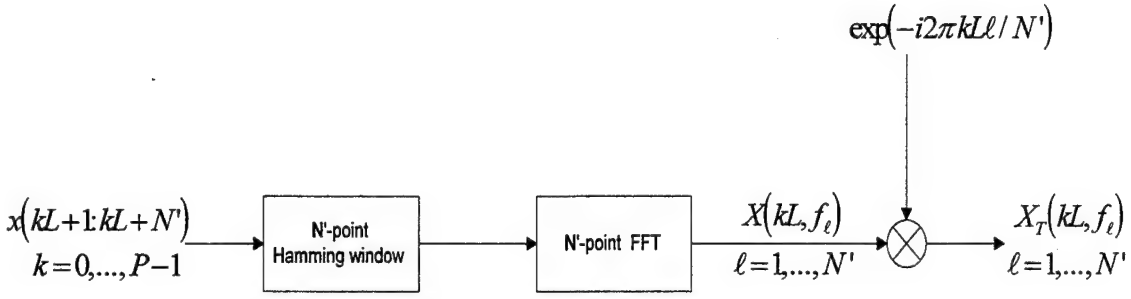

Figure 3 Computation of the Complex Demodulates

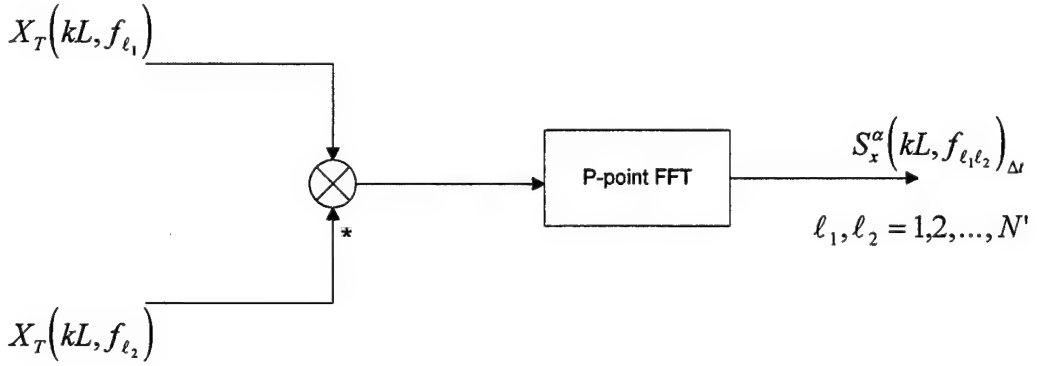

Figure 4 Implementation of the FFT Accumulation Method

An advantage of having complex demodulates is that there is no need to worry with a correction factor to take care of the phase shift introduced by overlap processing. The last multiplier in Figure 3 (i. e., complex exponential) provides the correction to compensate for the overlap processing artifacts.

The MATLAB codes that compute and plot the SCD function estimate using the FAM method are called AUTOFAM and CROSSFAM. AUTOFAM computes and plots the auto spectral correlation density function (amount of correlation between frequency shifted versions of a given real or complex valued signal) estimate. CROSSFAM computes and plots the cross spectral correlation density function estimate for two different real or complex valued signals.

The inputs required for these programs are the signal(s), the sampling frequency (f_s), the desired frequency resolution (Δf), and the desired resolution in cyclic frequency ($\Delta\alpha$). In the case of two signals, the sampling frequencies must be the same.

The programs are listed in Appendices B and C.

B. STRIP SPECTRAL CORRELATION ALGORITHM (SSCA)

In the SSCA algorithm, the complex demodulate of one of the signals is computed in the same way it is done for the FAM method (channelization). The complex demodulated sequence is directly multiplied by the complex conjugate of the other signal. Then, the resultant signal is smoothed in time by means of an

N-point FFT. Here, N is the total number of data points ($N = PL$).

Figure 5 shows the implementation of the SSCA. The complex demodulated component $X_T\left(kL, f_{\ell_1}\right)$ is obtained as shown in Figure 3.

It appears that the complex demodulate $X_T\left(kL, f_{\ell_1}\right)$ is at a sampling rate f_s/L due to the introduction of the decimation factor L, and consequently it can not be directly multiplied by $x[n]$ which is at a sampling rate f_s. However, the demodulated sequence is interpolated to match the sampling rate of $x[n]$ by means of a process called replication. Replication is accomplished by holding the value of each complex demodulate sample for L samples [Ref.2].

The MATLAB codes generated to compute and plot the SCD function estimate for given signal(s) using the SSCA method are called AUTOSSCA and CROSSSSCA. AUTOSSCA computes and plots the auto spectral correlation density function (amount of correlation between frequency shifted versions of a given signal) estimate. CROSSSSCA computes and plots the cross spectral correlation density function estimate for two real or complex valued signals.

The inputs required for these routines are the signal(s), the sampling frequency (f_s), the desired frequency resolution (Δf), and the desired resolution in cyclic frequency ($\Delta\alpha$). In the case of two signals, the sampling frequencies must be the same.

The codes are given in Appendices D and E.

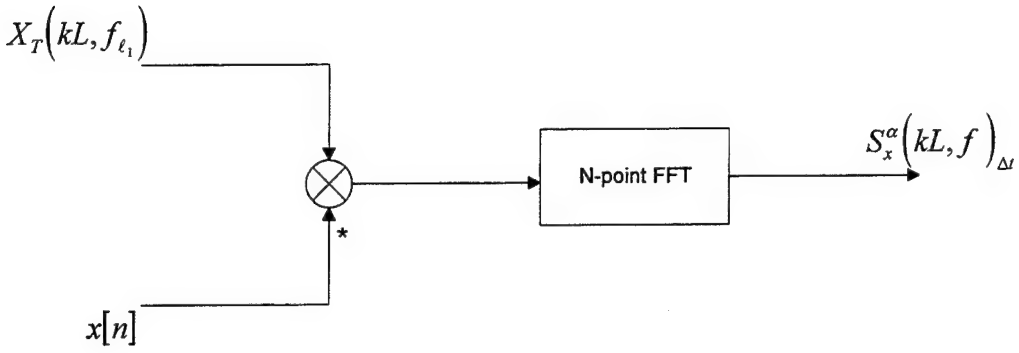

Figure 5 Implementation of the SSCA

V. EXPERIMENTAL RESULTS

In this chapter, the theoretical results of computing the SCD function for some analog and digital modulated signals are presented, together with the experimental results obtained as output from the programs AUTOFAM and AUTOSSCA. An interpretation of the results is also provided.

A. ANALOG MODULATED SIGNALS

1. Amplitude-Modulated (AM) Signal

Consider the following amplitude-modulated (AM) signal, $x[n]$, given by

$$x[n] = a[n]p[n], \tag{20}$$

where $a[n]$ is a purely stationary low pass message signal with power spectral density $S_a(f)$, and $p[n]$ is a sinusoidal carrier wave given by

$$p[n] = \cos(2\pi f_o n + \phi_o). \tag{21}$$

In Eq. 21, $f_o = F_o/F_s$ is the carrier digital frequency and ϕ_o is the carrier phase. F_o is the carrier frequency in Hz and F_s is the sampling frequency in Hz.

The SCD function for this amplitude-modulated (AM) sine wave is given by

$$S_x^{\alpha}(f) = \begin{cases} \frac{1}{4}S_a(f+f_o) + \frac{1}{4}S_a(f-f_o), & \alpha = 0 \\ \frac{1}{4}S_a(f)\, e^{\pm i2\phi_o}, & \alpha = \pm 2f_o \\ 0, & otherwise. \end{cases} \tag{22}$$

Details of the derivation are given in Appendix A.

When $a[n]$ is a tone, some of the assumptions made to obtain Eq. 22 are not valid. If the message $a[n]$ is a tone at digital frequency f_a given by

$$a[n] = \cos(2\pi f_a n), \tag{23}$$

then it is necessary to go through the same steps as for a stationary lowpass signal with no spectral lines in the message's power spectral density (PSD), as shown in Appendix A.

Let us assume that $x[n]$ is an amplitude-modulated single-sideband (AMSSB) signal, obtained by transmitting only the lower-side frequency, given by

$$x[n] = \frac{1}{2}\left[\cos(2\pi f_a n)\cdot\cos(2\pi f_o n + \phi_o) + \sin(2\pi f_a n)\cdot\sin(2\pi f_o n + \phi_o)\right]$$

$$= \frac{1}{2}\cos\left[2\pi(f_o - f_a)n + \phi_o\right]. \tag{24}$$

Since the cyclic autocorrelation function (ACF) is given by

$$R_x^{\alpha}[\ell] = \left\langle x[n]\, x^*[n-\ell]\, e^{-i2\pi\alpha n}\right\rangle e^{i\pi\alpha\ell}, \tag{25}$$

replacing $x[n]$ and $x[n-\ell]$ by Eq. 24 leads to,

$$R_x^{\alpha}[\ell] = \frac{1}{4}\cos\left[2\pi(f_o - f_a)\ell\right] e^{i\pi\alpha\ell}\left\langle e^{-i2\pi\alpha n}\right\rangle +$$

$$\frac{1}{8}e^{i\pi[\alpha-2(f_o-f_a)]\ell}\left\langle e^{i2\pi[\alpha-2(f_o-f_a)]n}\right\rangle e^{i2\phi_o}+\frac{1}{8}e^{i\pi[\alpha+2(f_o-f_a)]\ell}\left\langle e^{-i2\pi[\alpha+2(f_o-f_a)]n}\right\rangle e^{-i2\phi_o}. \quad (26)$$

This can be rewritten as

$$R_x^\alpha[\ell]=\begin{cases}\frac{1}{4}\cos\left[2\pi(f_o-f_a)\ell\right], & \alpha=0\\ \frac{1}{8}e^{\pm i2\phi_o}, & \alpha=\pm2(f_o-f_a).\end{cases} \quad (27)$$

The SCD is the Fourier transform of the cyclic autocorrelation function. Therefore, the SCD is given by the Fourier transform of Eq. 27 leading to

$$S_x^\alpha(f)=\begin{cases}\frac{1}{8}\left[\delta(f-f_o+f_a)+\delta(f+f_o-f_a)\right], & \alpha=0\\ \frac{1}{8}\delta(f)e^{\pm i2\phi_o}, & \alpha=\pm2(f_o-f_a).\end{cases} \quad (28)$$

Now, let us suppose that $x[n]$ is an amplitude-modulated double-sideband supressed carrier (AMDSB-SC) signal given by

$$x[n]=\cos(2\pi f_a n)\cdot\cos(2\pi f_o n+\phi_o). \quad (29)$$

This can be written using a trigonometric identity as

$$x[n]=\frac{1}{2}\left\{\cos\left[2\pi(f_o+f_a)n+\phi_o\right]+\cos\left[2\pi(f_o-f_a)n+\phi_o\right]\right\}. \quad (30)$$

So, replacing $x[n]$ and $x[n-\ell]$ by Eq. 30 into Eq. 25 leads to,

$$R_x^\alpha[\ell]=\frac{1}{8}\left[\cos2\pi(f_o+f_a)\ell+\cos2\pi(f_o-f_a)\ell\right]e^{i\pi\alpha\ell}\left\langle e^{-i2\pi\alpha n}\right\rangle+$$

$$\frac{1}{16}e^{i\pi[\alpha-2(f_o+f_a)]\ell}\left\langle e^{-i2\pi[\alpha-2(f_o+f_a)]n}\right\rangle e^{i2\phi_o}+\frac{1}{16}e^{i\pi[\alpha+2(f_o-f_a)]\ell}\left\langle e^{-i2\pi(\alpha-2f_a)n}\right\rangle+$$

$$\frac{1}{16}e^{i\pi[\alpha-2(f_o-f_a)]\ell}\left\langle e^{-i2\pi(\alpha-2f_o)n}\right\rangle e^{i2\phi_o}+\frac{1}{16}e^{i\pi[\alpha+2(f_o+f_a)]\ell}\left\langle e^{-i2\pi[\alpha+2(f_o+f_a)]n}\right\rangle e^{-i2\phi_o}+$$

$$\frac{1}{16}e^{i\pi[\alpha+2(f_o-f_a)]\ell}\left\langle e^{-i2\pi(\alpha+2f_o)n}\right\rangle e^{-i2\phi_o}+\frac{1}{16}e^{i\pi[\alpha-2(f_o-f_a)]\ell}\left\langle e^{-i2\pi(\alpha+2f_a)n}\right\rangle+$$

$$\frac{1}{16}e^{i\pi[\alpha+2(f_o+f_a)]\ell}\left\langle e^{-i2\pi(\alpha+2f_a)n}\right\rangle+\frac{1}{16}e^{i\pi[\alpha-2(f_o+f_a)]\ell}\left\langle e^{-i2\pi(\alpha-2f_o)n}\right\rangle e^{i2\phi_o}+$$

$$\frac{1}{16}e^{i\pi[\alpha-2(f_o-f_a)]\ell}\left\langle e^{-i2\pi[\alpha-2(f_o-f_a)]n}\right\rangle e^{i2\phi_o}+\frac{1}{16}e^{i\pi[\alpha+2(f_o+f_a)]\ell}\left\langle e^{-i2\pi(\alpha+2f_o)n}\right\rangle e^{-i2\phi_o}+$$

$$\frac{1}{16}e^{i\pi[\alpha-2(f_o+f_a)]\ell}\left\langle e^{-i2\pi(\alpha-2f_a)n}\right\rangle+\frac{1}{16}e^{i\pi[\alpha+2(f_o-f_a)]\ell}\left\langle e^{-i2\pi[\alpha+2(f_o-f_a)]n}\right\rangle e^{-i2\phi_o}. \qquad (31)$$

This can be rewritten as

$$R_x^{\alpha}[\ell]=\begin{cases}\frac{1}{8}\left[\cos 2\pi(f_o+f_a)\ell+\cos 2\pi(f_o-f_a)\ell\right], & \alpha=0\\ \frac{1}{16}e^{i2\pi f_o\ell}+\frac{1}{16}e^{-i2\pi f_o\ell}=\frac{1}{8}\cos 2\pi f_o\ell, & \alpha=\pm 2f_a\\ \frac{1}{16}e^{\pm i2\phi_o}, & \alpha=\pm 2(f_o-f_a)\\ \frac{1}{8}e^{\pm i2\phi_o}\cos 2\pi f_a\ell, & \alpha=\pm 2f_o\\ \frac{1}{16}e^{\pm i2\phi_o}, & \alpha=\pm 2(f_o+f_a).\end{cases} \qquad (32)$$

Therefore, the SCD is given by the Fourier transform of Eq. 32 leading to

$$S_x^{\alpha}(f)=\begin{cases}\frac{1}{16}\left[\delta(f-f_o-f_a)+\delta(f-f_o+f_a)+\delta(f+f_o-f_a)+\delta(f+f_o+f_a)\right], & \alpha=0\\ \frac{1}{16}\left[\delta(f-f_o)+\delta(f+f_o)\right], & \alpha=\pm 2f_a\\ \frac{1}{16}\delta(f)e^{\pm i2\phi_o}, & \alpha=\pm 2(f_o-f_a)\\ \frac{1}{16}\left[\delta(f-f_a)+\delta(f+f_a)\right]e^{\pm i2\phi_o}, & \alpha=\pm 2f_o\\ \frac{1}{16}\delta(f)e^{\pm i2\phi_o}, & \alpha=\pm 2(f_o+f_a).\end{cases} \qquad (33)$$

For the case where $x[n]$ is an amplitude-modulated double-sideband transmitted carrier (AMDSB-TC) signal given by

$$x[n]=\left[1+\cos(2\pi f_a n)\right]\cdot\cos(2\pi f_o n+\phi_o). \qquad (34)$$

This can be written using a trigonometric identity as

$$x[n]=\cos(2\pi\, f_o n)+\frac{1}{2}\left\{\cos\left[2\pi(f_o+f_a)n+\phi_o\right]+\cos\left[2\pi(f_o-f_a)n+\phi_o\right]\right\}. \qquad (35)$$

So, replacing $x[n]$ and $x[n-\ell]$ by Eq. 35 into Eq. 25 leads to,

$$R_x^{\alpha}[\ell]=\left\{\frac{1}{2}\cos(2\pi f_o\ell)+\frac{1}{8}\left[\cos 2\pi(f_o+f_a)\ell+\cos 2\pi(f_o-f_a)\ell\right]\right\}e^{i\pi\alpha\ell}\left\langle e^{-i2\pi\alpha n}\right\rangle+$$

$$\left\{\frac{1}{8}e^{i\pi[\alpha+2(f_o+f_a)]\ell}+\frac{1}{8}e^{i\pi[\alpha-2(f_o-f_a)]\ell}+\frac{1}{8}e^{i\pi(\alpha-2f_o)\ell}+\frac{1}{8}e^{i\pi(\alpha+2f_o)}\right\}\left\langle e^{-i2\pi(\alpha+f_a)n}\right\rangle+$$

$$\left\{\frac{1}{8}e^{i\pi[\alpha+2(f_o-f_a)]\ell}+\frac{1}{8}e^{i\pi[\alpha-2(f_o+f_a)]\ell}+\frac{1}{8}e^{i\pi(\alpha-2f_o)\ell}+\frac{1}{8}e^{i\pi(\alpha+2f_o)}\right\}\left\langle e^{-i2\pi(\alpha-f_a)n}\right\rangle+$$

$$\left\{\frac{1}{16}e^{i\pi[\alpha-2(f_o-f_a)]\ell}+\frac{1}{16}e^{i\pi[\alpha+2(f_o+f_a)]\ell}\right\}\left\langle e^{-i2\pi(\alpha+2f_a)n}\right\rangle+$$

$$\left\{\frac{1}{16}e^{i\pi[\alpha+2(f_o-f_a)]\ell}+\frac{1}{16}e^{i\pi[\alpha-2(f_o+f_a)]\ell}\right\}\left\langle e^{-i2\pi(\alpha-2f_a)n}\right\rangle+$$

$$\frac{1}{16}e^{i\pi[\alpha+2(f_o-f_a)]\ell}e^{-i2\phi_o}\left\langle e^{-i2\pi[\alpha+2(f_o-f_a)]n}\right\rangle+$$

$$\frac{1}{16}e^{i\pi[\alpha-2(f_o-f_a)]\ell}e^{i2\phi_o}\left\langle e^{-i2\pi[\alpha-2(f_o-f_a)]n}\right\rangle+$$

$$\left\{\frac{1}{8}e^{i\pi[\alpha+2(f_o-f_a)]\ell}+\frac{1}{8}e^{i\pi(\alpha+2f_o)\ell}\right\}e^{-i2\phi_o}\left\langle e^{-i2\pi[\alpha+(2f_o-f_a)]n}\right\rangle+$$

$$\left\{\frac{1}{8}e^{i\pi[\alpha-2(f_o-f_a)]\ell}+\frac{1}{8}e^{i\pi(\alpha-2f_o)\ell}\right\}e^{i2\phi_o}\left\langle e^{-i2\pi[\alpha-(2f_o-f_a)]n}\right\rangle+$$

$$\left\{\frac{1}{4}e^{i\pi(\alpha+2f_o)\ell}+\frac{1}{16}e^{i\pi[\alpha+2(f_o-f_a)]\ell}+\frac{1}{16}e^{i\pi[\alpha+2(f_o+f_a)]\ell}\right\}e^{-i2\phi_o}\left\langle e^{-i2\pi(\alpha+2f_o)n}\right\rangle+$$

$$\left\{\frac{1}{4}e^{i\pi(\alpha-2f_o)\ell}+\frac{1}{16}e^{i\pi[\alpha-2(f_o-f_a)]\ell}+\frac{1}{16}e^{i\pi[\alpha-2(f_o+f_a)]\ell}\right\}e^{i2\phi_o}\left\langle e^{-i2\pi(\alpha-2f_o)n}\right\rangle+$$

$$\left\{\frac{1}{8}e^{i\pi\left[\alpha+2\left(f_o+f_a\right)\right]\ell}+\frac{1}{8}e^{i\pi\left(\alpha+2f_o\right)\ell}\right\}e^{-i2\phi_o}\left\langle e^{-i2\pi\left[\alpha+\left(2f_o+f_a\right)\right]n}\right\rangle+$$

$$\left\{\frac{1}{8}e^{i\pi\left[\alpha-2\left(f_o+f_a\right)\right]\ell}+\frac{1}{8}e^{i\pi\left(\alpha-2f_o\right)\ell}\right\}e^{i2\phi_o}\left\langle e^{-i2\pi\left[\alpha-\left(2f_o+f_a\right)\right]n}\right\rangle+$$

$$\frac{1}{16}e^{i\pi\left[\alpha+2\left(f_o+f_a\right)\right]\ell}e^{-i2\phi_o}\left\langle e^{-i2\pi\left[\alpha+2\left(f_o+f_a\right)\right]n}\right\rangle+$$

$$\frac{1}{16}e^{i\pi\left[\alpha-2\left(f_o+f_a\right)\right]\ell}e^{i2\phi_o}\left\langle e^{-i2\pi\left[\alpha-2\left(f_o+f_a\right)\right]n}\right\rangle. \qquad (36)$$

This can be rewritten as

$$R_x^{\alpha}[\ell]=\begin{cases}\frac{1}{8}\cos\left[2\pi\left(f_o-f_a\right)\ell\right]+\frac{1}{2}\cos\left(2\pi f_o\ell\right)+\frac{1}{8}\cos\left[2\pi\left(f_o+f_a\right)\ell\right], & \alpha=0\\ \frac{1}{4}\cos\left[\pi\left(2f_o-f_a\right)\ell\right]+\frac{1}{4}\cos\left[\pi\left(2f_o+f_a\right)\ell\right], & \alpha=\pm f_a\\ \frac{1}{8}\cos\left(2\pi f_o\ell\right), & \alpha=\pm 2f_a\\ \frac{1}{16}e^{\pm i2\phi_o}, & \alpha=\pm 2\left(f_o-f_a\right)\\ \frac{1}{4}\cos\left(\pi f_a\ell\right)e^{\pm i2\phi_o}, & \alpha=\pm\left(2f_o-f_a\right)\\ \left[\frac{1}{4}+\frac{1}{8}\cos\left(2\pi f_a\ell\right)\right]e^{\pm i2\phi_o}, & \alpha=\pm 2f_o\\ \frac{1}{4}\cos\left(\pi f_a\ell\right)e^{\pm i2\phi_o}, & \alpha=\pm\left(2f_o+f_a\right)\\ \frac{1}{16}e^{\pm i2\phi_o}, & \alpha=\pm 2\left(f_o+f_a\right).\end{cases} \qquad (37)$$

Therefore, the SCD is given by

$$S_x^{\alpha}(f)=\begin{cases}\frac{1}{16}\delta\left(f+f_o+f_a\right)+\frac{1}{4}\delta\left(f+f_o\right)+\frac{1}{16}\delta\left(f+f_o-f_a\right)+\frac{1}{16}\delta\left(f-f_o+f_a\right)+\frac{1}{4}\delta\left(f-f_o\right)+\frac{1}{16}\delta\left(f-f_o-f_a\right), & \alpha=0\\ \frac{1}{8}\delta\left(f+f_o+\frac{f_a}{2}\right)+\frac{1}{8}\delta\left(f+f_o-\frac{f_a}{2}\right)+\frac{1}{8}\delta\left(f-f_o+\frac{f_a}{2}\right)+\frac{1}{8}\delta\left(f-f_o-\frac{f_a}{2}\right), & \alpha=\pm f_a\\ \frac{1}{16}\delta\left(f+f_o\right)+\frac{1}{16}\delta\left(f-f_o\right), & \alpha=\pm 2f_a\\ \frac{1}{16}\delta(f)e^{\pm i2\phi_o}, & \alpha=\pm 2\left(f_o-f_a\right)\\ \left[\frac{1}{8}\delta\left(f+\frac{f_a}{2}\right)+\frac{1}{8}\delta\left(f-\frac{f_a}{2}\right)\right]e^{\pm i2\phi_o}, & \alpha=\pm\left(2f_o-f_a\right)\\ \left[\frac{1}{16}\delta\left(f+f_a\right)+\frac{1}{4}\delta(f)+\frac{1}{16}\delta\left(f-f_a\right)\right]e^{\pm i2\phi_o}, & \alpha=\pm 2f_o\\ \left[\frac{1}{8}\delta\left(f+\frac{f_a}{2}\right)+\frac{1}{8}\delta\left(f-\frac{f_a}{2}\right)\right]e^{\pm i2\phi_o}, & \alpha=\pm\left(2f_o-f_a\right)\\ \frac{1}{16}\delta(f)e^{\pm i2\phi_o}, & \alpha=\pm 2\left(f_o+f_a\right).\end{cases} \qquad (38)$$

The results obtained from AUTOFAM and AUTOSSCA are presented as a sequence of three plots, for each of the signals utilized. This presentation is maintained throughout (i. e., Figure 6 - Figure 41). The first plot is a surface plot that shows the magnitude of the SCD function estimate in each region of the bifrequency plane with coordinates f and α. The second plot is a two-dimensional contour plot. It gives a better view of the position of the features in the bifrequency plane. The third plot is a set of two-dimensional slices of the SCD function estimate for fixed values of the cyclic frequency α.

Figures 6 - 11 show the results obtained by using the programs AUTOFAM and AUTOSSCA on an amplitude-modulated single-side band (AMSSB) signal. For $f_a = 512\,Hz$ and $f_o = 2048\,Hz$, Equation 28 leads to the following result:

$$S_x^{\alpha}(f) = \begin{cases} \frac{1}{8}\left[\delta(f-1536)+\delta(f+1536)\right], & \alpha = 0 \\ \frac{1}{8}\delta(f)e^{\pm i2\phi_o}, & \alpha = \pm 3072\,Hz. \end{cases} \tag{39}$$

So, according to Eq. 39, ones expect to obtain peaks at $f = \pm 1536 Hz$ for $\alpha = 0$, and at $f = 0$ for $\alpha = \pm 3072 Hz$. The results in Figures 6-11 are in agreement with the theoretical results in Eq. 39 and show that AUTOFAM gives a clearer picture than AUTOSSCA. This is even true when AUTOSSCA uses a finer resolution in cyclic frequency (i. e., $\Delta\alpha = 64\,Hz$ for AUTOFAM versus $\Delta\alpha = 32\,Hz$ for AUTOSSCA).

The results obtained for an amplitude-modulated double-side band

suppressed-carrier (AMDSB-SC) are presented in Figures 12-17. For $f_a = 512\,Hz$ and $f_o = 2048\,Hz$, Equation 33 leads to the following result:

$$S_x^{\alpha}(f) = \begin{cases} \frac{1}{16}\left[\delta(f-2560)+\delta(f-1536)+\delta(f+1536)+\delta(f+2560)\right], & \alpha = 0 \\ \frac{1}{16}\left[\delta(f-2048)+\delta(f+2048)\right], & \alpha = \pm 1024Hz \\ \frac{1}{16}\delta(f), & \alpha = \pm 3072Hz \\ \frac{1}{16}\left[\delta(f-512)+\delta(f+512)\right], & \alpha = \pm 4096Hz \\ \frac{1}{16}\delta(f), & \alpha = \pm 5120Hz. \end{cases} \tag{40}$$

According to Eq. 40, ones expect to have four peaks at $f = \pm 1536Hz$ and $f = \pm 2560Hz$, for $\alpha = 0$; two peaks at $f = \pm 2048Hz$, for $\alpha = \pm 1024Hz$; one peak at $f = 0$, for $\alpha = \pm 3072Hz$; two peaks at $f = \pm 512Hz$, for $\alpha = \pm 4096Hz$; and a peak at $f = 0$, for $\alpha = \pm 5120Hz$. Figures 12-17 confirm the theoretical results as given by Eq. 40.

The results for an amplitude-modulated double-side band transmitted-carrier (AMDSB-TC) are presented in Figures 18-23. For $f_a = 512\,Hz$ and $f_o = 2048\,Hz$, Equation 38 leads to the following result:

$$S_x^{\alpha}(f) = \begin{cases} \frac{1}{16}\delta(f+2560)+\frac{1}{4}\delta(f+2048)+\frac{1}{16}\delta(f+1536)+\frac{1}{16}\delta(f-1536)+\frac{1}{4}\delta(f-2048)+\frac{1}{16}\delta(f-2560), & \alpha = 0 \\ \frac{1}{8}\delta(f+2304)+\frac{1}{8}\delta(f+1792)+\frac{1}{8}\delta(f-1792)+\frac{1}{8}\delta(f-2304), & \alpha = \pm 512Hz \\ \frac{1}{16}\delta(f+2048)+\frac{1}{16}\delta(f-2048), & \alpha = \pm 1024Hz \\ \frac{1}{16}\delta(f)e^{\pm 12\phi_o}, & \alpha = \pm 3072Hz \\ \left[\frac{1}{8}\delta(f+256)+\frac{1}{8}\delta(f-256)\right]e^{\pm 12\phi_o}, & \alpha = \pm 3584Hz \\ \left[\frac{1}{16}\delta(f+512)+\frac{1}{4}\delta(f)+\frac{1}{16}\delta(f512_a)\right]e^{\pm 12\phi_o}, & \alpha = \pm 4096Hz \\ \left[\frac{1}{8}\delta(f+256)+\frac{1}{8}\delta(f-256)\right]e^{\pm 12\phi_o}, & \alpha = \pm 4608Hz \\ \frac{1}{16}\delta(f)e^{\pm 12\phi_o}, & \alpha = \pm 5120Hz. \end{cases} \tag{41}$$

According to Eq. 41, ones expect to have two big peaks at $f = \pm 2048Hz$

and four smaller peaks at $f = \pm 1536 Hz$ and $f = \pm 2560 Hz$, for $\alpha = 0$; four peaks at $f = \pm 1792 Hz$ and $f = \pm 2304 Hz$, for $\alpha = \pm 512 Hz$; two peaks at $f = \pm 2048 Hz$, for $\alpha = \pm 1024 Hz$; one peak at $f = 0$, for $\alpha = \pm 3072 Hz$; two peaks at $f = \pm 256 Hz$, for $\alpha = \pm 3584 Hz$; a big peak at $f = 0$ and two smaller peaks at $f = \pm 512 Hz$, for $\alpha = \pm 4096 Hz$; two peaks at $f = \pm 256 Hz$, for $\alpha = \pm 4608 Hz$; and a peak at $f = 0$, for $\alpha = \pm 5120 Hz$. Figures 18-23 verify the theoretical results of Eq. 41.

To have a reliable estimation of the spectral correlation density function is necessary that the product $\Delta t \, \Delta f >> 1$ [Ref. 1]. This condition requires that $\Delta f >> \Delta \alpha$. In some of the results obtained (i. e., as in Figure 21), this requirement was not met. Computational limitations did not allow for a better resolution in the plots, since this translates to generating a large amount of data, making impossible to obtain a plot on the printer and/or on the screen with the available PC and workstation resources.

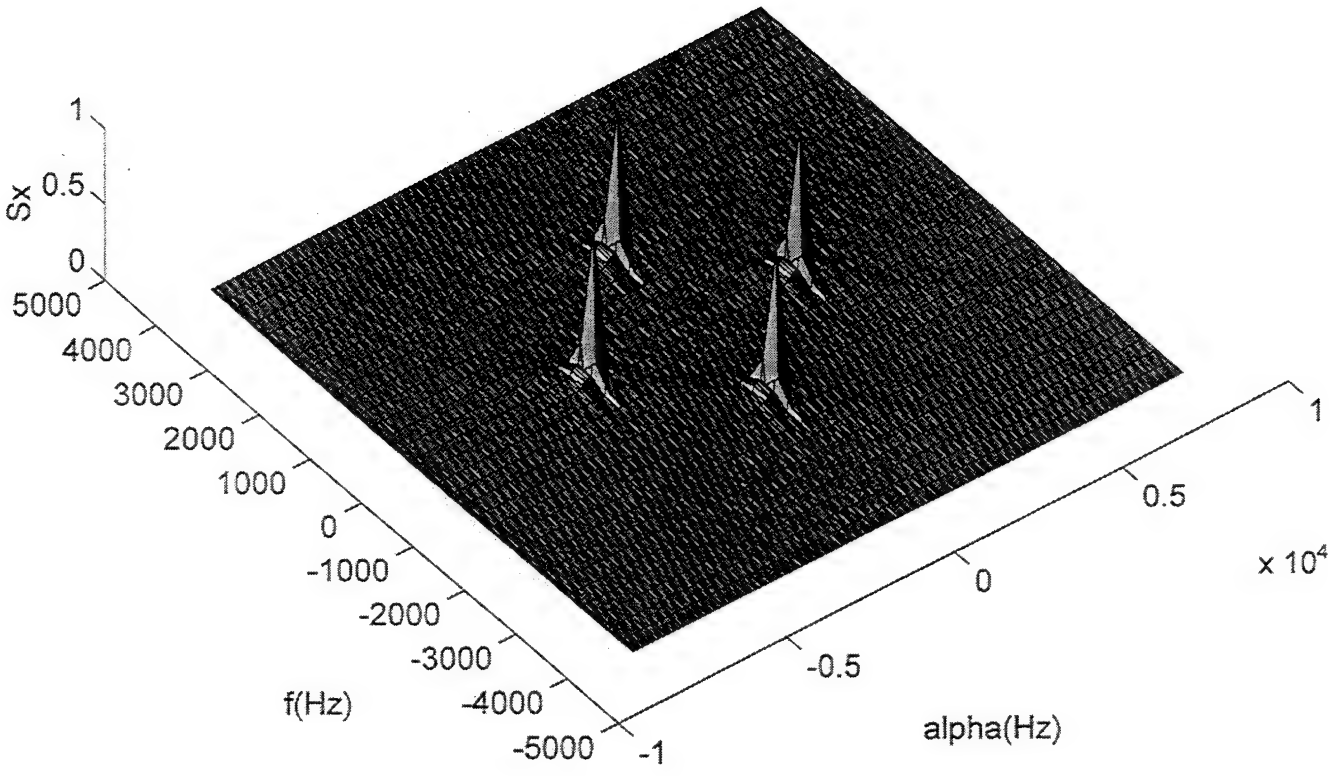

Figure 6 Surface plot of the SCD estimate magnitude for an Amplitude Modulated (AM) Single-Side Band Signal, using AUTOFAM, with the following parameters: $\Delta f = 256Hz$, $\Delta\alpha = 64Hz$, $f_c = 2048Hz$, $f_t = 512Hz$, and $f_s = 8192Hz$, where f_c is the carrier frequency, f_t is the tonal frequency, and f_s is the sampling frequency.

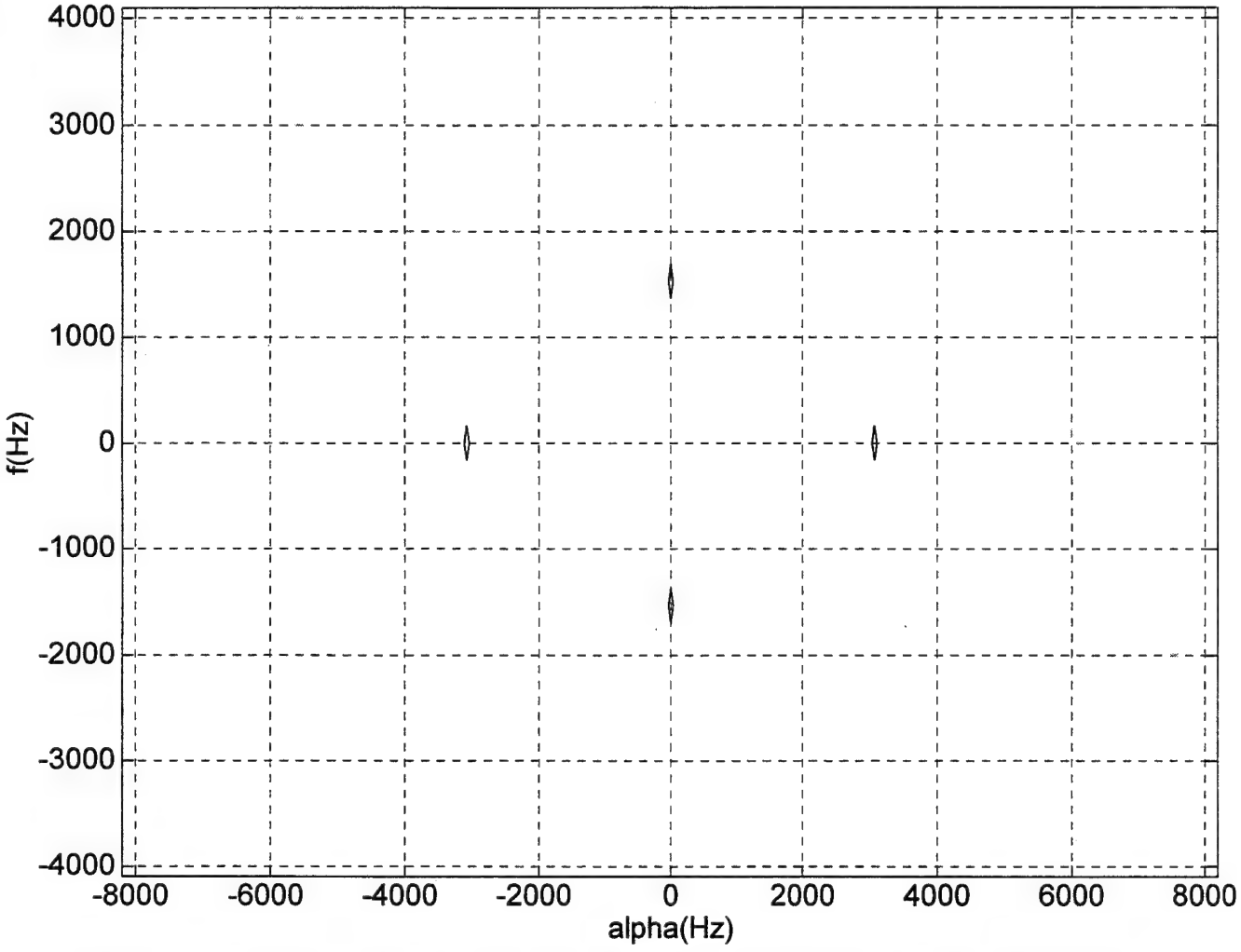

Figure 7 Contour plot of the SCD estimate magnitude for an Amplitude Modulated (AM) Single-Side Band Signal, using AUTOFAM, with the following parameters: $\Delta f = 256Hz$, $\Delta\alpha = 64Hz$, $f_c = 2048Hz$, $f_t = 512Hz$, and $f_s = 8192Hz$, where f_c is the carrier frequency, f_t is the tonal frequency, and f_s is the sampling frequency.

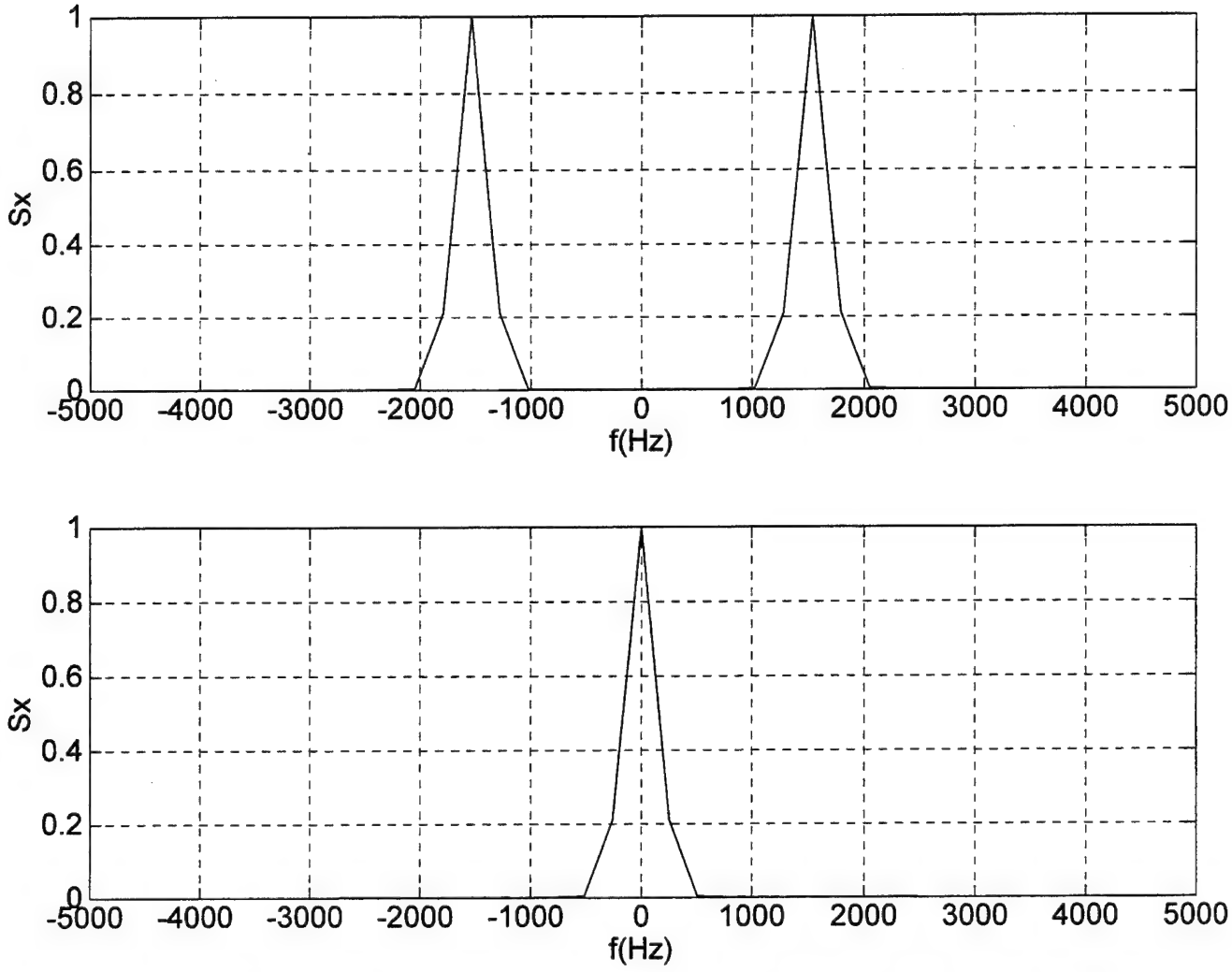

Figure 8 Plots of the SCD estimate magnitude for an Amplitude Modulated (AM) Single-Side Band Signal, using AUTOFAM, for $\alpha = 0$ and $\alpha = 3072Hz$, respectively, with the following parameters: $\Delta f = 256Hz$, $\Delta\alpha = 64Hz$, $f_c = 2048Hz$, $f_t = 512Hz$, and $f_s = 8192Hz$, where f_c is the carrier frequency, f_t is the tonal frequency, and f_s is the sampling frequency.

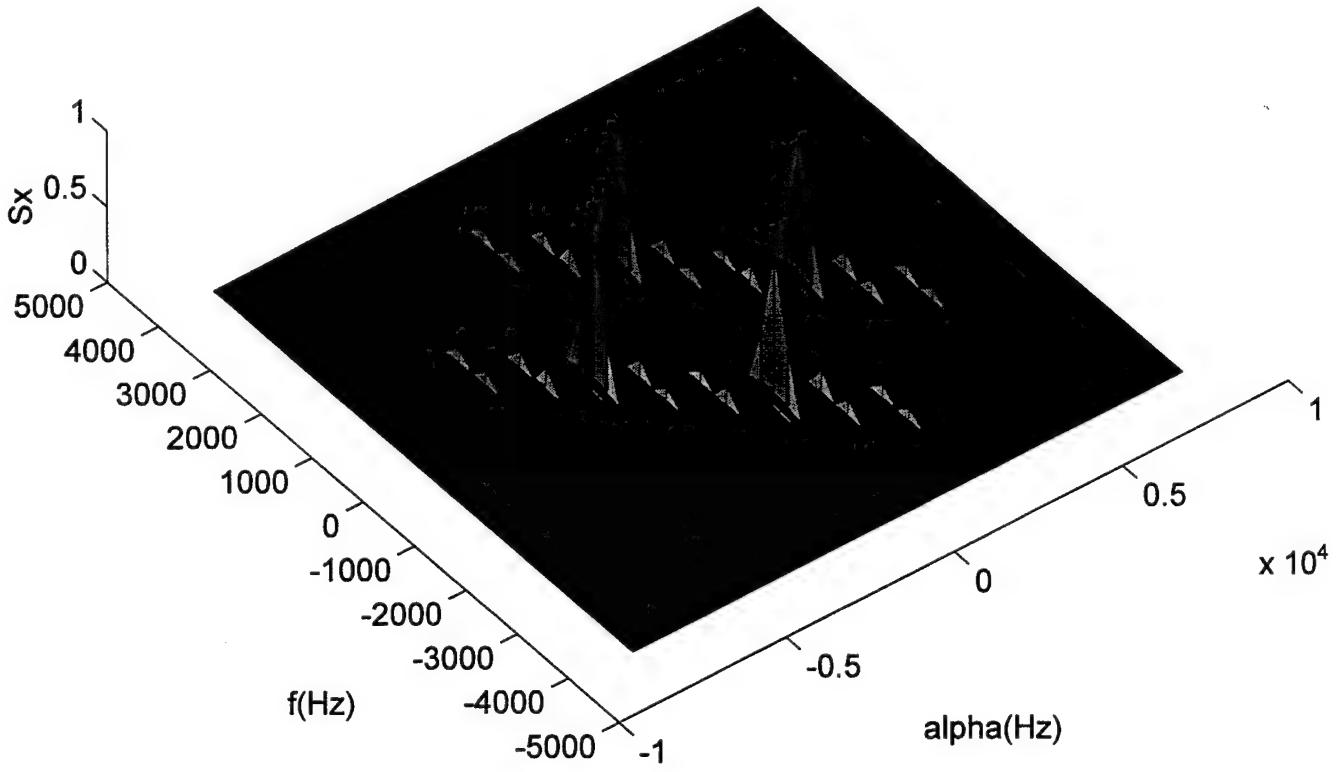

Figure 9 Surface plot of the SCD estimate magnitude for an Amplitude Modulated (AM) Single-Side Band Signal, using AUTOSSCA, with the following parameters: $\Delta f = 256Hz$, $\Delta\alpha = 32Hz$, $f_c = 2048Hz$, $f_t = 512Hz$, and $f_s = 8192Hz$, where f_c is the carrier frequency, f_t is the tonal frequency, and f_s is the sampling frequency.

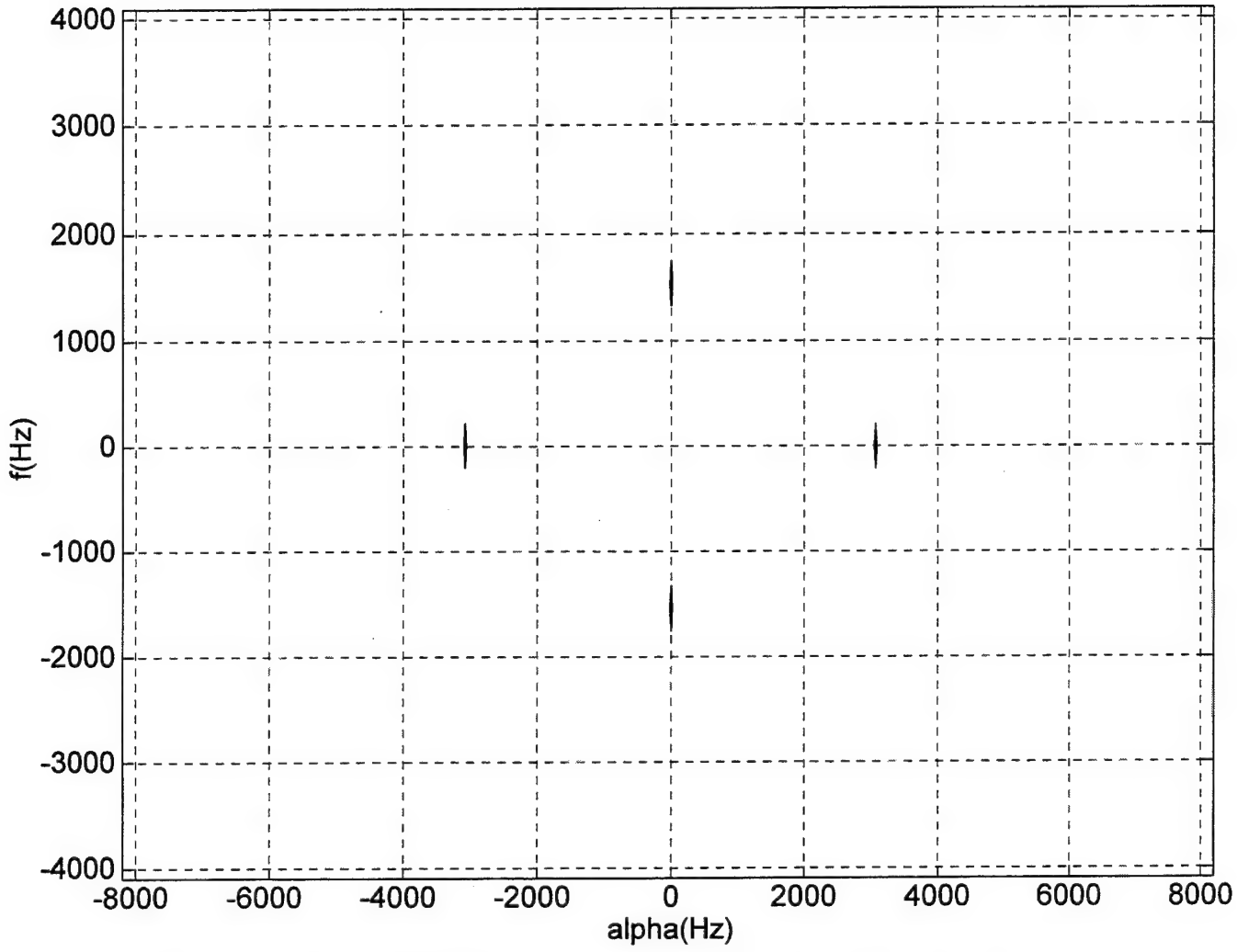

Figure 10 Contour plot of the SCD estimate magnitude for an Amplitude Modulated (AM) Single-Side Band Signal, using AUTOSSCA, with the following parameters: $\Delta f = 256Hz$, $\Delta\alpha = 32Hz$, $f_c = 2048Hz$, $f_t = 512Hz$, and $f_s = 8192Hz$, where f_c is the carrier frequency, f_t is the tonal frequency, and f_s is the sampling frequency

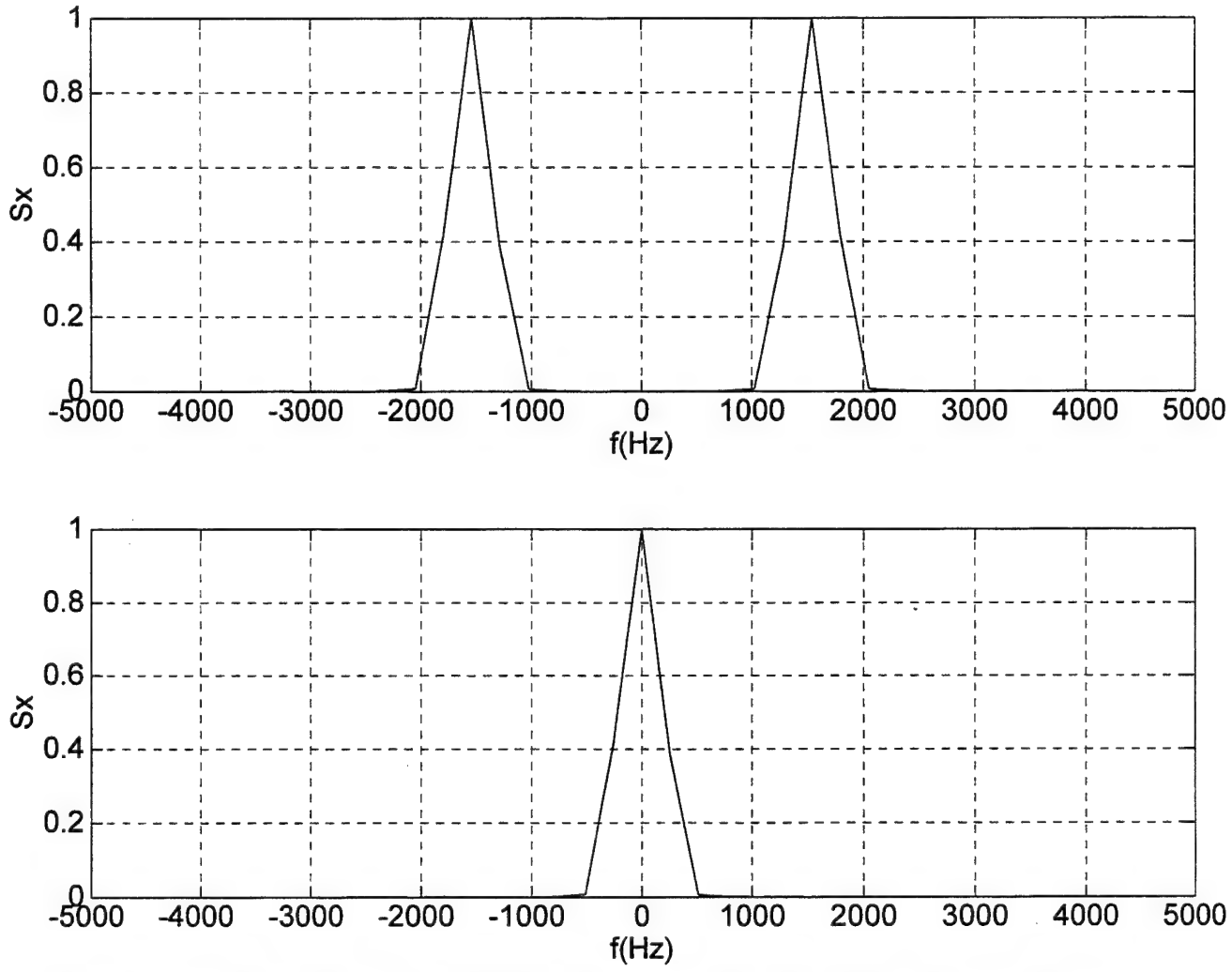

Figure 11 Plots of the SCD estimate magnitude for an Amplitude Modulated (AM) Single-Side Band Transmitted Carrier Signal, using AUTOSSCA, for $\alpha = 0$ and $\alpha = 3072Hz$, respectively, with the following parameters: $\Delta f = 256Hz$, $\Delta\alpha = 32Hz$, $f_c = 2048Hz$, $f_t = 512Hz$, and $f_s = 8192Hz$, where f_c is the carrier frequency, f_t is the tonal frequency, and f_s is the sampling frequency.

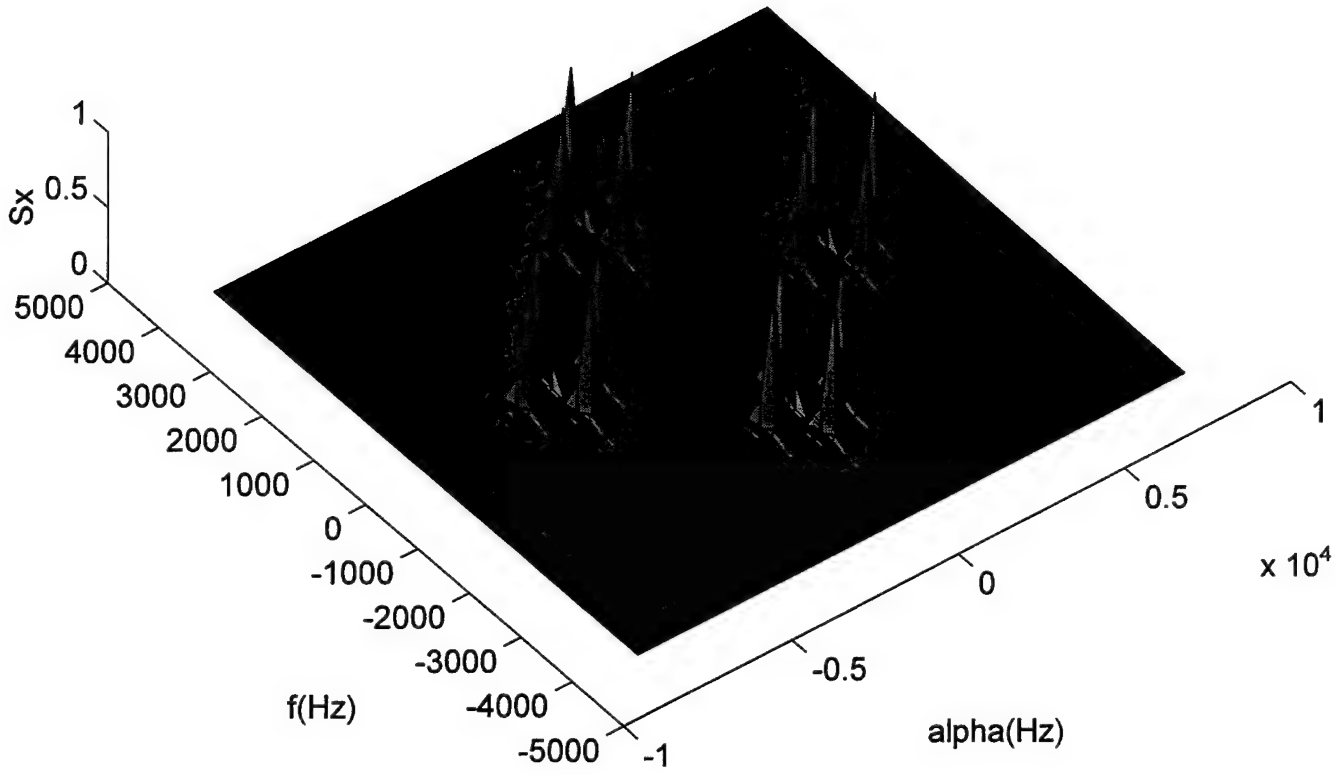

Figure 12 Surface plot of the SCD estimate magnitude for an Amplitude Modulated (AM) Double-Side Band Supressed Carrier Signal, using AUTOFAM, with the following parameters: $\Delta f = 256Hz$, $\Delta\alpha = 32Hz$, $f_c = 2048Hz$, $f_t = 512Hz$, and $f_s = 8192Hz$, where f_c is the carrier frequency, f_t is the tonal frequency, and f_s is the sampling frequency.

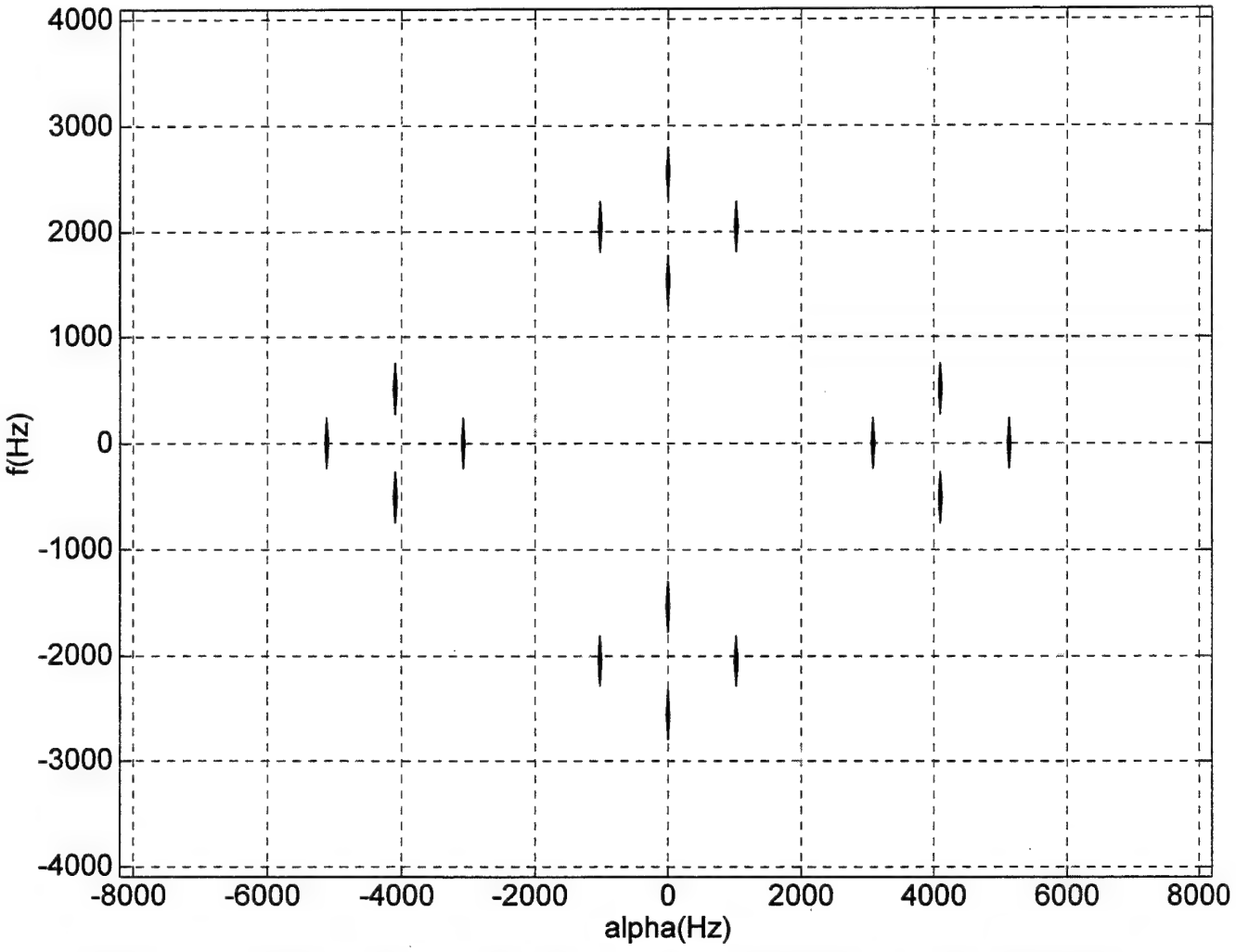

Figure 13 Contour plot of the SCD estimate magnitude for an Amplitude Modulated (AM) Double-Sided Band Supressed Carrier Signal, using AUTOFAM, with the following parameters: $\Delta f = 256Hz$, $\Delta\alpha = 32Hz$, $f_c = 2048Hz$, $f_t = 512Hz$, and $f_s = 8192Hz$, where f_c is the carrier frequency, f_t is the tonal frequency, and f_s is the sampling frequency.

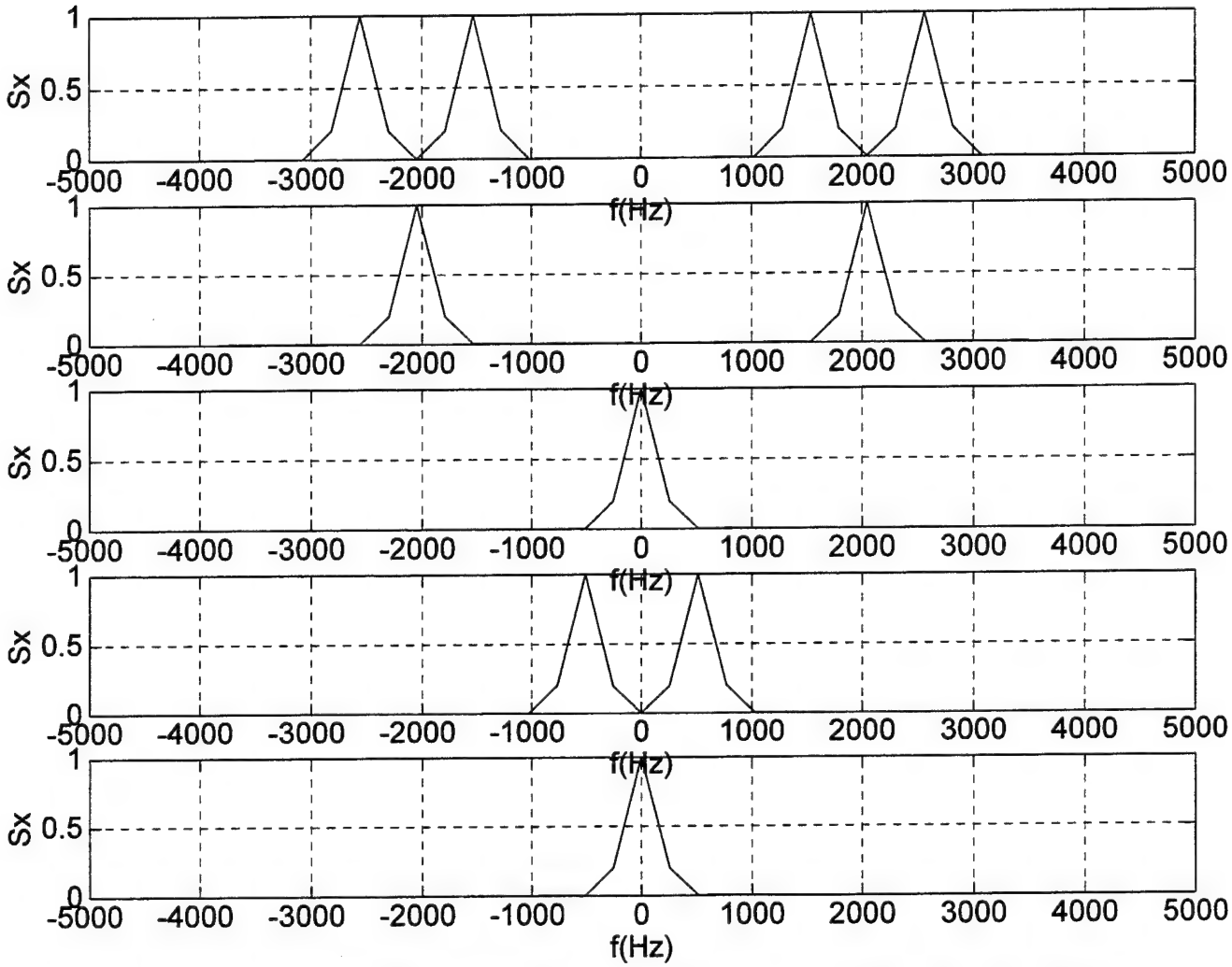

Figure 14 Plots of the SCD estimate magnitude for an Amplitude Modulated (AM) Double-Side Band Supressed Carrier Signal, using AUTOFAM, for $\alpha = 0$, $\alpha = 1024Hz$, $\alpha = 3072Hz$, $\alpha = 4096Hz$, and $\alpha = 5120Hz$, respectively, with the following parameters: $\Delta f = 256Hz$, $\Delta\alpha = 32Hz$, $f_c = 2048Hz$, $f_t = 512Hz$, and $f_s = 8192Hz$, where f_c is the carrier frequency, f_t is the tonal frequency, and f_s is the sampling frequency.

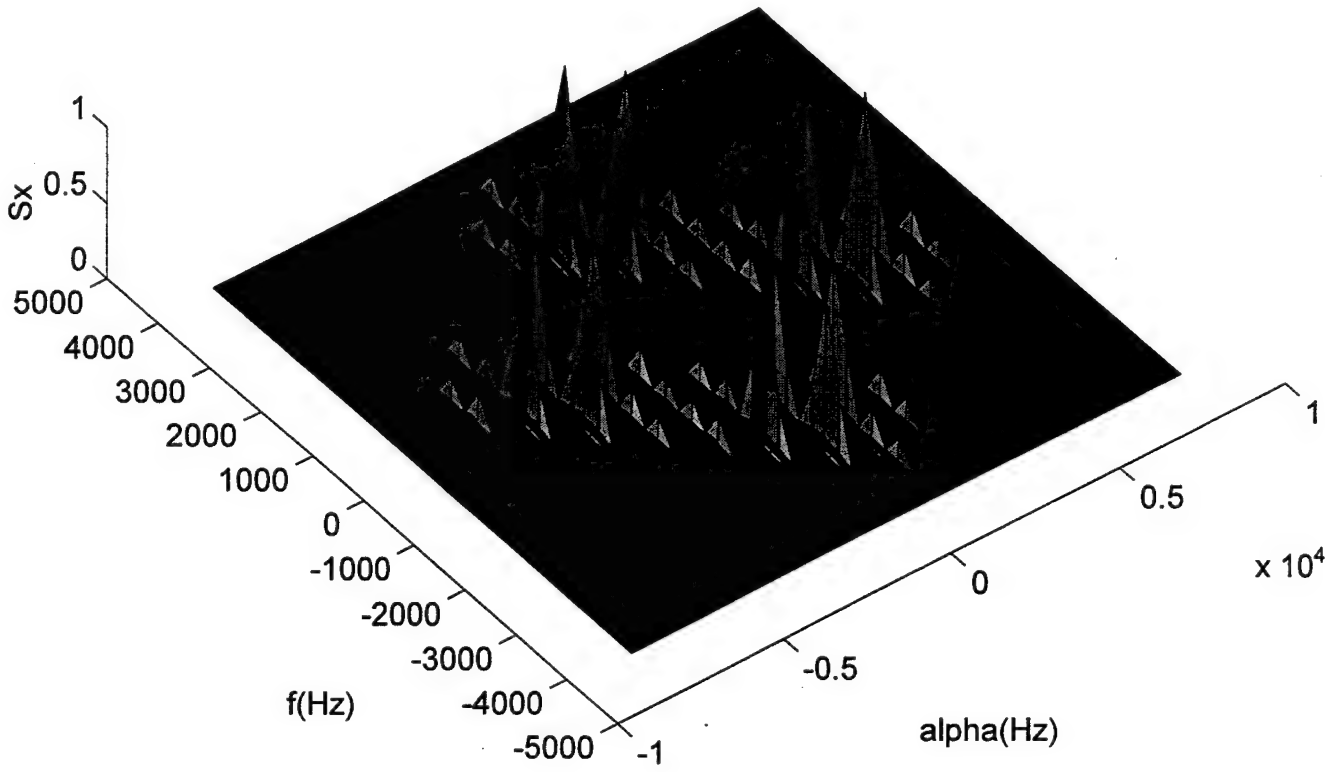

Figure 15 Surface plot of the SCD estimate magnitude for an Amplitude Modulated (AM) Double-Side Band Supressed Carrier Signal, using AUTOSSCA, with the following parameters: $\Delta f = 256Hz$, $\Delta\alpha = 32Hz$, $f_c = 2048Hz$, $f_t = 512Hz$, and $f_s = 8192Hz$, where f_c is the carrier frequency, f_t is the tonal frequency, and f_s is the sampling frequency.

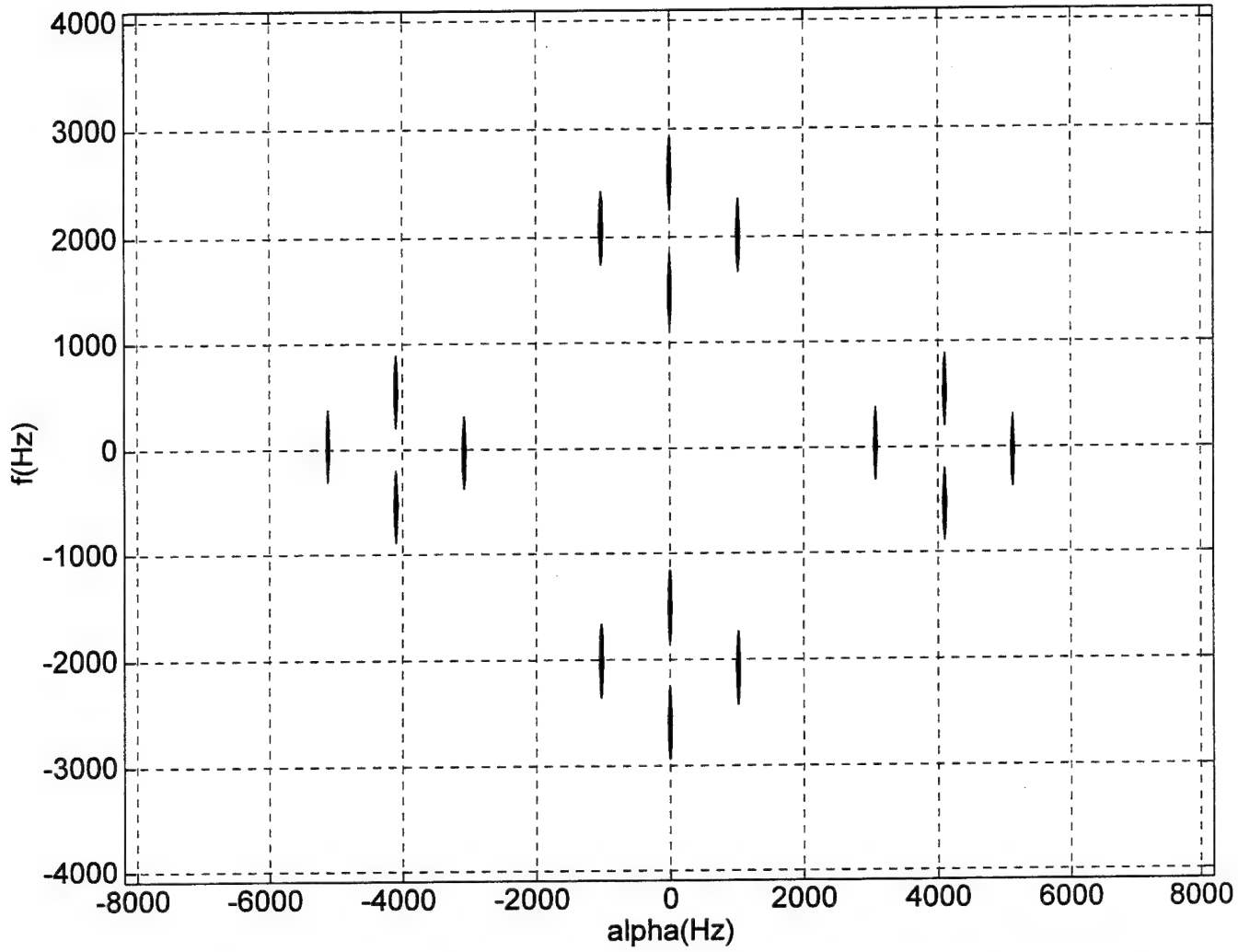

Figure 16 Contour plot of the SCD estimate magnitude for an Amplitude Modulated (AM) Double-Sided Band Supressed Carrier Signal, using AUTOSSCA, with the following parameters: $\Delta f = 256Hz$, $\Delta\alpha = 32Hz$, $f_c = 2048Hz$, $f_t = 512Hz$, and $f_s = 8192Hz$, where f_c is the carrier frequency, f_t is the tonal frequency, and f_s is the sampling frequency.

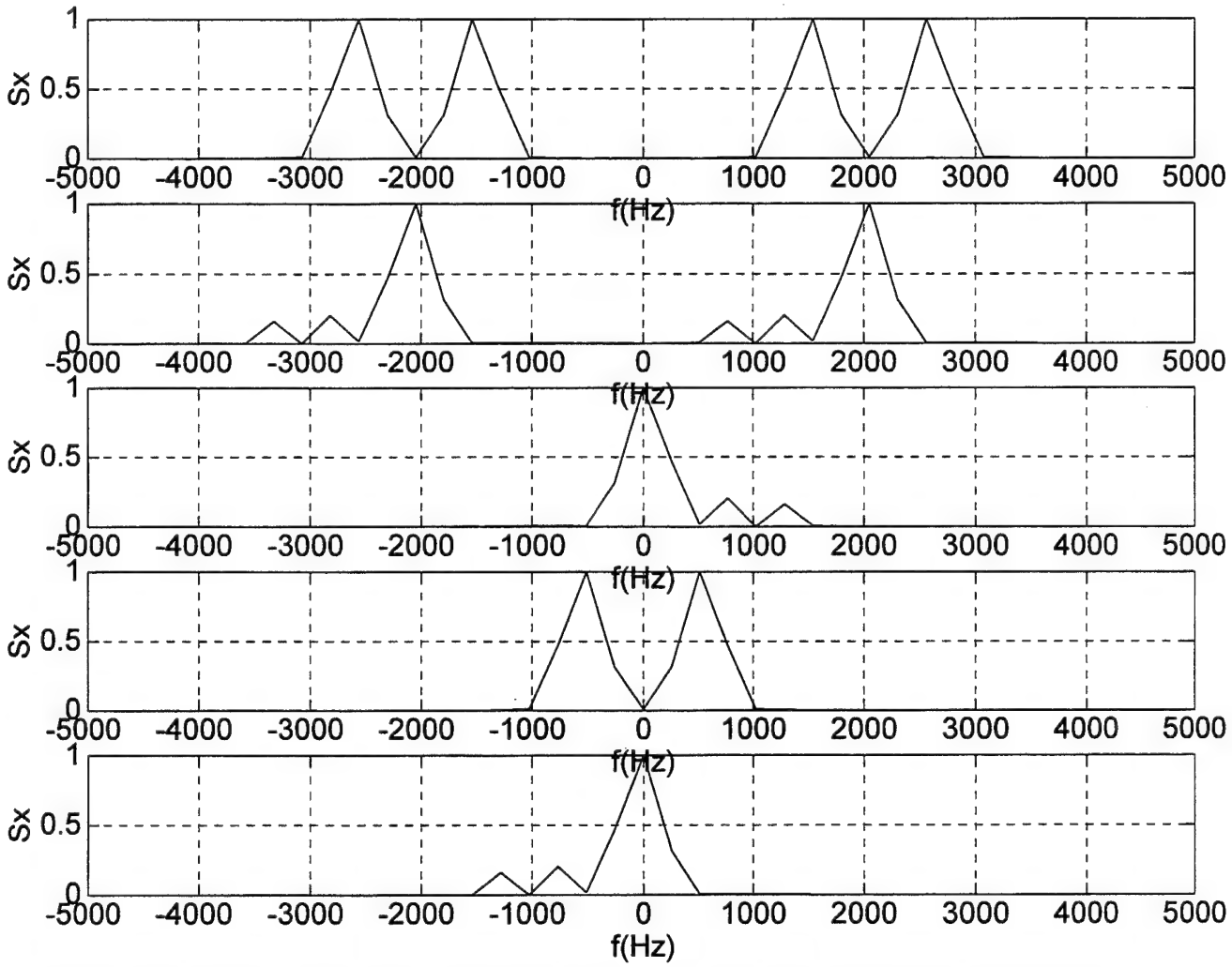

Figure 17 Plots of the SCD estimate magnitude for an Amplitude Modulated (AM) Double-Side Band Supressed Carrier Signal, using AUTOSSCA, for $\alpha = 0$, $\alpha = 1024Hz$, $\alpha = 3072Hz$, $\alpha = 4096Hz$, and $\alpha = 5120Hz$, respectively, with the following parameters: $\Delta f = 256Hz$, $\Delta\alpha = 32Hz$, $f_c = 2048Hz$, $f_t = 512Hz$, and $f_s = 8192Hz$, where f_c is the carrier frequency, f_t is the tonal frequency, and f_s is the sampling frequency.

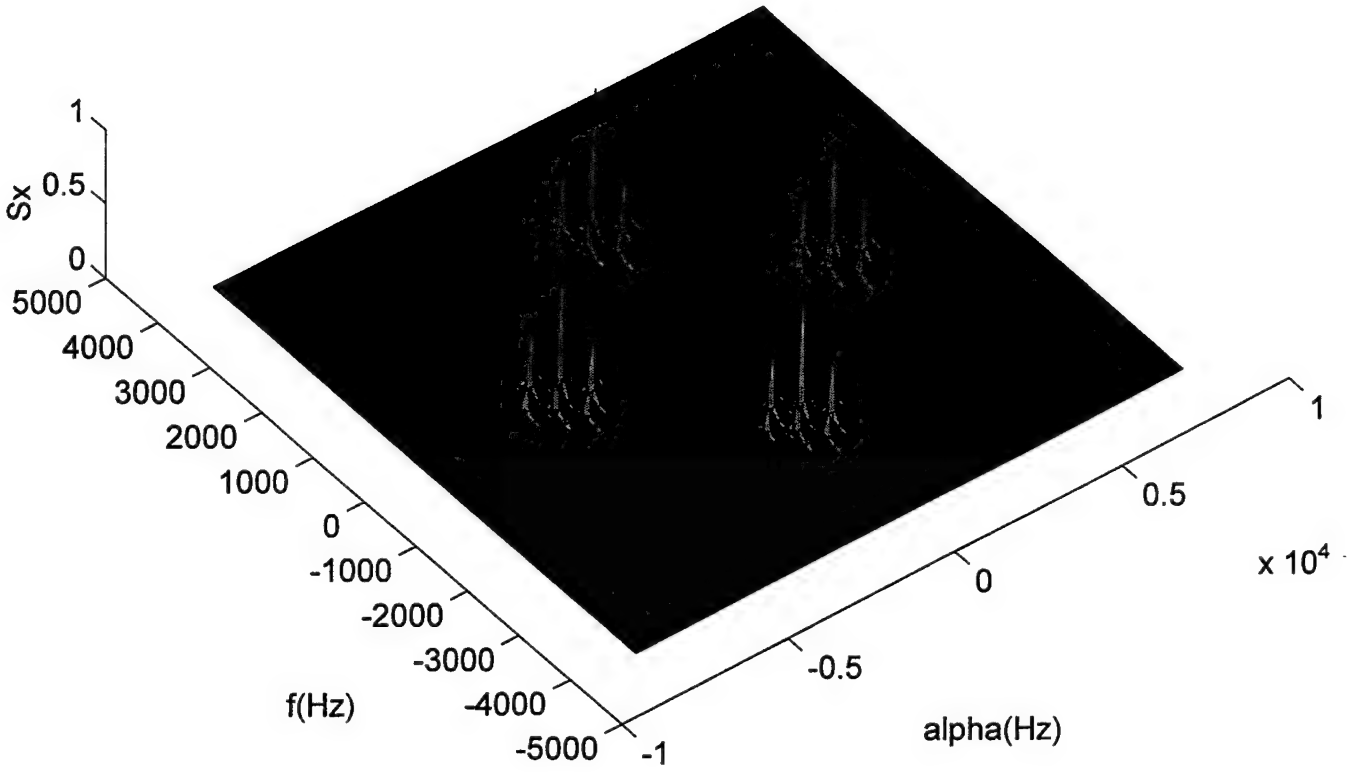

Figure 18 Surface plot of the SCD estimate magnitude for an Amplitude Modulated (AM) Double-Side Band Transmitted Carrier Signal, using AUTOFAM, with the following parameters: $\Delta f = 128Hz$, $\Delta\alpha = 32Hz$, $f_c = 2048Hz$, $f_t = 512Hz$, and $f_s = 8192Hz$, where f_c is the carrier frequency, f_t is the tonal frequency, and f_s is the sampling frequency.

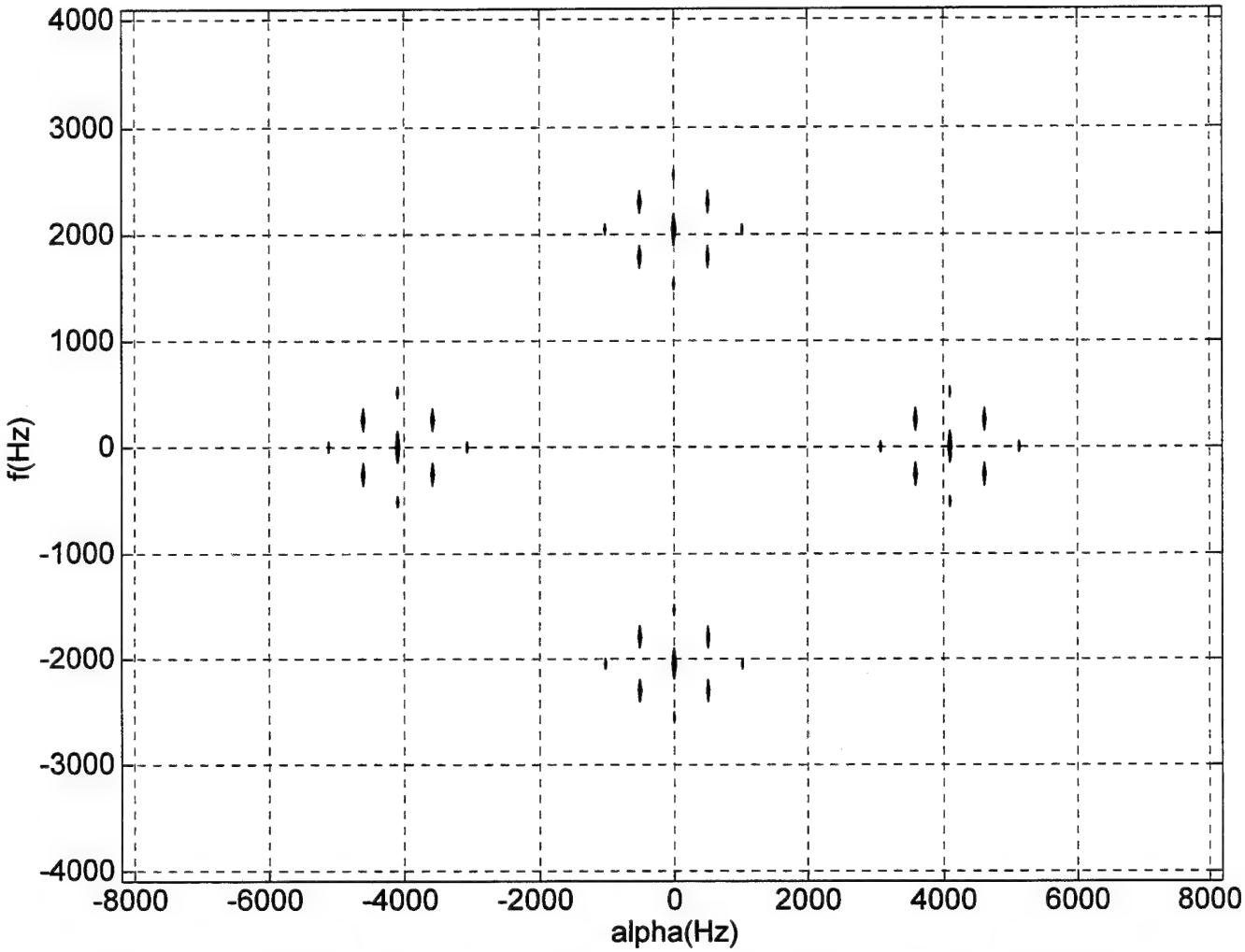

Figure 19 Contour plot of the SCD estimate magnitude for an Amplitude Modulated (AM) Double-Sided Band Transmitted Carrier Signal, using AUTOFAM, with the following parameters: $\Delta f = 128Hz$, $\Delta\alpha = 32Hz$, $f_c = 2048Hz$, $f_t = 512Hz$, and $f_s = 8192Hz$, where f_c is the carrier frequency, f_t is the tonal frequency, and f_s is the sampling frequency.

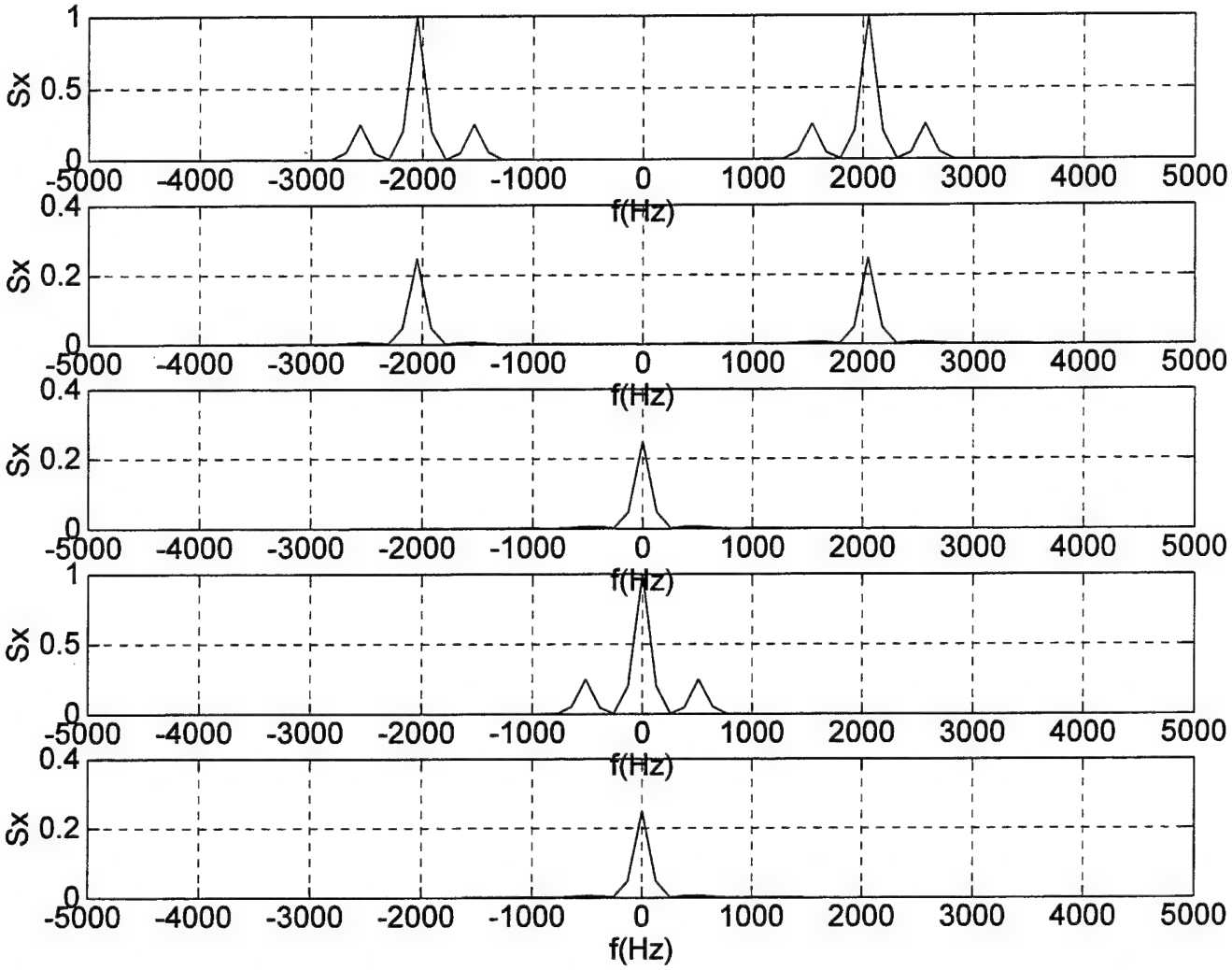

Figure 20 Plots of the SCD estimate magnitude for an Amplitude Modulated (AM) Double-Side Band Transmitted Carrier Signal, using AUTOFAM, for $\alpha = 0$, $\alpha = 1024Hz$, $\alpha = 3072Hz$, $\alpha = 4096Hz$, and $\alpha = 5120Hz$, respectively, with the following parameters: $\Delta f = 128Hz$, $\Delta\alpha = 32Hz$, $f_c = 2048Hz$, $f_t = 512Hz$, and $f_s = 8192Hz$, where f_c is the carrier frequency, f_t is the tonal frequency, and f_s is the sampling frequency.

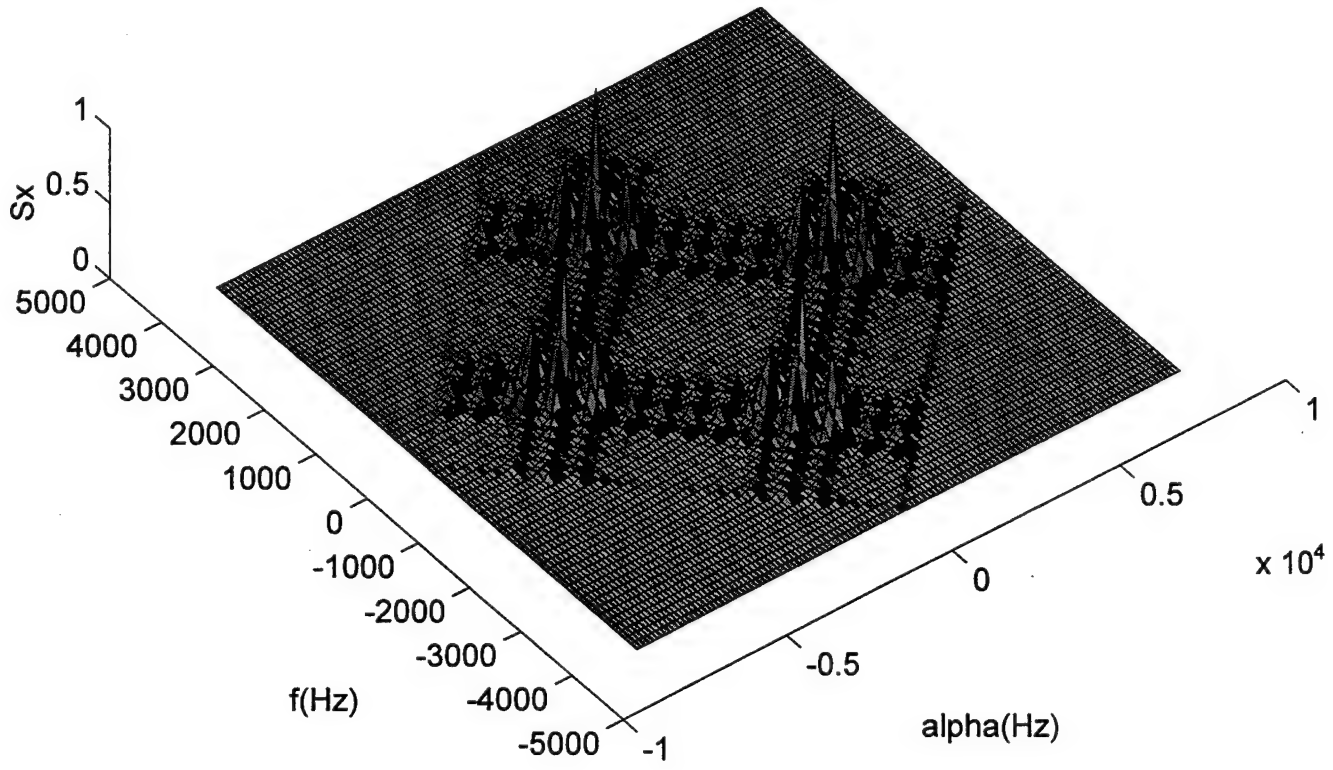

Figure 21 Surface plot of the SCD estimate magnitude for an Amplitude Modulated (AM) Double-Side Band Transmitted Carrier Signal, using AUTOSSCA, with the following parameters: $\Delta f = 128Hz$, $\Delta\alpha = 128Hz$, $f_c = 2048Hz$, $f_t = 512Hz$, and $f_s = 8192Hz$, where f_c is the carrier frequency, f_t is the tonal frequency, and f_s is the sampling frequency.

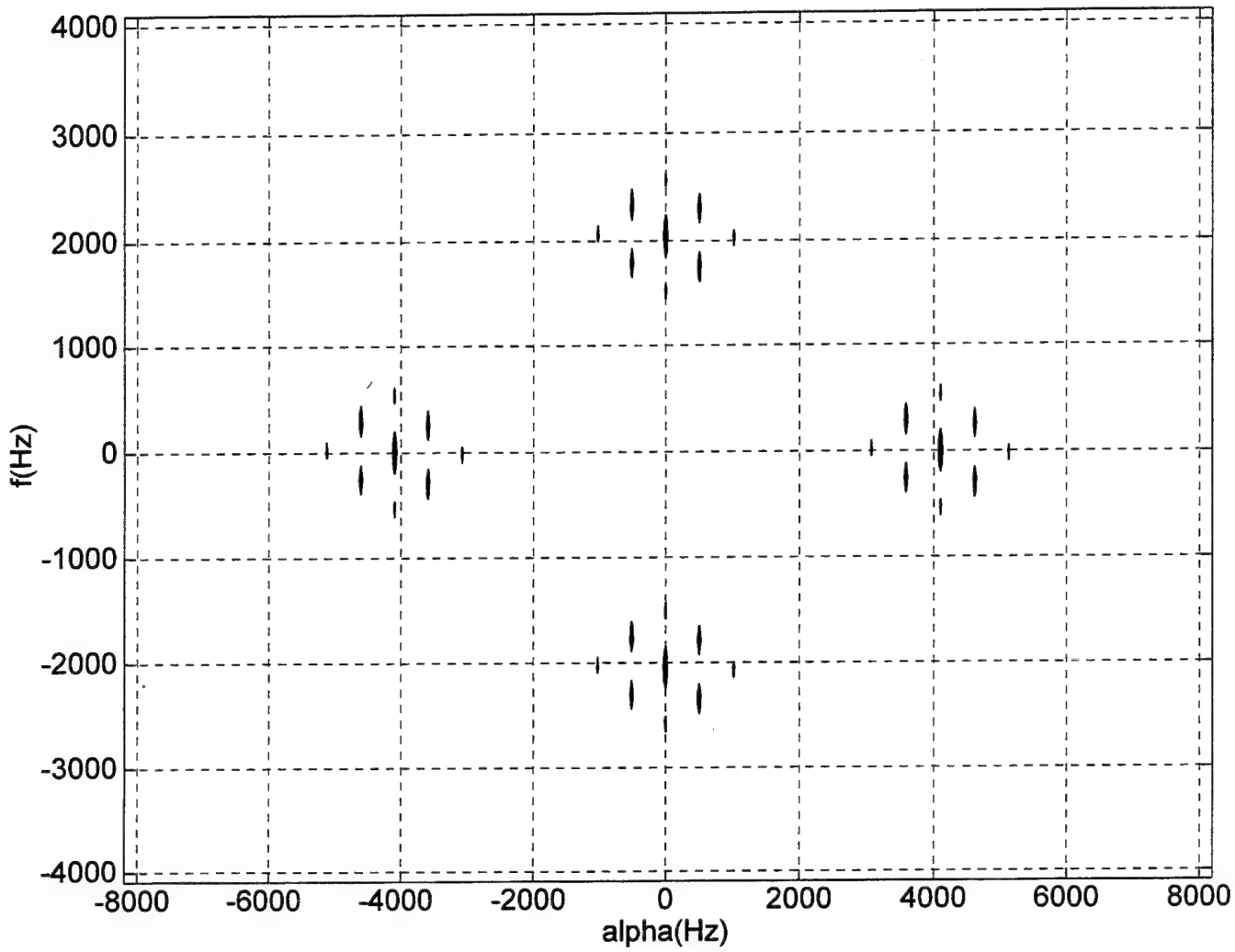

Figure 22 Contour plot of the SCD estimate magnitude for an Amplitude Modulated (AM) Double-Sided Band Transmitted Carrier Signal, using AUTOSSCA, with the following parameters: $\Delta f = 128Hz$, $\Delta\alpha = 32Hz$, $f_c = 2048Hz$, $f_t = 512Hz$, and $f_s = 8192Hz$, where f_c is the carrier frequency, f_t is the tonal frequency, and f_s is the sampling frequency.

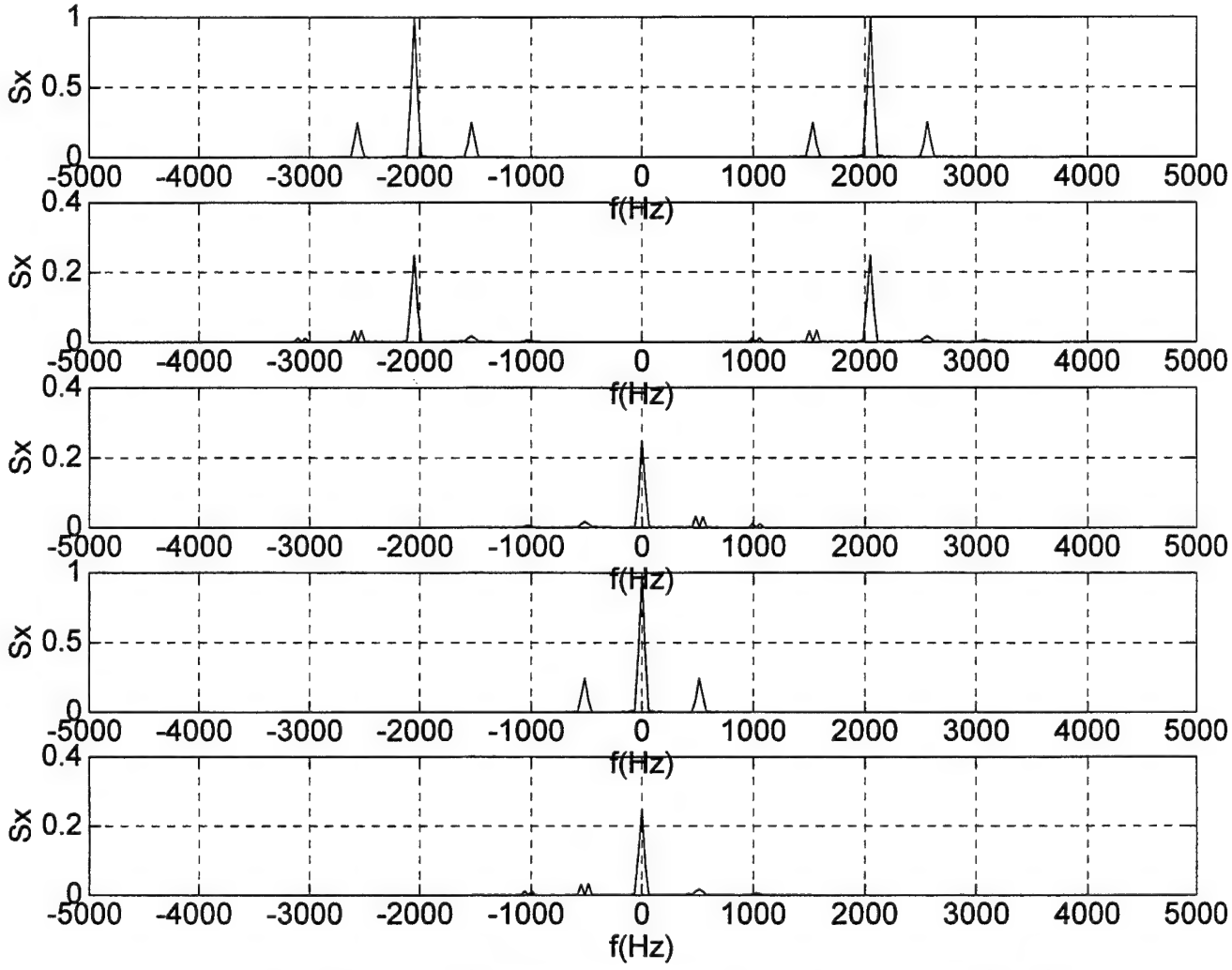

Figure 23 Plots of the SCD estimate magnitude for an Amplitude Modulated (AM) Double-Side Band Transmitted Carrier Signal, using AUTOSSCA, for $\alpha = 0$, $\alpha = 1024Hz$, $\alpha = 3072Hz$, $\alpha = 4096Hz$, and $\alpha = 5120Hz$, respectively, with the following parameters: $\Delta f = 32Hz$, $\Delta\alpha = 32Hz$, $f_c = 2048Hz$, $f_t = 512Hz$, and $f_s = 8192Hz$, where f_c is the carrier frequency, f_t is the tonal frequency, and f_s is the sampling frequency.

2. Pulse-Amplitude Modulated (PAM) Signal

In the previous section, consider the following form for the carrier wave, $p[n]$,

$$p[n] = \sum_{m=-\infty}^{\infty} \delta(n - mN_o) \tag{42}$$

where N_o is the pulse period. If the product $x[n] = a[n]p[n]$ is filtered using a pulse form with impulse-response $q[n]$, then the result is the pulse-amplitude modulation(PAM) signal

$$y[n] = \sum_{m=-\infty}^{\infty} a[mN_o]\, q[n - mN_o]. \tag{43}$$

The cyclic spectra for the PAM signal, when $a[n]$ is stationary, is given by

$$S_y^{\alpha}(f) = \begin{cases} \frac{1}{T_o} Q\left(f + \frac{\alpha}{2}\right) Q^*\left(f - \frac{\alpha}{2}\right) S_a\left(f + \frac{\alpha}{2}\right), & \alpha = \frac{k}{T_o} \\ 0, & \alpha \neq \frac{k}{T_o} \end{cases} \tag{44}$$

where $Q(f)$ is the Fourier transform of the pulse form $q[n]$, and $S_a(f)$ is the power spectral density of the signal $a[n]$.

Figures 24-29 show surface and contour plots of the SCD estimate magnitude for a PAM signal which is modulated by a random sequence of zeros and ones.

From Eq. 44, ones expect to obtain something different from zero just at

cyclic frequencies that are multiple of the bit rate. Figures 24-29 verify the result obtained in Eq. 44. The poor resolution is more obvious in these examples, making it difficult to obtain the appropriate SCD representation for the signal.

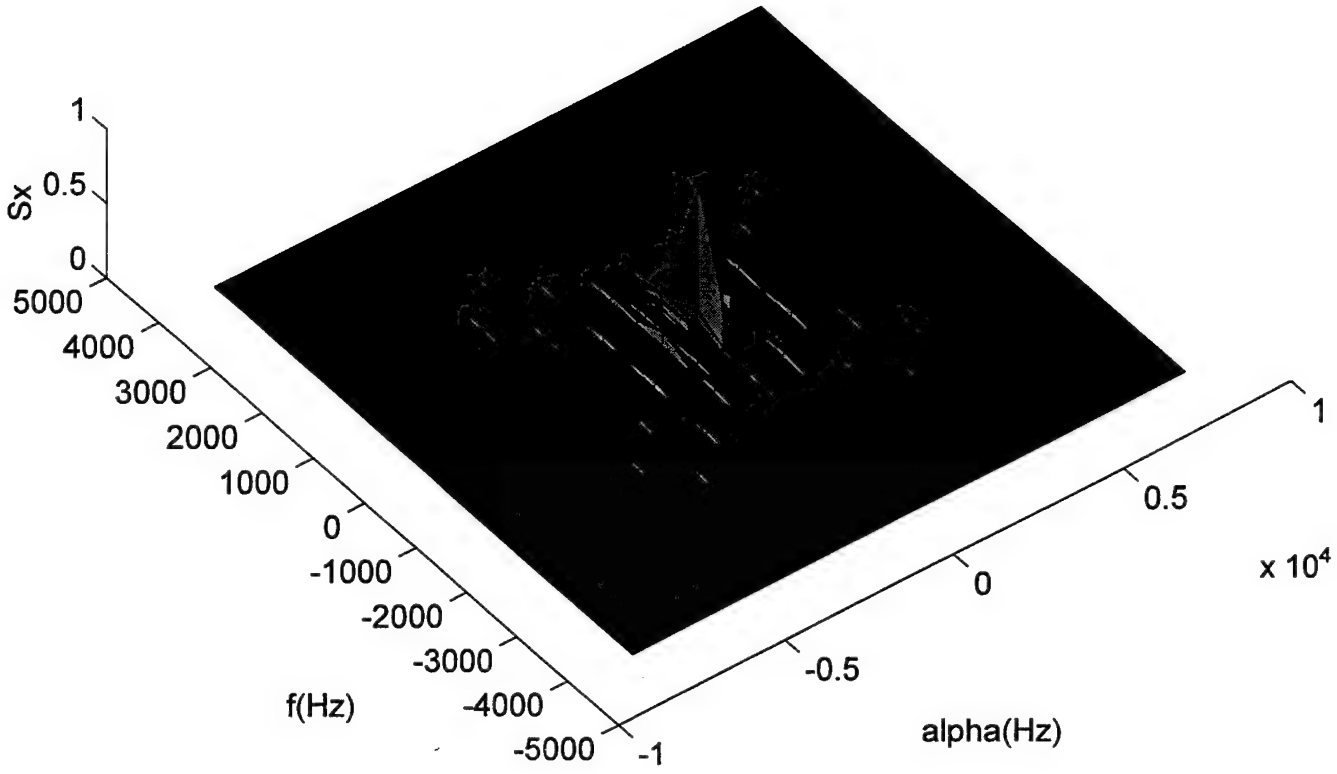

Figure 24 Surface plot of the SCD estimate magnitude for a Pulse-Amplitude Modulated (PAM) Signal, using AUTOFAM, with the following parameters: $\Delta f = 512Hz$, $\Delta\alpha = 16Hz$, $r_b = 1024Hz$, and $f_s = 8192Hz$, where r_b is the bit rate, and f_s is the sampling frequency.

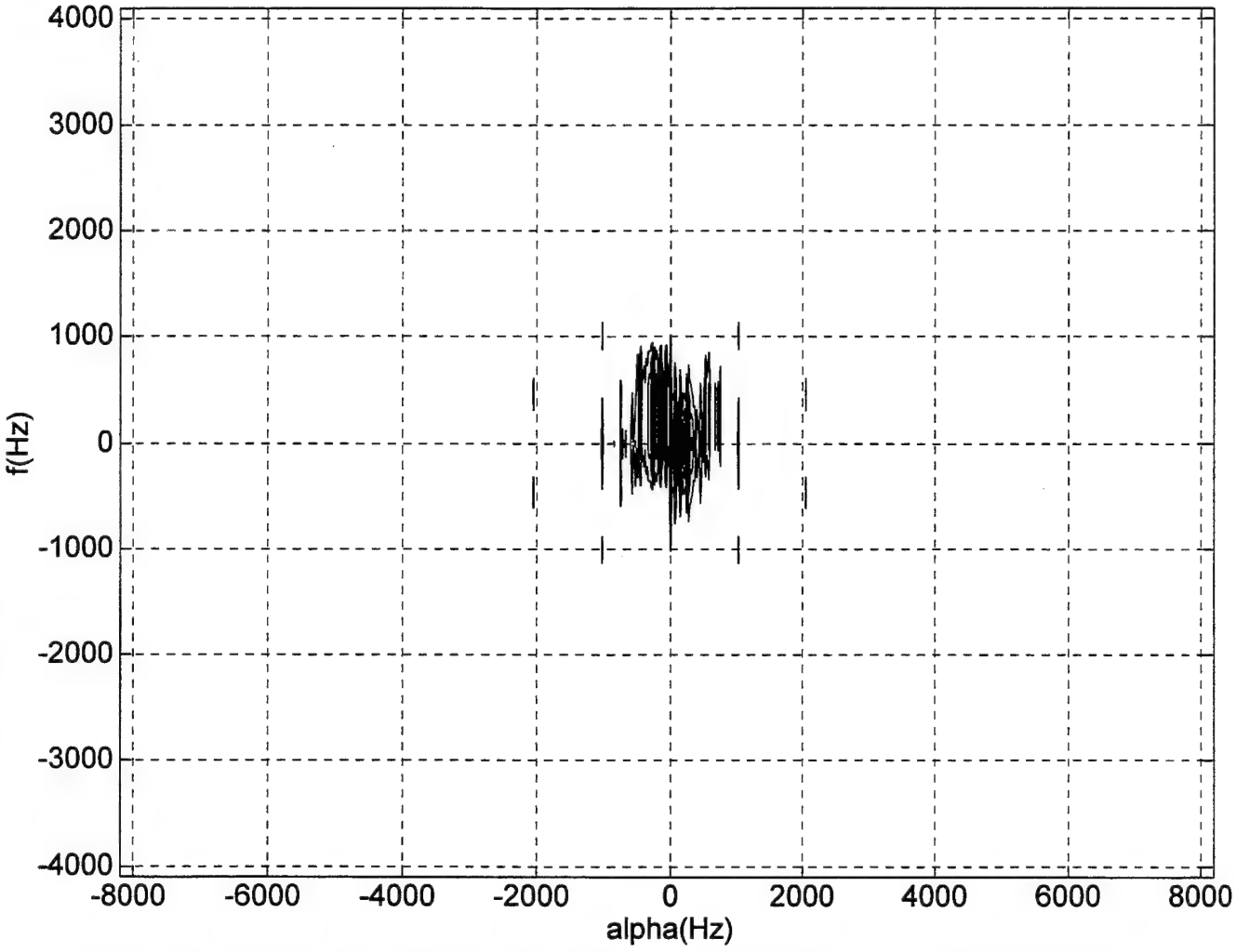

Figure 25 Contour plot of the SCD estimate magnitude for a Pulse-Amplitude Modulated (PAM) Signal, using AUTOFAM, with the following parameters: $\Delta f = 512Hz$, $\Delta\alpha = 16Hz$, $r_b = 1024Hz$, and $f_s = 8192Hz$, where r_b is the bit rate, and f_s is the sampling frequency.

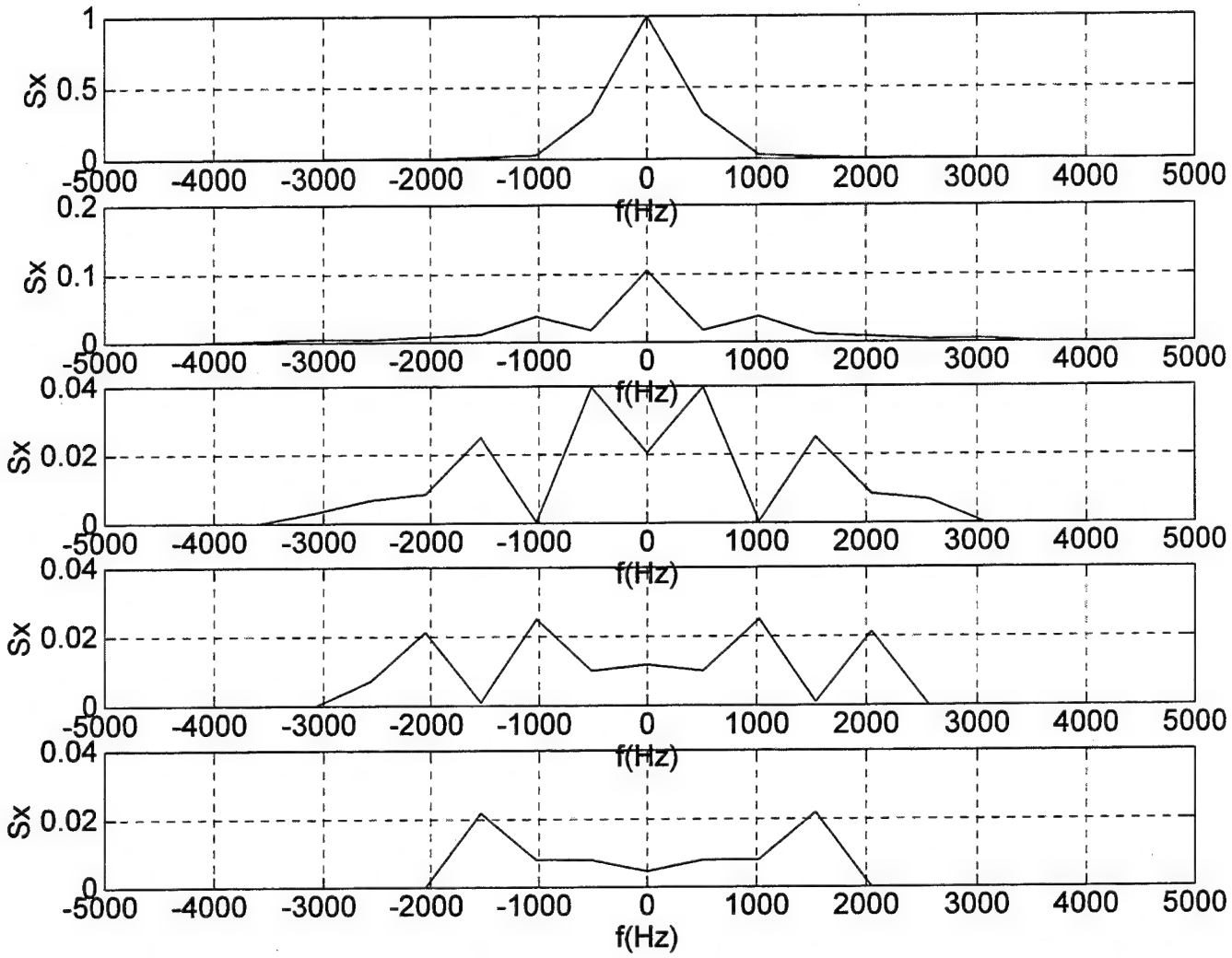

Figure 26 Plots of the SCD estimate magnitude for a Pulse-Amplitude Modulated (PAM) Signal, using AUTOFAM, for $\alpha = 0$, $\alpha = 1024Hz$, $\alpha = 2048Hz$, $\alpha = 3072Hz$, and $\alpha = 4096Hz$, respectively, with the following parameters: $\Delta f = 512Hz$, $\Delta\alpha = 16Hz$, $r_b = 1024Hz$, and $f_s = 8192Hz$, where r_b is the bit rate, and f_s is the sampling frequency.

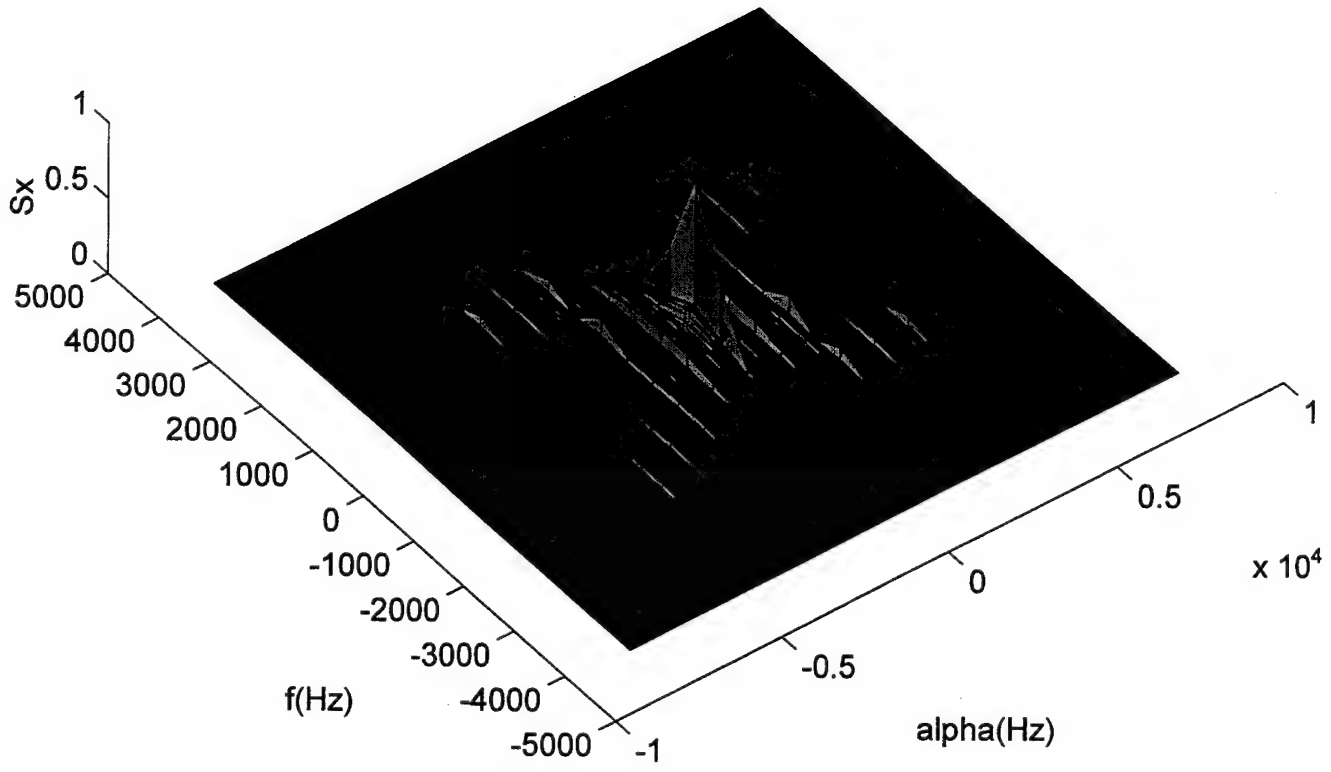

Figure 27 Surface plot of the SCD estimate magnitude for a Pulse-Amplitude Modulated (PAM) Signal, using AUTOSSCA, with the following parameters: $\Delta f = 512Hz$, $\Delta\alpha = 16Hz$, $r_b = 1024Hz$, and $f_s = 8192Hz$, where r_b is the bit rate, and f_s is the sampling frequency.

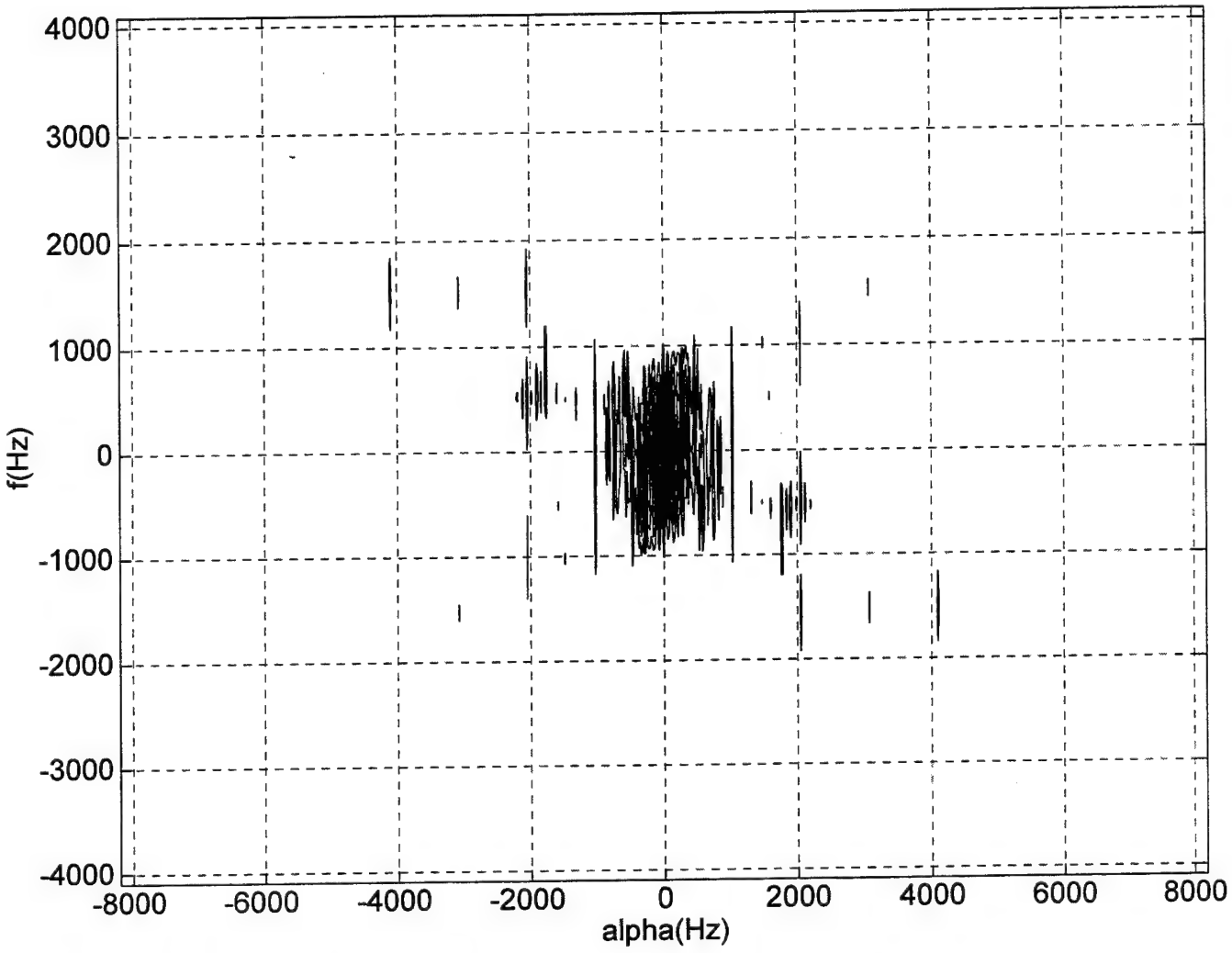

Figure 28 Contour plot of the SCD estimate magnitude for a Pulse-Amplitude Modulated (PAM) Signal, using AUTOSSCA, with the following parameters: $\Delta f = 512Hz$, $\Delta\alpha = 16Hz$, $r_b = 1024Hz$, and $f_s = 8192Hz$, where r_b is the bit rate, and f_s is the sampling frequency.

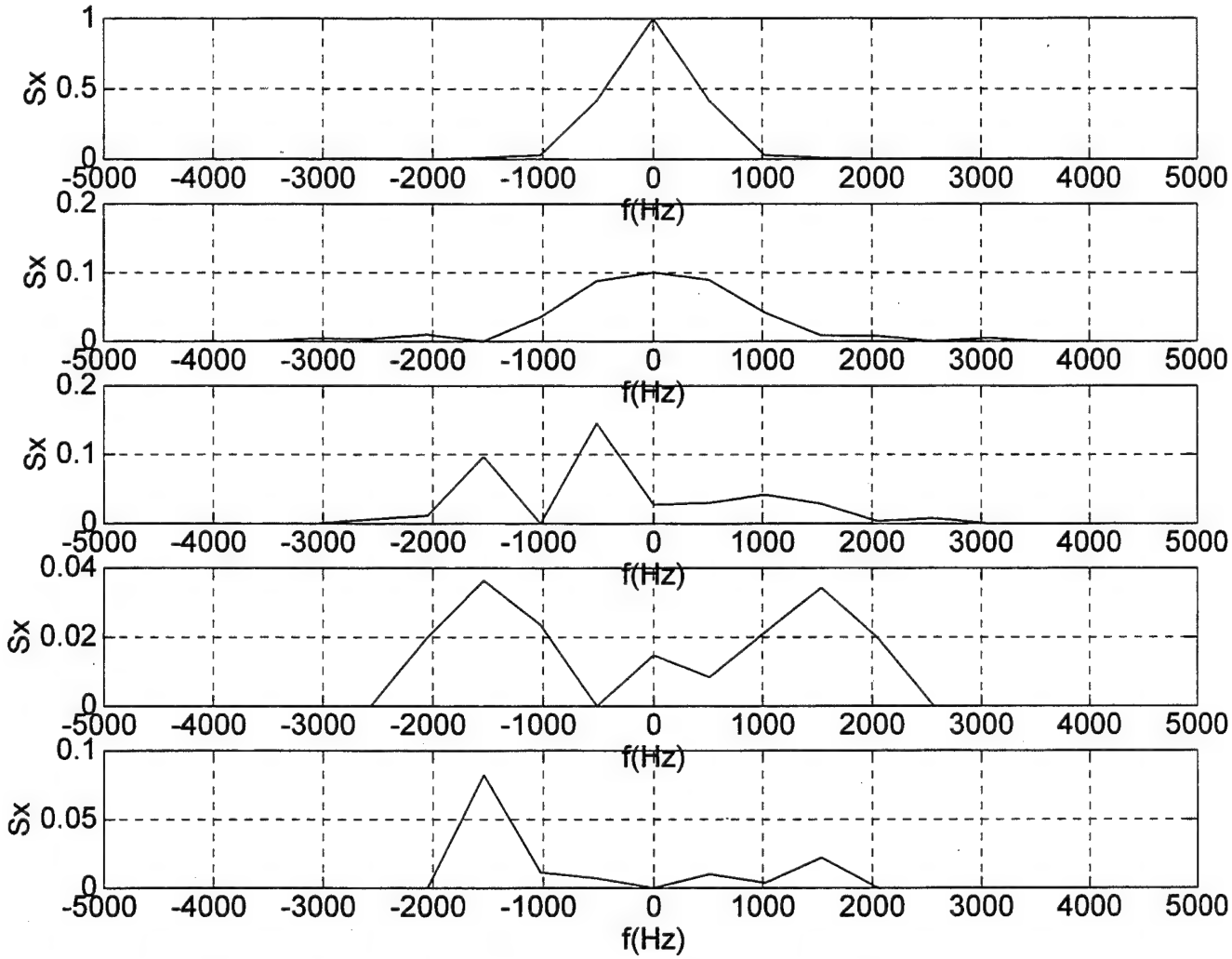

Figure 29 Plots of the SCD estimate magnitude for a Pulse-Amplitude Modulated (PAM) Signal, using AUTOSSCA, for $\alpha = 0$, $\alpha = 1024Hz$, $\alpha = 2048Hz$, $\alpha = 3072Hz$, and $\alpha = 4096Hz$, respectively, with the following parameters: $\Delta f = 512Hz$, $\Delta\alpha = 16Hz$, $r_b = 1024Hz$, and $f_s = 8192Hz$, where r_b is the bit rate, and f_s is the sampling frequency.

B. DIGITAL MODULATED SIGNALS

1. Amplitude Shift Keying (ASK) Signal

An ASK signal is simply an AM signal

$$x[n] = a[n]\cos\left(2\pi\frac{f_o}{f_s}n + \phi_o\right), \tag{45}$$

in which the amplitude message $a[n]$ is a M-ary PAM signal

$$a[n] = \sum_{k=-\infty}^{\infty} a_k\, q\left(n - kN_o - n_o\right). \tag{46}$$

The spectral correlation density function for this ASK signal is given by

$$\begin{aligned} S_x^\alpha(f) = \frac{1}{4N_o}\Bigg\{\Bigg[& Q\left(f + f_o + \frac{\alpha}{2}\right) Q^*\left(f + f_o - \frac{\alpha}{2}\right) S_a^\alpha\left(f + f_o\right) \\ & + Q\left(f - f_o + \frac{\alpha}{2}\right) Q^*\left(f - f_o - \frac{\alpha}{2}\right) S_a^\alpha\left(f - f_o\right)\Bigg] e^{-i2\pi\alpha n_o} \\ & + Q\left(f + \frac{\alpha}{2} + f_o\right) Q^*\left(f - \frac{\alpha}{2} - f_o\right) S_a^{\alpha+2f_o}(f)\, e^{-i\left[2\pi(\alpha+2f_o)n_o + 2\phi_o\right]} \\ & + Q\left(f + \frac{\alpha}{2} - f_o\right) Q^*\left(f - \frac{\alpha}{2} + f_o\right) S_a^{\alpha-2f_o}(f)\, e^{-i\left[2\pi(\alpha-2f_o)n_o - 2\phi_o\right]}\Bigg\}. \end{aligned} \tag{47}$$

For a full-duty cycle rectangle pulse, $q[n]$ is given by

$$q[n] = \begin{cases} 1, & |n| \le N_o/2 \\ 0, & |n| > N_o/2 \end{cases}. \tag{48}$$

Its Fourier transform is given by

$$Q(f) = \frac{\sin(\pi f N_o)}{\pi f}. \tag{49}$$

Details on this result can be found in Reference 9.

Figures 30-41 present the outputs from AUTOFAM and AUTOSSCA for some ASK signals. Figures 30-35 present the results for an ASK signal with bit rate $r_b = 2048Hz$, and Figures 36-41 present the results for the same signal with $r_b = 1024Hz$. As $f_o = 2048Hz$, from Eq. 47, ones expect to obtain a representation which is a combination of four PAM signals centered at $f = \pm f_o = \pm 2048Hz$, for $\alpha = 0$, and at $f = 0$, for $\alpha = \pm 2f_o = \pm 4096Hz$. The results obtained in Figures 30-41 confirm that expectation.

2. Binary-Phase Shift Keying (BPSK) Signal

A phase-shift keying (PSK) signal is just a phase-modulated (PM) carrier

$$x[n] = \cos\left(2\pi \frac{f_o}{f_s} n + \phi[n]\right) \tag{50}$$

in which the phase $\phi[n]$ is a M-ary PAM signal

$$\phi[n] = \sum_{m=-\infty}^{\infty} a[mN_o] q[n - mN_o]. \tag{51}$$

Hence, the cyclic spectra for the BPSK signal, $x[n]$, is given by Eq. 47, already computed for a M-ary ASK signal. Of course, the results are the same as for the M-ary ASK signal and are given by Figures 30-41.

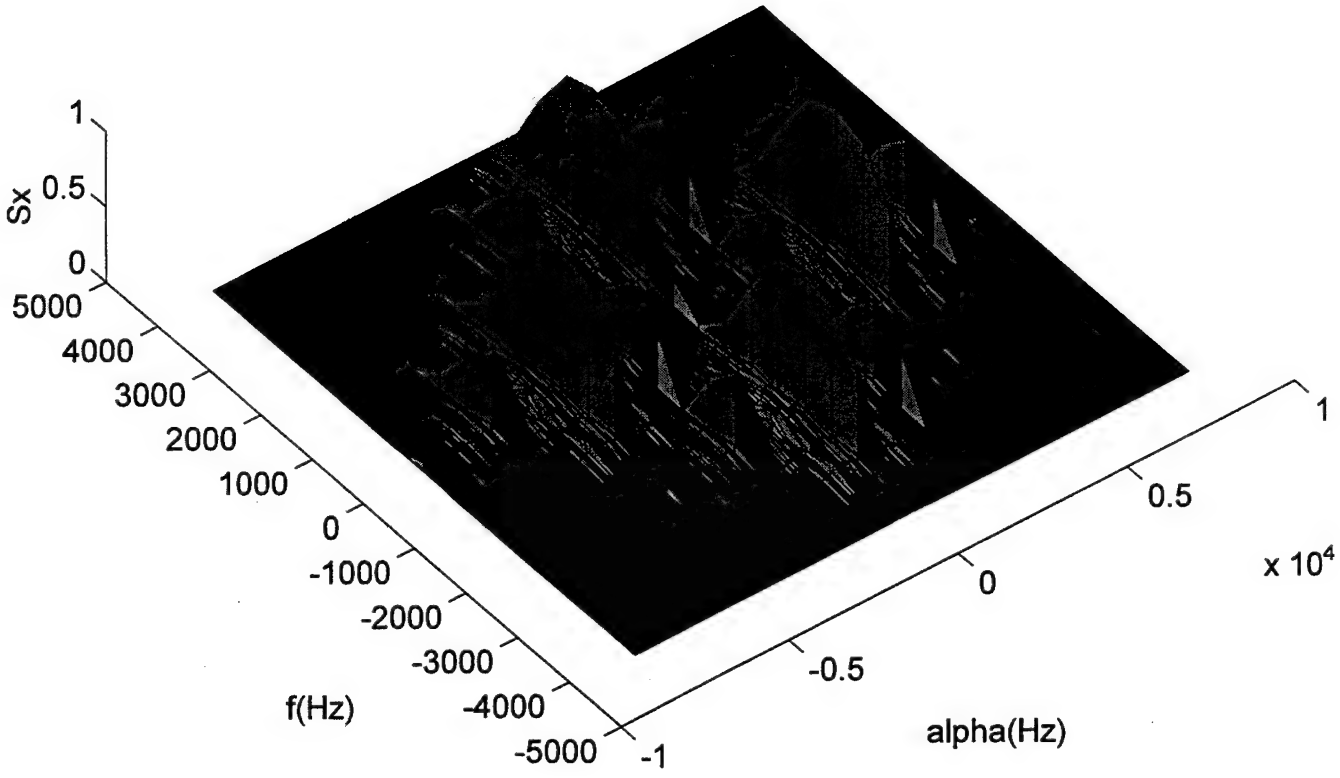

Figure 30 Surface plot of the SCD estimate magnitude for an Amplitude Shift Keying (ASK) or a Binary Phase Shift Keying (BPSK) Signal, using AUTOFAM, with the following parameters: $\Delta f = 512Hz$, $\Delta\alpha = 16Hz$, $f_c = 2048Hz$, $r_b = 2048Hz$, and $f_s = 8192Hz$, where f_c is the carrier frequency, r_b is the bit rate, and f_s is the sampling frequency.

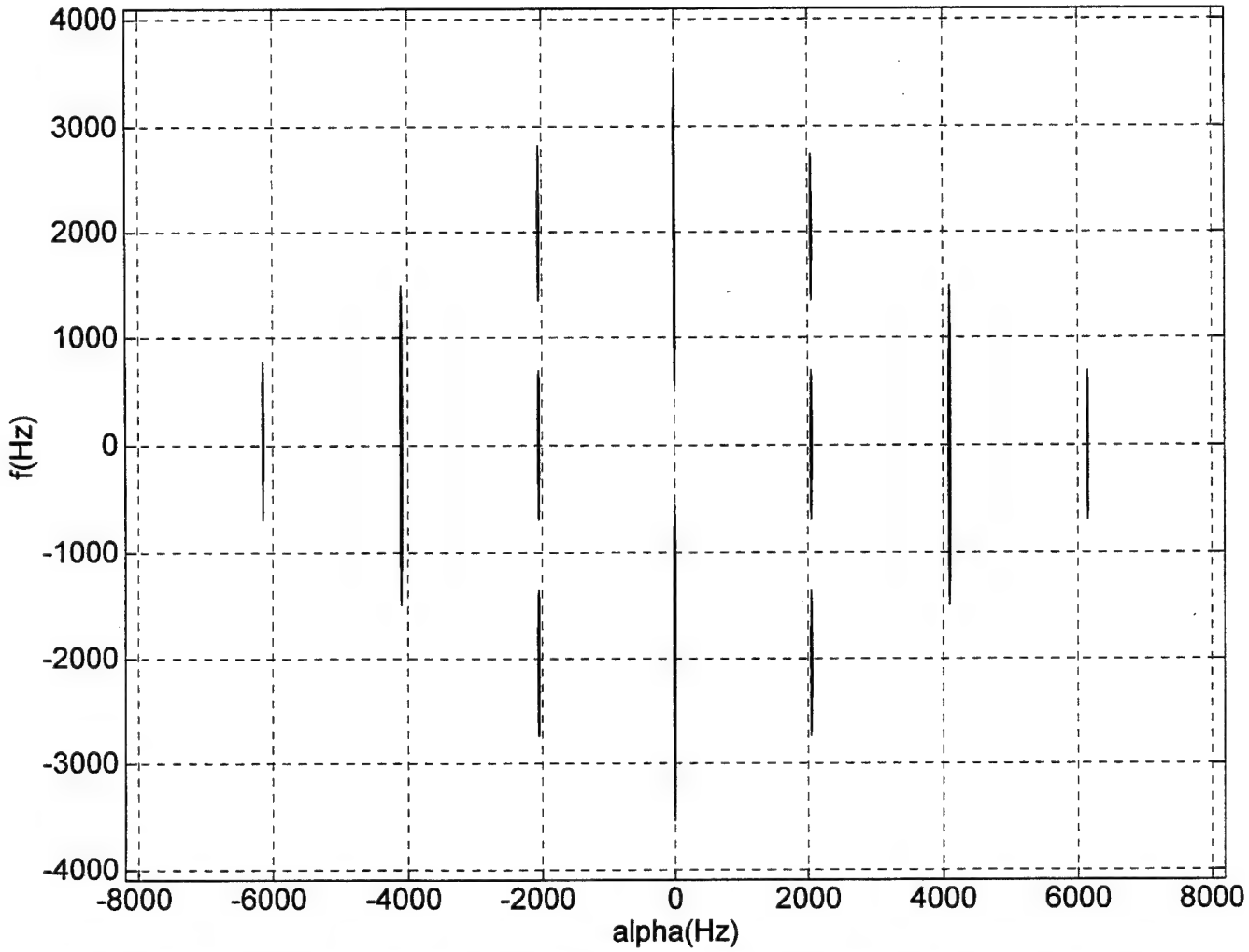

Figure 31 Contour plot of the SCD estimate magnitude for an Amplitude Shift Keying (ASK) or a Binary Phase Shift Keying (BPSK) Signal, using AUTOFAM, with the following parameters: $\Delta f = 512Hz$, $\Delta\alpha = 16Hz$, $f_c = 2048Hz$, $r_b = 2048Hz$, and $f_s = 8192Hz$, where f_c is the carrier frequency, r_b is the bit rate, and f_s is the sampling frequency.

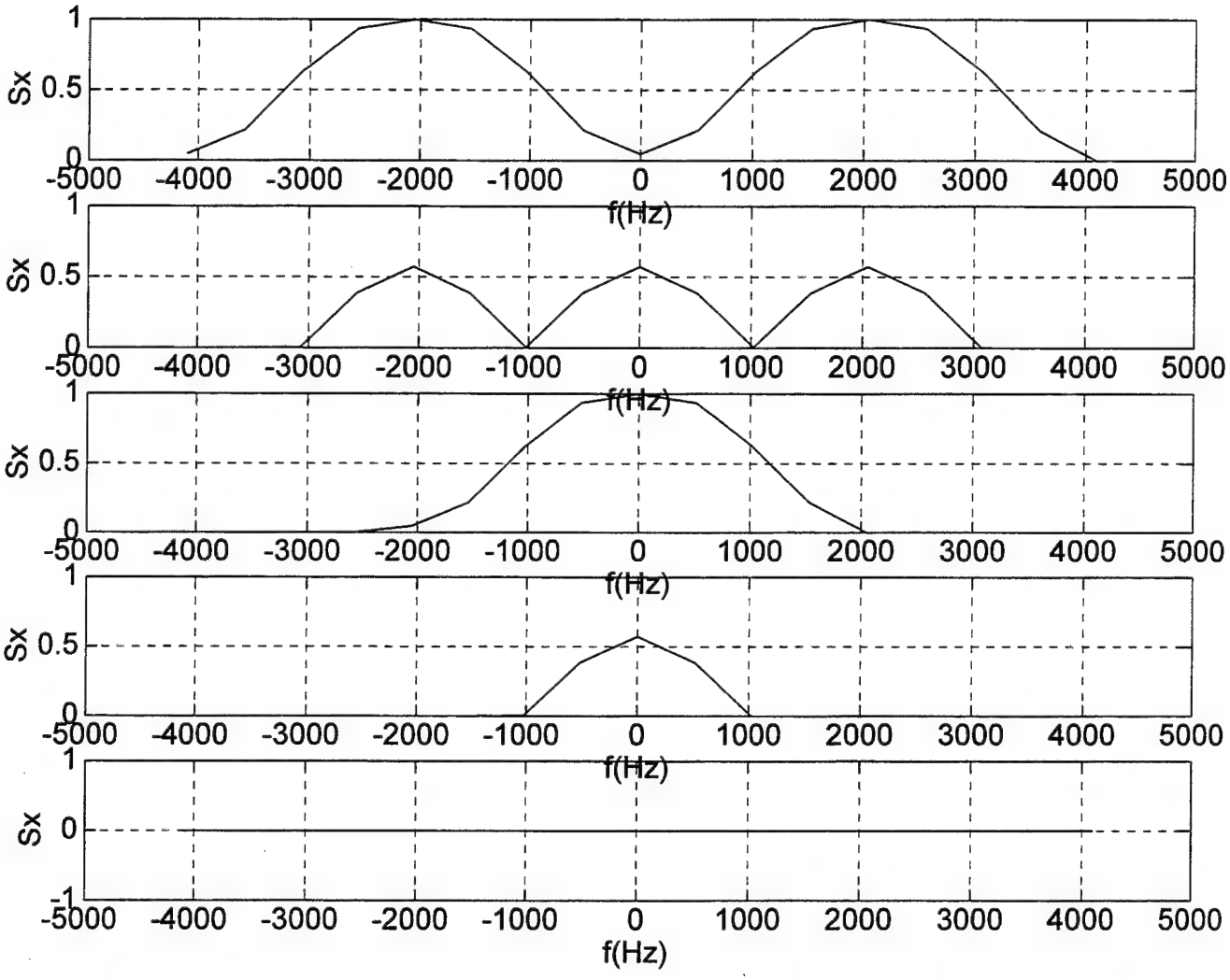

Figure 32 Plots of the SCD estimate magnitude for an Amplitude Shift Keying (ASK) or a Binary Phase Shift Keying (BPSK) Signal, using AUTOFAM, for $\alpha = 0$, $\alpha = 2048Hz$, $\alpha = 4096Hz$, and $\alpha = 6144Hz$, respectively, with the following parameters: $\Delta f = 512Hz$, $\Delta\alpha = 16Hz$, $f_c = 2048Hz$, $r_b = 2048Hz$, and $f_s = 8192Hz$, where f_c is the carrier frequency, r_b is the bit rate, and f_s is the sampling frequency.

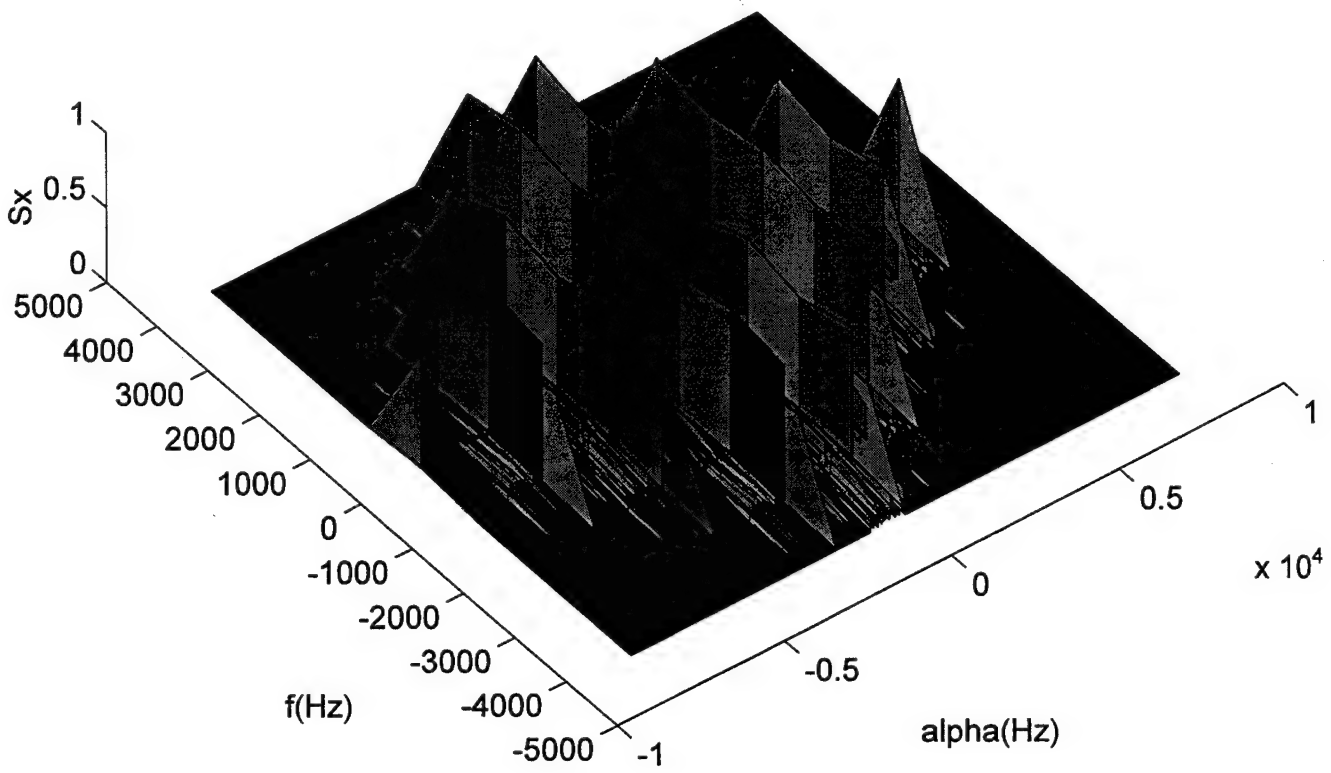

Figure 33 Surface plot of the SCD estimate magnitude for an Amplitude Shift Keying (ASK) or a Binary Phase Shift Keying (BPSK) Signal, using AUTOSSCA, with the following parameters: $\Delta f = 1024Hz$, $\Delta\alpha = 8Hz$, $f_c = 2048Hz$, $r_b = 2048Hz$, and $f_s = 8192Hz$, where f_c is the carrier frequency, r_b is the bit rate, and f_s is the sampling frequency.

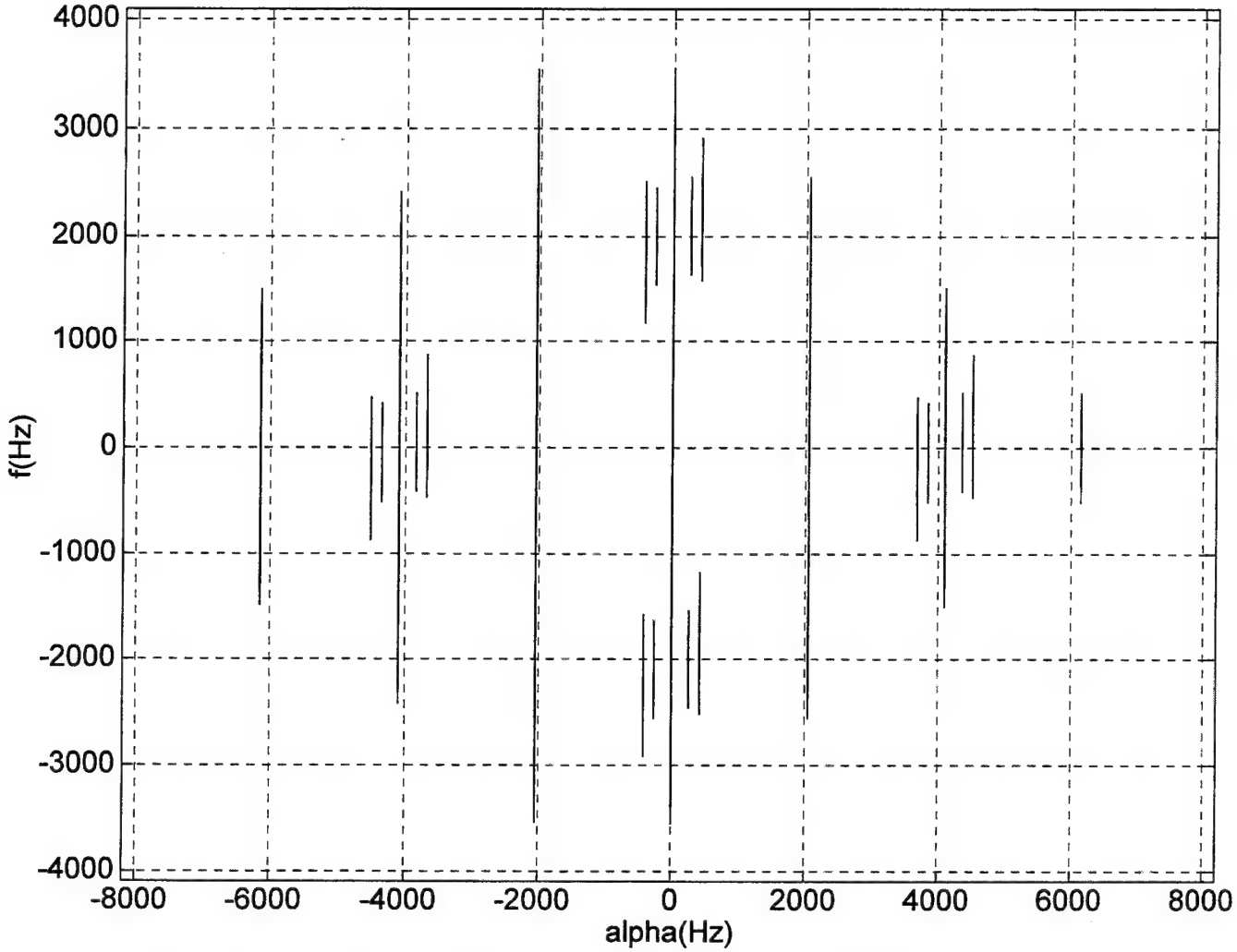

Figure 34 Contour plot of the SCD estimate magnitude for an Amplitude Shift Keying (ASK) or a Binary Phase Shift Keying (BPSK) Signal, using AUTOSSCA, with the following parameters: $\Delta f = 1024Hz$, $\Delta\alpha = 8Hz$, $f_c = 2048Hz$, $r_b = 2048Hz$, and $f_s = 8192Hz$, where f_c is the carrier frequency, r_b is the bit rate, and f_s is the sampling frequency.

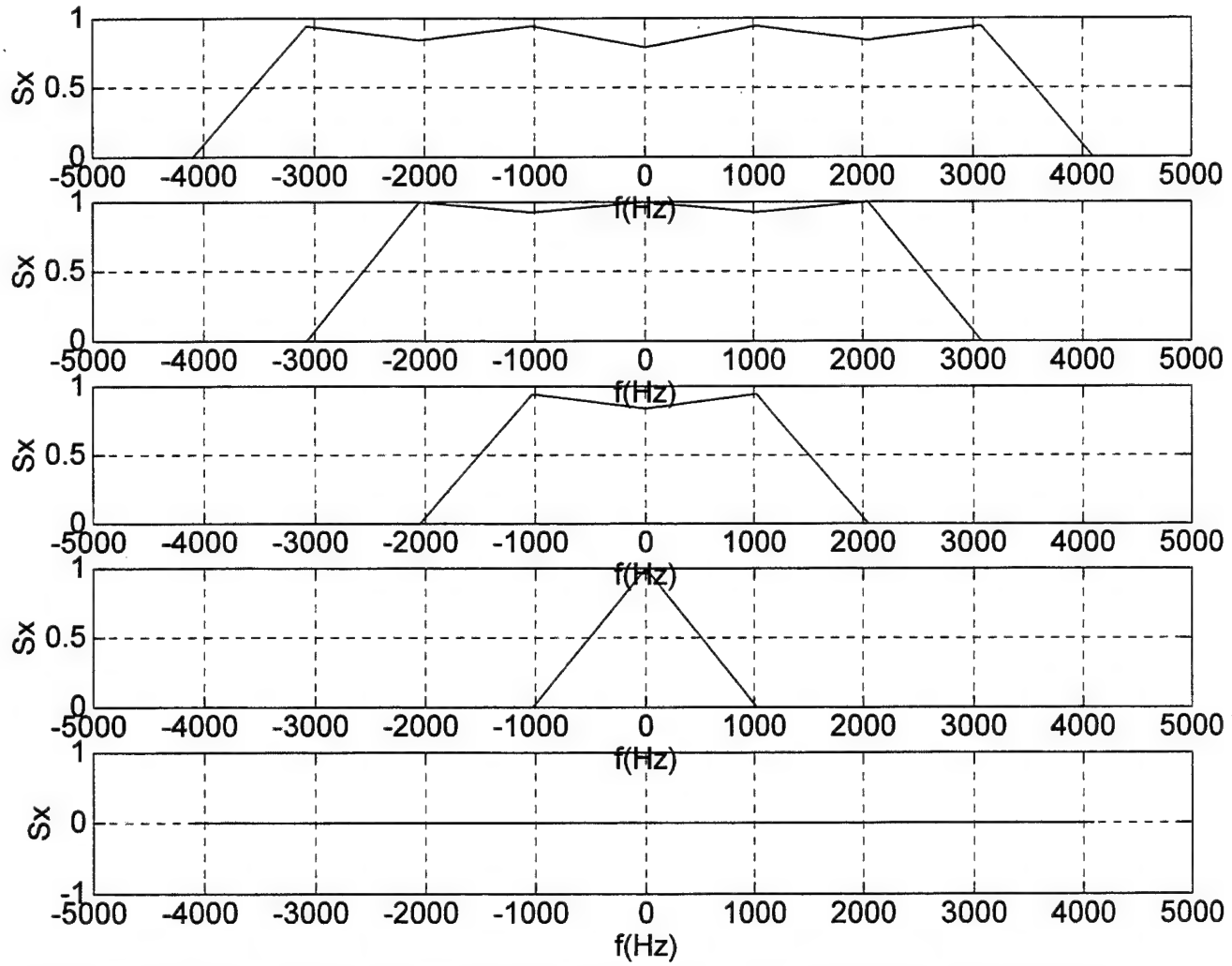

Figure 35 Plots of the SCD estimate magnitude for an Amplitude Shift Keying (ASK) or a Binary Phase Shift Keying (BPSK) Signal, using AUTOSSCA, for $\alpha = 0$, $\alpha = 2048Hz$, $\alpha = 4096Hz$, and $\alpha = 6144Hz$, respectively, with the following parameters: $\Delta f = 1024Hz$, $\Delta\alpha = 8Hz$, $f_c = 2048Hz$, $r_b = 2048Hz$, and $f_s = 8192Hz$, where f_c is the carrier frequency, r_b is the bit rate, and f_s is the sampling frequency.

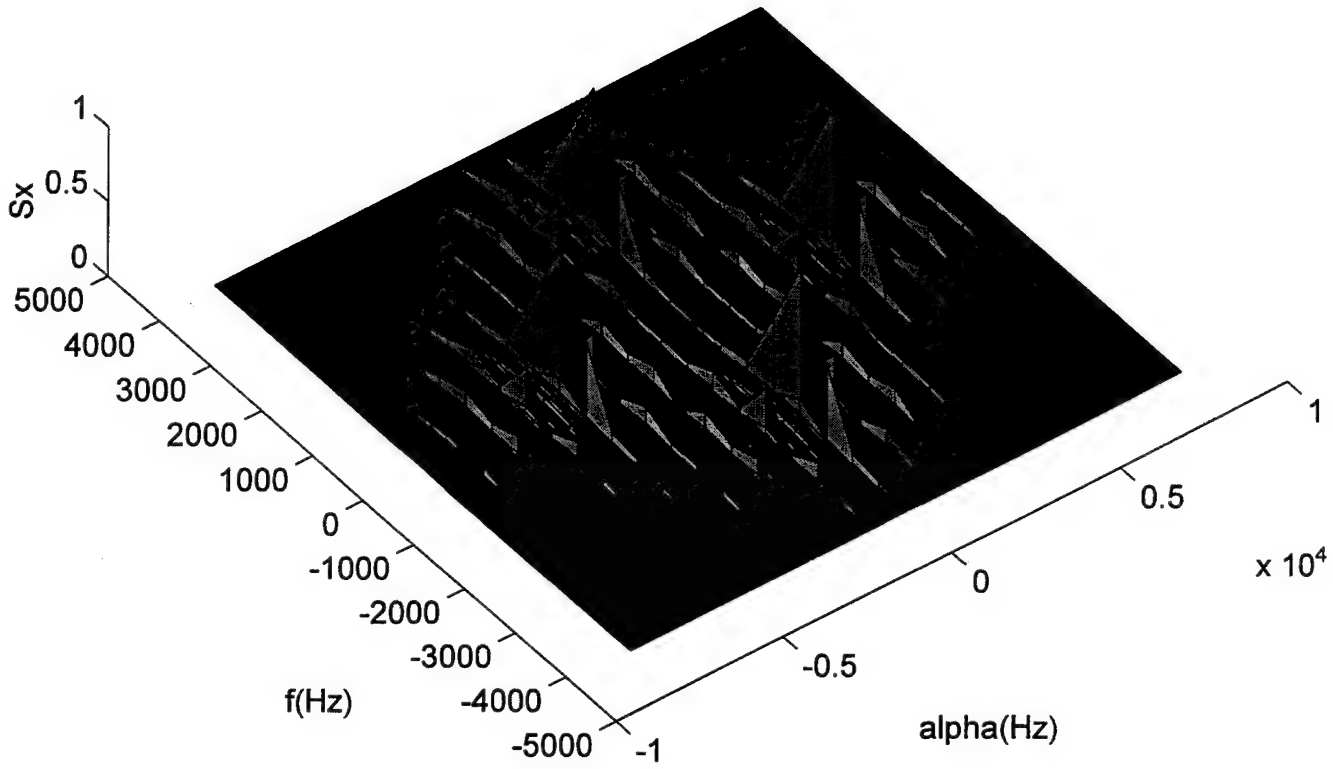

Figure 36 Surface plot of the SCD estimate magnitude for an Amplitude Shift Keying (ASK) or a Binary Phase Shift Keying (BPSK) Signal, using AUTOFAM, with the following parameters: $\Delta f = 512Hz$, $\Delta\alpha = 16Hz$, $f_c = 2048Hz$, $r_b = 1024Hz$, and $f_s = 8192Hz$, where f_c is the carrier frequency, r_b is the bit rate, and f_s is the sampling frequency.

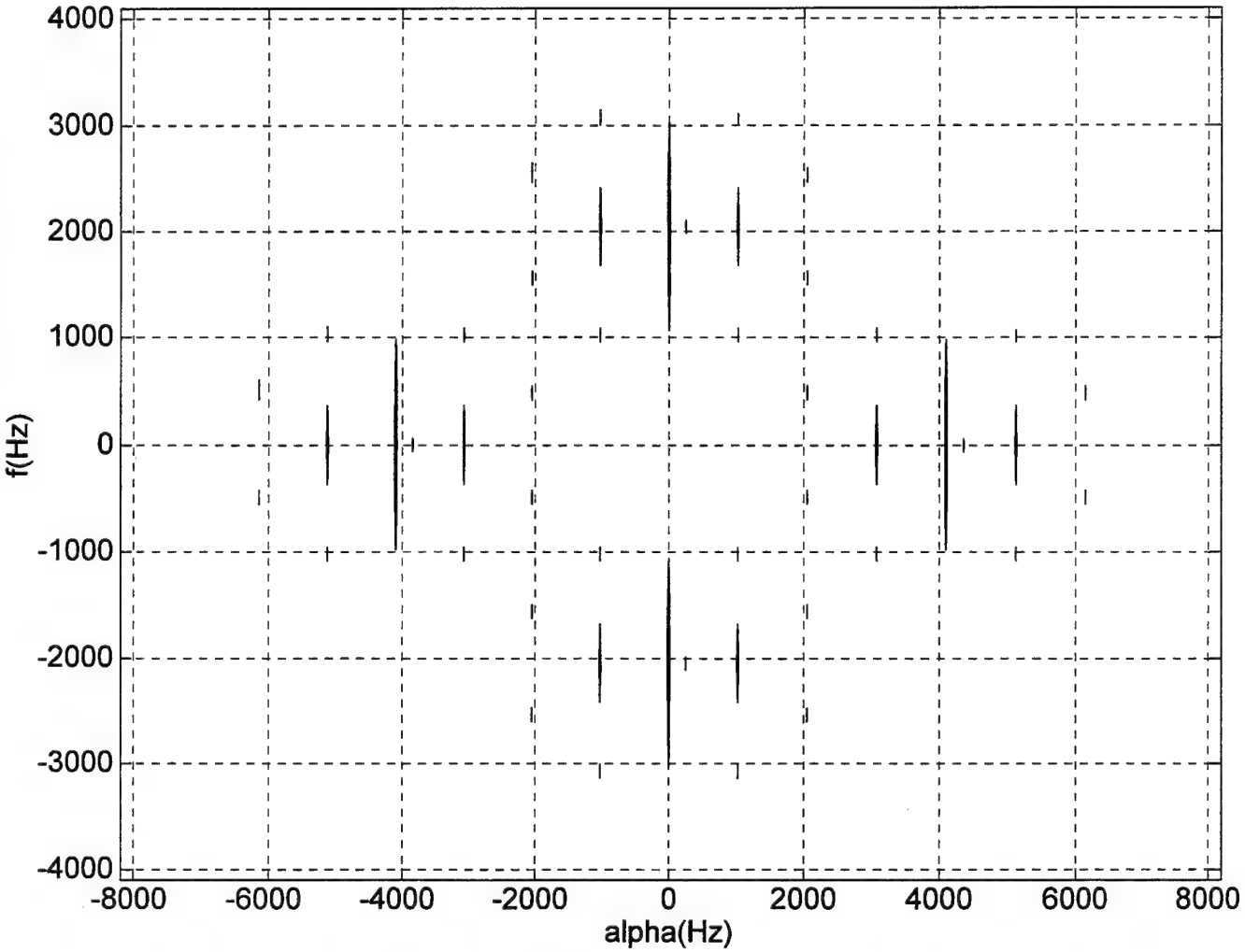

Figure 37 Contour plot of the SCD estimate magnitude for an Amplitude Shift Keying (ASK) or a Binary Phase Shift Keying (BPSK) Signal, using AUTOFAM, with the following parameters: $\Delta f = 512Hz$, $\Delta\alpha = 16Hz$, $f_c = 2048Hz$, $r_b = 1024Hz$, and $f_s = 8192Hz$, where f_c is the carrier frequency, r_b is the bit rate, and f_s is the sampling frequency.

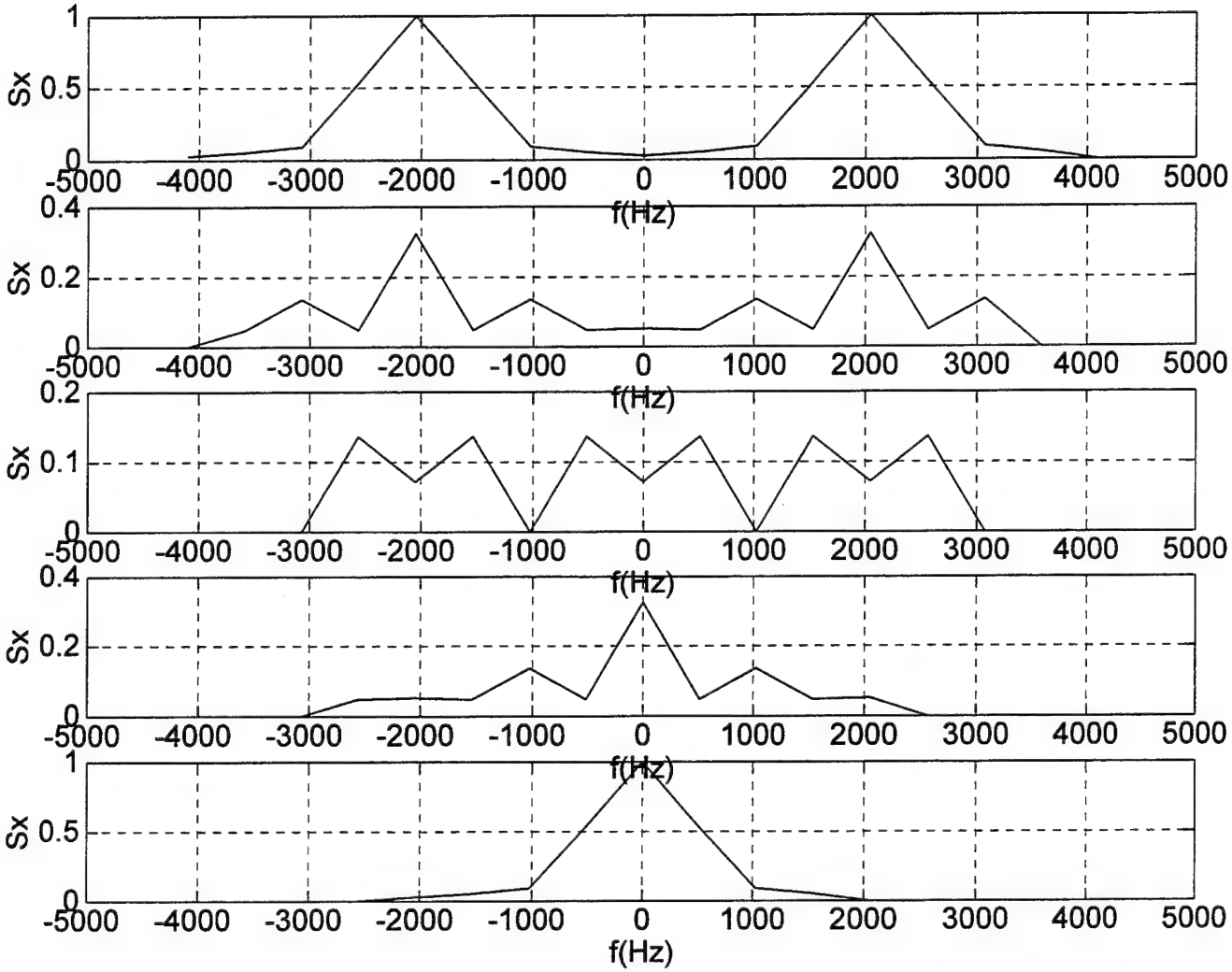

Figure 38 Plots of the SCD estimate magnitude for an Amplitude Shift Keying (ASK) or a Binary Phase Shift Keying (BPSK) Signal, using AUTOFAM, for $\alpha = 0$, $\alpha = 1024Hz$, $\alpha = 2048Hz$, $\alpha = 3072Hz$, and $\alpha = 4096Hz$, respectively, with the following parameters: $\Delta f = 512Hz$, $\Delta\alpha = 16Hz$, $f_c = 2048Hz$, $r_b = 1024Hz$, and $f_s = 8192Hz$, where f_c is the carrier frequency, r_b is the bit rate, and f_s is the sampling frequency.

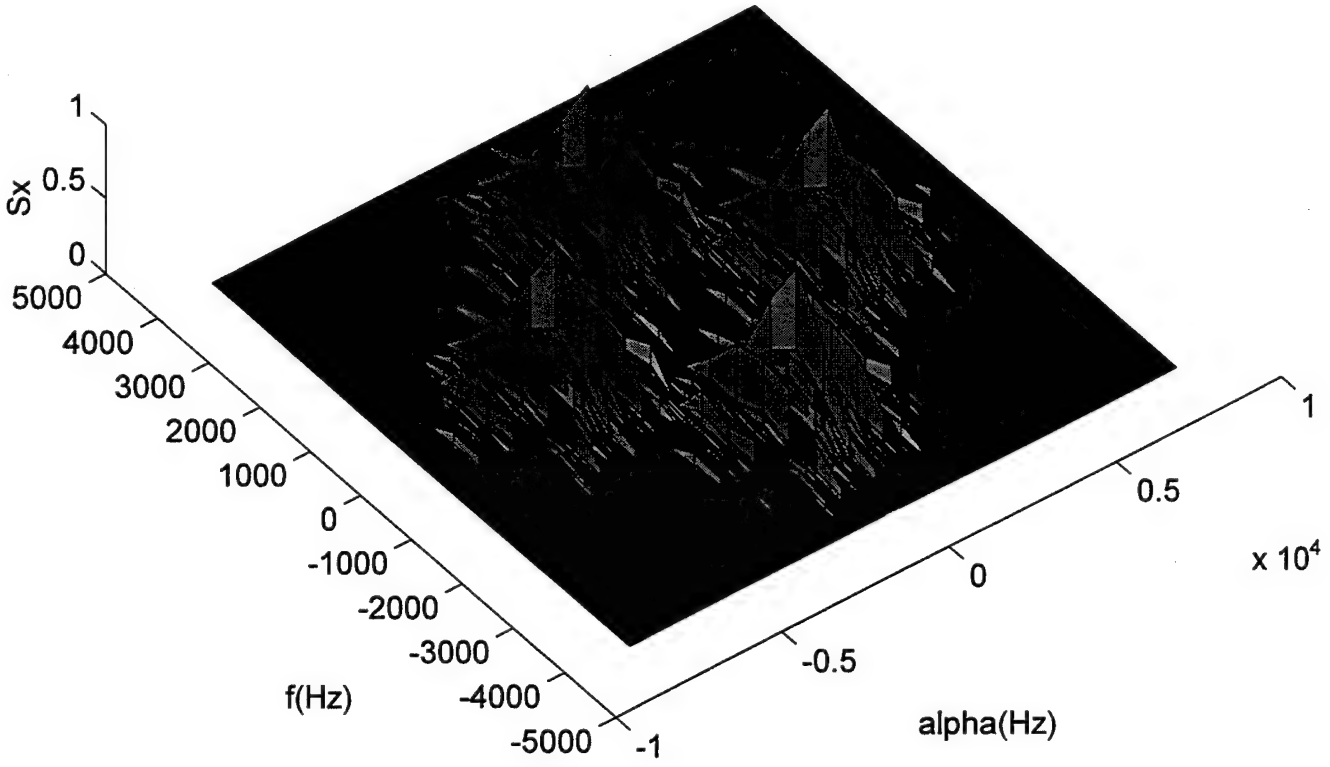

Figure 39 Surface plot of the SCD estimate magnitude for an Amplitude Shift Keying (ASK) or a Binary Phase Shift Keying (BPSK) Signal, using AUTOSSCA, with the following parameters: $\Delta f = 512Hz$, $\Delta\alpha = 16Hz$, $f_c = 2048Hz$, $r_b = 1024Hz$, and $f_s = 8192Hz$, where f_c is the carrier frequency, r_b is the bit rate, and f_s is the sampling frequency.

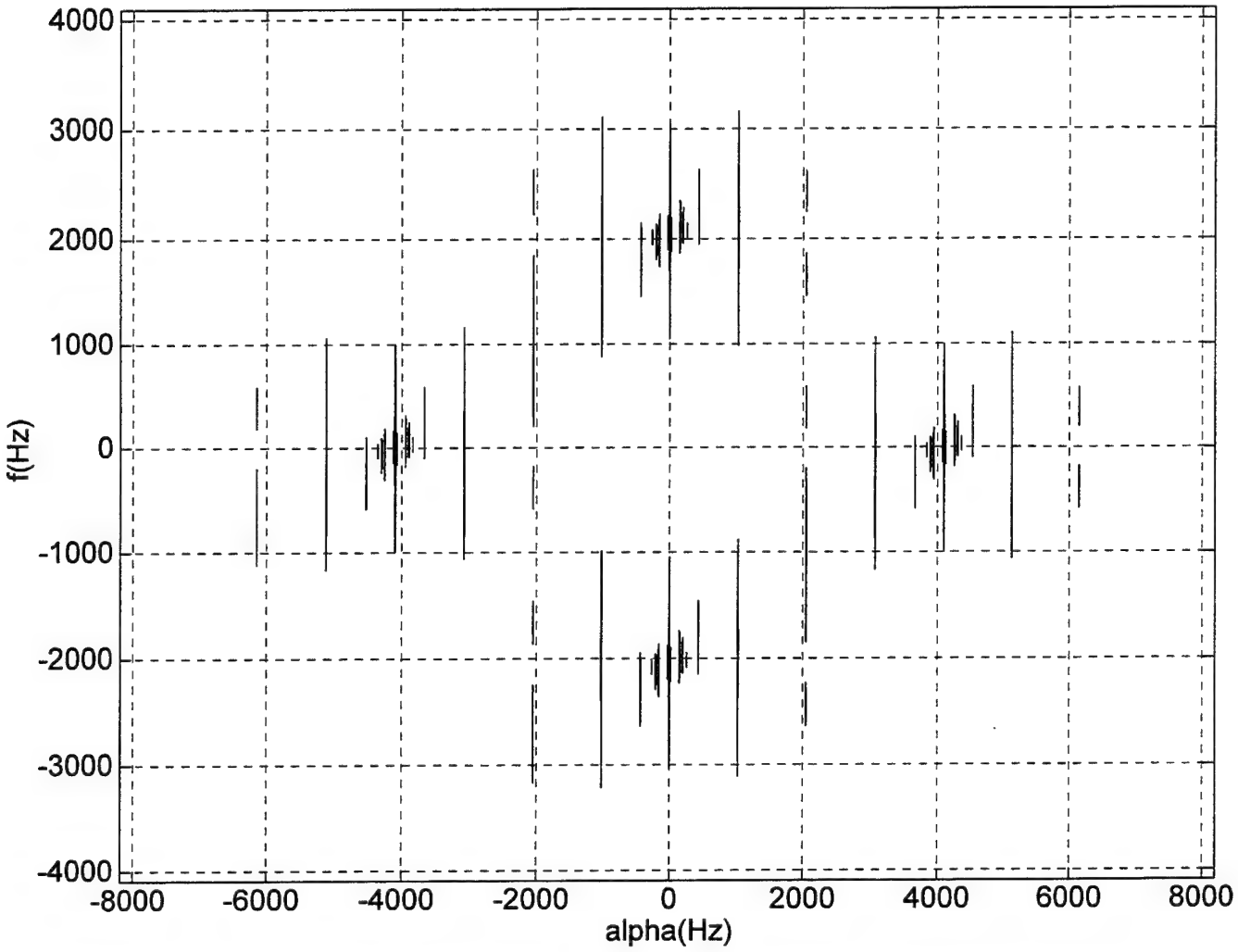

Figure 40 Contour plot of the SCD estimate magnitude for an Amplitude Shift Keying (ASK) or a Binary Phase Shift Keying (BPSK) Signal, using AUTOSSCA, with the following parameters: $\Delta f = 512Hz$, $\Delta\alpha = 4Hz$, $f_c = 2048Hz$, $r_b = 1024Hz$, and $f_s = 8192Hz$, where f_c is the carrier frequency, r_b is the bit rate, and f_s is the sampling frequency.

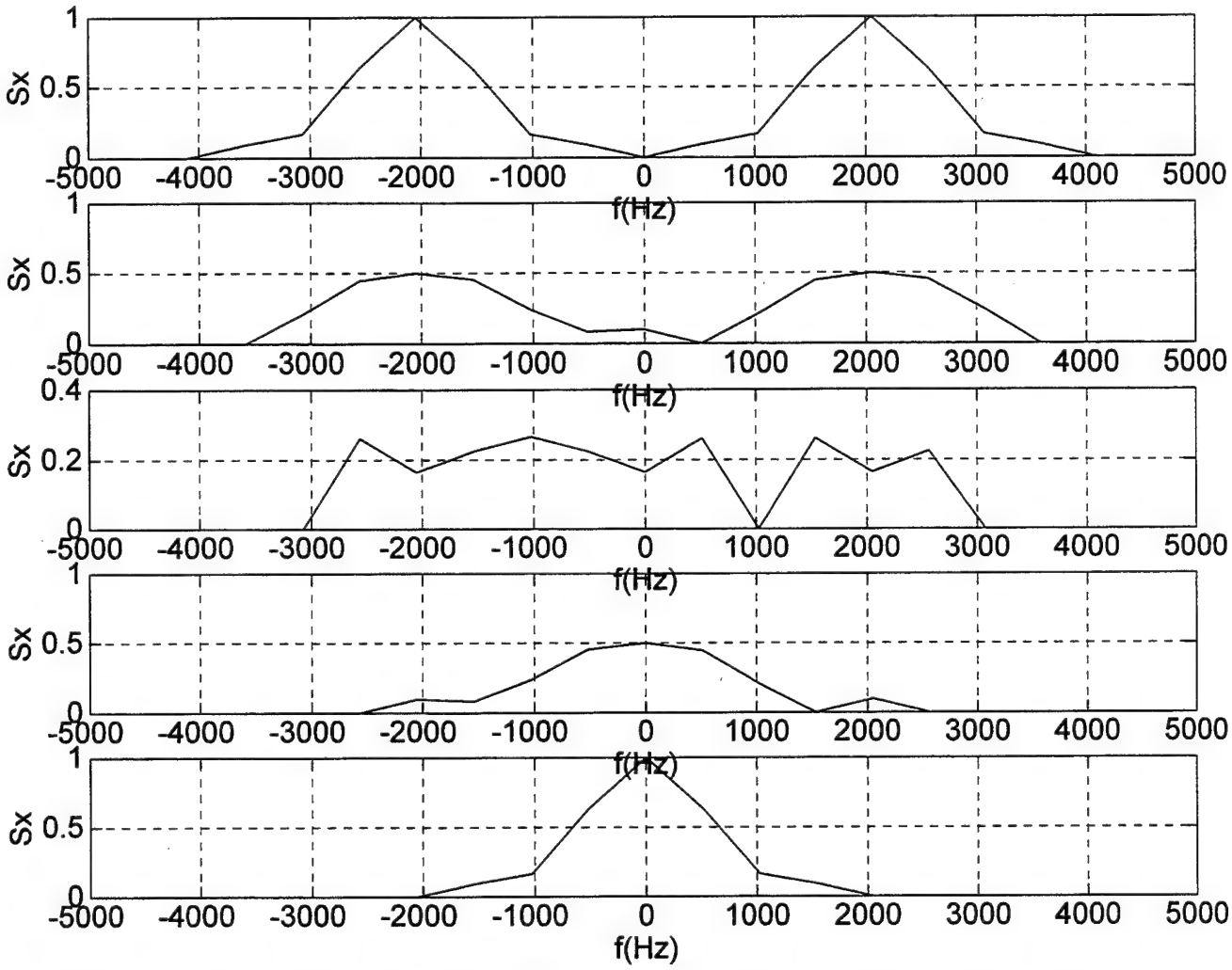

Figure 41 Plots of the SCD estimate magnitude for an Amplitude Shift Keying (ASK) or a Binary Phase Shift Keying (BPSK) Signal, using AUTOSSCA, for $\alpha = 0$, $\alpha = 1024Hz$, $\alpha = 2048Hz$, $\alpha = 3072Hz$, and $\alpha = 4096Hz$, respectively, with the following parameters: $\Delta f = 512Hz$, $\Delta\alpha = 16Hz$, $f_c = 2048Hz$, $r_b = 1024Hz$, and $f_s = 8192Hz$, where f_c is the carrier frequency, r_b is the bit rate, and f_s is the sampling frequency.

VI. CONCLUSIONS

A. SUMMARY

The purpose of this thesis was to implement the FAM and the SSCA methods in MATLAB, allowing students, researchers, and engineers to take advantage of the power of the cyclic analysis methods for solving signal detection and modulation identification problems. Since MATLAB is user friendly and easily portable to other operating systems, the implementation becomes a proving ground, easily modified and set up on other computer systems.

The two methods are implemented as user friendly as possible. The only inputs required for both are the signal(s), the sampling frequency (f_s), that should be the same for both, and the desired resolutions for spectrum frequency (f) and cyclic frequency (α). The results generated by both programs can be displayed in different ways, such as surface plots, contour plots, and cross-section plots.

Both programs generate a large amount of data when a good resolution is desired. As a consequence, limitations in computational as well as printing resources did not allow the presentation of more detailed plots. One can of course easily create averaged spectral correlation surfaces, with a coherent or power averaging method.

B. SUGGESTIONS

A step that was not possible to reach during this work was an analysis and experimentation of the performance of cyclic spectral analysis in a white-noise contaminated environment. A natural extension to this work is an analysis of how well cyclic analysis performs in a white and a colored noise environment such as the one imposed by the ocean to the receiving elements.

Computationally, cyclic spectral analysis is an expensive task. Therefore, any improvements to the speed of existing methods or even completely new fast algorithms are desirable.

During the development of this thesis, it was intended to replace some of the Fast Fourier Transform (FFT) operations by the fast Wavelet Transform. A follow on to this work is the replacement of the FFT operations by Wavelet Transforms, and an evaluation of how well the modified algorithm performs in terms of identification and computational cost.

APPENDIX A. CALCULATION OF THE SCD FUNCTION OF AN AMPLITUDE-MODULATED SIGNAL

Let us consider the amplitude-modulated (AM) signal

$$x[n] = a[n]\cos(2\pi f n), \tag{52}$$

where $a[n]$ is a stationary random lowpass signal with PSD $S_a(f)$, with no spectral lines in its PSD.

The fundamental parameter for second-order periodicity in discrete-time, called *cyclic autocorrelation function* and denoted by $R_x^\alpha[\ell]$, is given by

$$R_x^\alpha[\ell] = \left\langle x[n]\, x^*[n-\ell]\, e^{-i2\pi\alpha n} \right\rangle e^{i\pi\alpha\ell}. \tag{53}$$

We can look at $R_x^\alpha[\ell]$ from the following point of view:

Let $u[n] = x[n]\, e^{-i\pi\alpha n}$ and $v[n] = x[n]\, e^{+i\pi\alpha n}$, then

$$\begin{aligned} R_x^\alpha[\ell] &= \left\langle x[n] e^{-i\pi\alpha n}\; x^*[n-\ell] e^{-i\pi\alpha n}\; e^{i\pi\alpha\ell} \right\rangle \\ &= \left\langle x[n] e^{-i\pi\alpha n}\; x^*[n-\ell] e^{-i\pi\alpha(n-\ell)} \right\rangle \\ &= \left\langle x[n] e^{-i\pi\alpha n}\; \left\{ x[n-\ell] e^{i\pi\alpha(n-\ell)} \right\}^* \right\rangle \\ &= \left\langle u[n]\, v^*[n-\ell] \right\rangle \\ &= R_{uv}[\ell] \end{aligned} \tag{54}$$

But, since $u[n] = x[n]\, e^{-i\pi\alpha n}$,

$$R_u[\ell] = \langle u[n]\, u^*[n-\ell] \rangle$$

$$= \langle x[n] e^{-i\pi\alpha n}\, x^*[n-\ell] e^{i\pi\alpha(n-\ell)} \rangle$$

$$= \langle x[n]\, x^*[n-\ell] \rangle\, e^{-i\pi\alpha\ell}$$

$$= R_x[\ell]\, e^{-i\pi\alpha\ell}$$

$$= R_x[\ell] e^{-i2\pi\left(\frac{\alpha}{2}\right)\ell} \tag{55}$$

and taking the Fourier transform leads to

$$S_u(f) = S_x(f) \otimes \delta\left(f + \frac{\alpha}{2}\right) = S_x\left(f + \frac{\alpha}{2}\right). \tag{56}$$

Similarly, if $v[n] = x[n]\, e^{i\pi\alpha n}$, then

$$R_v[\ell] = R_x[\ell] e^{i2\pi\left(\frac{\alpha}{2}\right)\ell}, \tag{57}$$

and

$$S_v(f) = S_x\left(f - \frac{\alpha}{2}\right). \tag{58}$$

Thus, we can redefine the second-order periodicity, by saying that $x[n]$ exhibits second-order periodicity if and only if frequency translates (frequency-shifted versions) of $x[n]$ are correlated with each other.

As long as the mean values of the frequency translates $u[n]$ and $v[n]$ are zero (i. e., $\langle u[n] \rangle = 0$ and $\langle v[n] \rangle = 0$), $x[n]$ does not contain finite-amplitude

additive sine-wave components at $\pm\alpha/2$ and therefore $S_x(f)$ has no spectral lines at $f=\pm\alpha/2$. The crosscorrelation $R_{uv}[\ell]$ is actually a temporal crosscovariance $K_{uv}[\ell]$, that is,

$$K_{uv}[\ell]=\left\langle\left\{u[n]-\langle u[n]\rangle\right\}\left\{v[n-\ell]-\langle v[n-\ell]\rangle\right\}^*\right\rangle$$

$$=\left\langle u[n]\,v^*[n-\ell]\right\rangle$$

$$=R_{uv}[\ell]\,. \tag{59}$$

Based on this, we can define a *temporal correlation coefficient,* the magnitude of which is upper bounded by unity, for frequency translates since

$$\gamma_x^{\alpha}[\ell]=\frac{R_x^{\alpha}[\ell]}{R_x[0]}=\frac{K_{uv}[\ell]}{\left(K_u[0]K_v[0]\right)^{1/2}}\,. \tag{60}$$

Since $a[n]$ is a real stationary random ($R_a^{\alpha}[\ell]\equiv 0$, for all $\alpha\neq 0$) signal with zero mean (i. e., $\langle a[n]\rangle=0$), the cyclic autocorrelation function of $x[n]$ is given by

$$R_x^{\alpha}[\ell]=\left\langle x[n]\,x^*[n-\ell]\,e^{-i2\pi\alpha n}\right\rangle e^{i\pi\alpha\ell}$$

$$=\left\langle a[n]\cos\left(2\pi f_o n+\theta\right)a^*[n-\ell]\cos\left[2\pi f_o(n-\ell)+\theta\right]e^{-i2\pi\alpha n}\right\rangle e^{i\pi\alpha\ell}$$

$$=\left\langle a[n]\,a^*[n-\ell]\frac{1}{2}\left\{\cos\left(2\pi f_o\ell\right)+\cos\left[2\pi f_o(2n-\ell)+2\theta\right]\right\}e^{-i2\pi\alpha n}\right\rangle e^{i\pi\alpha\ell}$$

$$= \frac{1}{2}\cos(2\pi f_o \ell)\left\langle a[n]a^*[n-\ell]e^{-i2\pi\alpha n}\right\rangle e^{i\pi\alpha\ell}$$

$$+ \frac{1}{2}\left\langle a[n]a^*[n-\ell]\cos[2\pi f_o(2n-\ell)+2\theta]e^{-i2\pi\alpha n}\right\rangle e^{i\pi\alpha\ell}$$

$$= \frac{1}{2}\cos(2\pi f_o \ell)\, R_a^\alpha[\ell] + \frac{1}{2}\left\langle a[n]a^*[n-\ell]\frac{e^{i[2\pi f_o(2n-\ell)+2\theta]} + e^{-i[2\pi f_o(2n-\ell)+2\theta]}}{2} e^{-i2\pi\alpha n}\right\rangle e^{i\pi\alpha\ell}$$

$$= \frac{1}{2}R_a^\alpha[\ell]\cos(2\pi f_o \ell) + \frac{1}{4}e^{i2\theta}\left\langle a[n]a^*[n-\ell]e^{-i2\pi(\alpha-2f_o)n}\right\rangle e^{i\pi(\alpha-2f_o)\ell}$$

$$+ \frac{1}{4}e^{-i2\theta}\left\langle a[n]a^*[n-\ell]e^{-i2\pi(\alpha+2f_o)n}\right\rangle e^{i\pi(\alpha+2f_o)\ell}$$

$$= \frac{1}{2}R_a^\alpha[\ell]\cos(2\pi f_o \ell) + \frac{1}{4}e^{i2\theta}\, R_a^{\alpha-2f_o}[\ell] + \frac{1}{4}e^{-i2\theta}\, R_a^{\alpha+2f_o}[\ell].$$

(61)

But since $a[n]$ is a stationary signal (i. e., $R_a^\alpha[\ell] \equiv 0$ for all $\alpha \neq 0$), the only non-zero contributions are at $\alpha = 0$ and $\alpha = \pm 2f_o$. Thus, the cyclic autocorrelation function becomes

$$R_x^\alpha[\ell] = \begin{cases} \frac{1}{4}e^{\pm i2\theta}R_a[\ell], & \alpha = 2f_o \\ \frac{1}{2}R_a[\ell]\cos(2\pi f_o \ell), & \alpha = 0 \\ 0, & otherwise \end{cases} \qquad (62)$$

Defining the temporal correlation coefficient as

$$\delta_x^\alpha[\ell] = \frac{R_x^\alpha[\ell]}{R_x[0]}, \tag{63}$$

where $R_x[0] = R_x^\alpha[\ell]$ for $\alpha = 0$, computed at $\ell = 0$, so $R_x[0] = R_a[0]/2$.

So, $\delta_x^\alpha[\ell]$ becomes

$$\delta_x^\alpha[\ell] = \begin{cases} \dfrac{\frac{1}{4}e^{\pm i2\theta}R_a[\ell]}{\frac{1}{2}R_a[0]} = \frac{1}{2}e^{\pm i2\theta}\delta_a[\ell], & \alpha = \pm 2f_o \\ \dfrac{\frac{1}{2}R_a[\ell]\cos(2\pi f_o \ell)}{\frac{1}{2}R_a[0]} = \delta_a[\ell]\cos(2\pi f_o \ell), & \alpha = 0. \end{cases} \tag{64}$$

Thus, the strength of correlation between $x[n]\,e^{-i\pi\alpha n}$ and $x[n-\ell]\,e^{-i\pi\alpha(n-\ell)}$ is given by

$$\left|\delta_x^\alpha[\ell]\right| = \begin{cases} \frac{1}{2}\left|\delta_a[\ell]\right|, & \alpha = \pm 2f_o \\ \left|\delta_a[\ell]\cos(2\pi f_o \ell)\right|, & \alpha = 0 \\ 0, & \textit{otherwise.} \end{cases} \tag{65}$$

It can be substantial for an amplitude-modulated signal, e.g., $\left|\delta_x^\alpha[0]\right| = 1/2$.

To localize in the frequency domain the average power $\left\langle |x[n]|^2 \right\rangle = R_x[0]$ in a stationary signal $x[n]$, we simply pass the signal $x[n]$ through a set of narrowband bandpass filters and then measure the average power at the output of the filters. In the limit when the bandwidths of these filters approach zero, the corresponding set of measurements of average power, normalized by the

bandwidth, constitute the "power spectral density (PSD) function", given by

$$S_x(f) = \lim_{B\to\infty} \frac{1}{B} \left\langle \left| h_B^f[n] \otimes x[n] \right|^2 \right\rangle, \tag{66}$$

where $h_B^f[n]$ is the discrete-impulse response of a bandpass filter with center frequency f, bandwidth B, and unity gain at the band center.

In a similar fashion, to localize in the frequency domain the correlation $\langle u[n] v^*[n] \rangle = \left\langle |x[n]|^2 e^{-i2\pi\alpha n} \right\rangle \equiv R_x^\alpha[0]$ of frequency-shifted versions $u[n]$ and $v[n]$ of a cyclostationary signal $x[n]$, we pass both of the two frequency translates $u[n]$ and $v[n]$ of $x[n]$ through the same set of bandpass filters. Again, in the limit when the bandwidth of these filters approach zero, the corresponding set of measurements of the temporal correlation of the filtered signals constitute the so called "spectral-correlation density (SCD) function", given by

$$S_x^\alpha(f) = \lim_{B\to 0} \frac{1}{B} \left\langle \left\{ h_B^f[n] \otimes u[n] \right\} \left\{ h_B^f[n] \otimes v[n] \right\}^* \right\rangle, \tag{67}$$

that yields the spectral density of correlation between $u[n]$ and $v[n]$ at frequency f, which is identical to the spectral density of correlation in $x[n]$ at frequencies $f + \alpha/2$ and $f - \alpha/2$.

It's a well known result, called "Wiener relation" as opposed to its probabilistic counterpart called "Wiener-Khinchin relation", that the PSD is equal to the Fourier transform of the autocorrelation function,

$$S_x(f) = \sum_{\ell=-\infty}^{\infty} R_x[\ell] e^{-i2\pi f\ell} . \tag{68}$$

Similarly, the SCD can be obtained by Fourier transforming the "cyclic autocorrelation function",

$$S_x^{\alpha}(f) = \sum_{\ell=-\infty}^{\infty} R_x^{\alpha}[\ell] e^{-i2\pi f\ell} . \tag{69}$$

This result is known as the "cyclic (periodic) Wiener relation".

We observe that since $R_x^{\alpha}[\ell]$ is periodic in α with period two, so is $S_x^{\alpha}(f)$.

$$\begin{aligned} R_x^{\alpha+2}[\ell] &= \left\langle x[n]\, x^*[n-\ell] e^{-i2\pi(\alpha+2)n} \right\rangle e^{i\pi(\alpha+2)\ell} \\ &= \left\langle x[n]\, x^*[n-\ell] e^{-i2\pi\alpha n}\, e^{-i4\pi n} \right\rangle e^{i\pi\alpha\ell}\, e^{i2\pi\ell} , \end{aligned} \tag{70}$$

and, since n and ℓ are integers,

$$e^{-i4\pi n} = e^{i2\pi\ell} = 1 , \tag{71}$$

so,

$$\begin{aligned} R_x^{\alpha+2}[\ell] &= \left\langle x[n]\, x^*[n-\ell] e^{-i2\pi\alpha n} \right\rangle e^{i\pi\alpha\ell} \\ &= R_x^{\alpha}[\ell] . \end{aligned} \tag{72}$$

Thus,

$$S_x^{\alpha+2}(f) = \sum_{\ell=-\infty}^{\infty} R_x^{\alpha+2}[\ell] e^{-i2\pi f\ell}$$

$$= \sum_{\ell=-\infty}^{\infty} R_x^{\alpha}[\ell] e^{-i2\pi f\ell}$$

$$= S_x^{\alpha}(f). \tag{73}$$

Also, since ℓ takes on only integer values, then $S_x^{\alpha}(f)$ is periodic in f with period one

$$S_x^{\alpha}(f+1) = \sum_{\ell=-\infty}^{\infty} R_x^{\alpha}[\ell] e^{-i2\pi(f+1)\ell}$$

$$= \sum_{\ell=-\infty}^{\infty} R_x^{\alpha}[\ell] e^{-i2\pi f\ell}\, e^{-i2\pi\ell}, \tag{74}$$

and, since ℓ is an integer, we have

$$e^{-i2\pi\ell} = 1, \tag{75}$$

then,

$$S_x^{\alpha}(f+1) = \sum_{\ell=-\infty}^{\infty} R_x^{\alpha}[\ell] e^{-i2\pi f\ell}$$

$$= S_x^{\alpha}(f). \tag{76}$$

Furthermore, $S_x^{\alpha}(f)$ also exhibits the following periodicity:

$$S_x^{\alpha+1}(f+1/2) = S_x^{\alpha}(f). \tag{77}$$

This is easily shown by

$$S_x^{\alpha+1}\left(f+\frac{1}{2}\right)=\sum_{\ell=-\infty}^{\infty}R_x^{\alpha+1}[\ell]e^{-i2\pi\left(f+\frac{1}{2}\right)\ell}$$

$$=\sum_{\ell=-\infty}^{\infty}\left\langle x[n]x^*[n-\ell]e^{-i2\pi(\alpha+1)n}\right\rangle e^{i\pi(\alpha+1)\ell}\ e^{-i2\pi f\ell}\ e^{-i\pi\ell}$$

$$=\sum_{\ell=-\infty}^{\infty}\left\langle x[n]x^*[n-\ell]e^{-i2\pi\alpha n}\ e^{-i2\pi n}\right\rangle e^{i\pi\alpha\ell}\ e^{i\pi\ell}\ e^{-i2\pi f\ell}\ e^{-i\pi\ell}$$

$$=\sum_{\ell=-\infty}^{\infty}\left\langle x[n]x^*[n-\ell]e^{-i2\pi\alpha n}\ e^{-i2\pi n}\right\rangle e^{i\pi\alpha\ell}\ e^{-i2\pi f\ell}\ , \tag{78}$$

and, since n is an integer, we have

$$e^{-i2\pi n}=1, \tag{79}$$

hence,

$$S_x^{\alpha+1}\left(f+\frac{1}{2}\right)=\sum_{\ell=-\infty}^{\infty}\left\langle x[n]x^*[n-\ell]e^{-i2\pi\alpha n}\right\rangle e^{i\pi\alpha\ell}\ e^{-i2\pi f\ell}$$

$$=\sum_{\ell=-\infty}^{\infty}R_x^{\alpha}[\ell]e^{-i2\pi f\ell}$$

$$=S_x^{\alpha}(f). \tag{80}$$

We also define a *spectral correlation coefficient*, $\rho_x^{\alpha}(f)$, given by

$$\rho_x^{\alpha}(f)=\frac{S_x^{\alpha}(f)}{\left[S_x\left(f+\frac{\alpha}{2}\right)S_x\left(f-\frac{\alpha}{2}\right)\right]^{\frac{1}{2}}}$$

$$= \frac{S_{uv}(f)}{\left[S_u(f)S_v(f)\right]^{\frac{1}{2}}}. \tag{81}$$

Since $\left|\rho_x^\alpha(f)\right|$ is bounded by $[0,1]$, it is a convenient measure of the degree of local spectral redundancy that results from spectral correlation.

Going back to the AM signal, by Fourier transforming the cyclic autocorrelation function, we get

$$S_x^\alpha(f) = \begin{cases} \frac{1}{4}e^{\pm i2\theta}S_a(f), & \alpha = \pm 2f_o \\ \frac{1}{4}S_a(f+f_o)+\frac{1}{4}S_a(f-f_o), & \alpha = 0 \\ 0, & otherwise \end{cases} \tag{82}$$

and so, the spectral correlation coefficient is given by:

$$S_x\left(f+\frac{\alpha}{2}\right) = S_x^\alpha(f), \text{ for } \alpha = 0, \text{ computed at } f+\frac{\alpha}{2}$$

$$= \frac{1}{4}S_a(f+f_o)+\frac{1}{4}S_a(f-f_o), \text{ computed at } f+\frac{\alpha}{2}$$

$$= \frac{1}{4}S_a\left(f+\frac{\alpha}{2}+f_o\right)+\frac{1}{4}S_a\left(f+\frac{\alpha}{2}-f_o\right). \tag{83}$$

Also,

$$S_x\left(f-\frac{\alpha}{2}\right) = \frac{1}{4}S_a\left(f-\frac{\alpha}{2}+f_o\right)+\frac{1}{4}S_a\left(f-\frac{\alpha}{2}-f_o\right). \tag{84}$$

So that, for $\alpha = 2f_o$,

$$S_x\left(f+\frac{\alpha}{2}\right)=S_x\left(f+f_o\right)=\frac{1}{4}S_a\left(f+2f_o\right)+\frac{1}{4}S_a\left(f\right), \tag{85}$$

and,

$$S_x\left(f-\frac{\alpha}{2}\right)=S_x\left(f-f_o\right)=\frac{1}{4}S_a\left(f\right)+\frac{1}{4}S_a\left(f-2f_o\right), \tag{86}$$

and for $\alpha=-2f_o$,

$$S_x\left(f+\frac{\alpha}{2}\right)=S_x\left(f-f_o\right)=\frac{1}{4}S_a\left(f\right)+\frac{1}{4}S_a\left(f-2f_o\right), \tag{87}$$

and,

$$S_x\left(f-\frac{\alpha}{2}\right)=S_x\left(f+f_o\right)=\frac{1}{4}S_a\left(f+2f_o\right)+\frac{1}{4}S_a\left(f\right), \tag{88}$$

and, for $\alpha=0$,

$$S_x\left(f+\frac{\alpha}{2}\right)=S_x\left(f\right)=\frac{1}{4}S_a\left(f+f_o\right)+\frac{1}{4}S_a\left(f-f_o\right), \tag{89}$$

and,

$$S_x\left(f-\frac{\alpha}{2}\right)=S_x\left(f\right)=\frac{1}{4}S_a\left(f+f_o\right)+\frac{1}{4}S_a\left(f-f_o\right), \tag{90}$$

then,

$$\rho_x^{\alpha}\left(f\right)=\begin{cases}\dfrac{S_a\left(f\right)e^{\pm i2\theta}}{\left\{\left[S_a\left(f+2f_o\right)+S_a\left(f\right)\right]\left[S_a\left(f\right)+S_a\left(f-2f_o\right)\right]\right\}^{\frac{1}{2}}}, & \alpha=\pm 2f_o \\ 1, & \alpha=0 \\ 0, & \textit{otherwise.}\end{cases} \tag{91}$$

Thus, the strength of correlation between the spectral components of $x[n]$ at frequencies $f+\alpha/2$ and $f-\alpha/2$ is unity (i. e., $\left|\rho_x^{\alpha}(f)\right|=1$, for $|f|<f_o$ and $\alpha=\pm 2f_o$), provided that $a[n]$ is bandlimited to $|f|\le f_o$. Hence $S_a(f)=0$ for $|f|\ge f_o$.

APPENDIX B. FUNCTION AUTOFAM

```
function [Sx,alphao,fo]=autofam(x,fs,df,dalpha)
%       AUTOFAM(X,FS,DF,DALPHA) computes the spectral auto-correlation
%       density function estimate of the signal X, by using the FFT
%       Accumulation Method(FAM). Make sure that DF is much bigger
%       than DALPHA in order to have a reliable estimate.
%
%       INPUTS:
%       X      - input column vector;
%       FS     - sampling rate;
%       DF     - desired frequency resolution; and
%       DALPHA - desired cyclic frequency resolution.
%
%       OUTPUTS:
%       SX     - spectral correlation density function estimate;
%       ALPHAO - cyclic frequency; and
%       FO     - spectrum frequency.
%
%       Author: E.L.Da Costa,9/28/95.

if nargin ~= 4
   error('Wrong number of arguments.');
end

%%%%%%%%%%%%%%%%%%%%%%%%%%%%
% Definition of Parameters %
%%%%%%%%%%%%%%%%%%%%%%%%%%%%
Np=pow2(nextpow2(fs/df));      % Number of input channels, defined
                               % by the desired frequency
                               % resolution(df) as follows:
                               % Np=fs/df, where fs is the original
                               % data sampling rate. It must be a
                               % power of 2 to avoid truncation or
```

```
                                % zero-padding in the FFT routines;
L=Np/4;                         % Offset between points in the same
                                % column at consecutive rows in the
                                % same channelization matrix. It
                                % should be chosen to be less than
                                % or equal to Np/4;
P=pow2(nextpow2(fs/dalpha/L)); % Number of rows formed in the
                                % channelization matrix, defined
                                % by the desired cyclic frequency
                                % resolution(dalpha) as follows:
                                % P=fs/dalpha/L.It must be a power
                                % of 2;
N=P*L;                          % Total number of points in the
                                % input data.

%%%%%%%%%%%%%%%%%%%%%%%%
% Input Channelization %
%%%%%%%%%%%%%%%%%%%%%%%%
if length(x)<N
   x(N)=0;
elseif length(x)>N
   x=x(1:N);
end
NN=(P-1)*L+Np;
xx=x;
xx(NN)=0;
xx=xx(:);
X=zeros(Np,P);
for k=0:P-1
    X(:,k+1)=xx(k*L+1:k*L+Np);
end

%%%%%%%%%%%%%
% Windowing %
%%%%%%%%%%%%%
```

```
a=hamming(Np);
XW=diag(a)*X;
XW=X;


%%%%%%%%%%%%%
% First FFT %
%%%%%%%%%%%%%
XF1=fft(XW);
XF1=fftshift(XF1);
XF1=[XF1(:,P/2+1:P) XF1(:,1:P/2)];

%%%%%%%%%%%%%%%%%%
% Downconversion %
%%%%%%%%%%%%%%%%%%
E=zeros(Np,P);
for k=-Np/2:Np/2-1
    for m=0:P-1
        E(k+Np/2+1,m+1)=exp(-i*2*pi*k*m*L/Np);
    end
end
XD=XF1.*E;
XD=conj(XD');

%%%%%%%%%%%%%%%%%%
% Multiplication %
%%%%%%%%%%%%%%%%%%
XM=zeros(P,Np^2);
for k=1:Np
    for l=1:Np
        XM(:,(k-1)*Np+l)=(XD(:,k).*conj(XD(:,l)));
    end
end

%%%%%%%%%%%%%
```

```
% Second FFT %
%%%%%%%%%%%%%
XF2=fft(XM);
XF2=fftshift(XF2);
XF2=[XF2(:,Np^2/2+1:Np^2) XF2(:,1:Np^2/2)];
XF2=XF2(P/4:3*P/4,:);
M=abs(XF2);
alphao=-1:1/N:1;
fo=-.5:1/Np:.5;
Sx=zeros(Np+1,2*N+1);
for k1=1:P/2+1
    for k2=1:Np^2
        if rem(k2,Np)==0
           l=Np/2-1;
        else
           l=rem(k2,Np)-Np/2-1;
        end
        k=ceil(k2/Np)-Np/2-1;
        p=k1-P/4-1;
        alpha=(k-l)/Np+(p-1)/L/P;
        f=(k+l)/2/Np;
        if alpha<-1 | alpha>1
           k2=k2+1;
        elseif f<-.5 | f>.5
           k2=k2+1;
        else
           kk=1+Np*(f+.5);
           ll=1+N*(alpha+1);
           Sx(kk,ll)=M(k1,k2);
        end
    end
end
```

APPENDIX C. FUNCTION AUTOSSCA

```
function [Sx,alphao,fo]=autossca(x,fs,df,dalpha)
%       AUTOSSCA(X,FS,DF,DALPHA) computes the spectral auto-
%       correlation density function estimate of the signal X,
%       by using the Strip Spectral Correlation Algorithm (SSCA).
%       Make sure that DF is much bigger than DALPHA in order to
%       have a reliable estimate.
%
%       INPUTS:
%       X       - input column vector;
%       FS      - sampling rate;
%       DF      - desired frequency resolution; and
%       DALPHA - desired cyclic frequency resolution.
%
%       OUTPUTS:
%       SX      - spectral auto-correlation density function estimate;
%       ALPHAO - cyclic frequency; and
%       FO      - spectrum frequency.
%
%       Author: E.L.Da Costa,9/28/95.

if nargin ~= 4
   error('Wrong number of arguments');
end

%%%%%%%%%%%%%%%%%%%%%%%%%%%%
% Definition of Parameters %
%%%%%%%%%%%%%%%%%%%%%%%%%%%%
Np=pow2(nextpow2(fs/df));          % Number of input channels, defined
                                   % by the desired frequency
                                   % resolution(df) as follows:
                                   % Np=fs/df, where fs is the original
                                   % data sampling rate. It must be a
```

```
                                % power of 2 to avoid truncation or
                                % zero-padding in the FFT routines;
L=Np/4;                         % Offset between points in the same
                                % column at consecutive rows in the
                                % same channelization matrix. It
                                % should be chosen to be less than
                                % or equal to Np/4;
P=pow2(nextpow2(fs/dalpha/L));  % Number of rows formed in the
                                % channelization matrix, defined by
                                % the desired cyclic frequency
                                % resolution(dalpha) as follows:
                                % P=fs/dalpha/L. It must be a power
                                % of 2;
N=P*L;                          % Total number of points in the
                                % input data.

%%%%%%%%%%%%%%%%%%%%%%%%
% Input Channelization %
%%%%%%%%%%%%%%%%%%%%%%%%
if length(x)<N
   x(N)=0;
   disp('you will not get the desired resolution in cyclic frequency');
   dalpha=fs/N;
   disp(['cyclic frequency resolution=',num2str(dalpha)]);
elseif length(x)>N
   x=x(1:N);
end
NN=(P-1)*L+Np;
xx=x;
xx(NN)=0;
xx=xx(:);
X=zeros(Np,P);
for k=0:P-1
    X(:,k+1)=xx(k*L+1:k*L+Np);
end
```

```
%%%%%%%%%%%%%
% Windowing %
%%%%%%%%%%%%%
a=hamming(Np);
XW=diag(a)*X;

%%%%%%%%%%%%%
% First FFT %
%%%%%%%%%%%%%
XF1=fft(XW);
XF1=fftshift(XF1);
XF1=[XF1(:,P/2+1:P) XF1(:,1:P/2)];

%%%%%%%%%%%%%%%%%%
% Downconversion %
%%%%%%%%%%%%%%%%%%
E=zeros(Np,P);
for k=-Np/2:Np/2-1
    for m=0:P-1
        E(k+Np/2+1,m+1)=exp(-i*2*pi*k*m*L/Np);
    end
end
XD=XF1.*E;

%%%%%%%%%%%%%%%
% Replication %
%%%%%%%%%%%%%%%
XR=zeros(Np,P*L);
for k=1:P
    XR(:,(k-1)*L+1:k*L)=XD(:,k)*ones(1,L);
end

%%%%%%%%%%%%%%%%%%
% Multiplication %
```

```
%%%%%%%%%%%%%%%%%%
xc=ones(Np,1)*x';
XM=XR.*xc;
XM=conj(XM');


%%%%%%%%%%%%%%
% Second FFT %
%%%%%%%%%%%%%%
XF2=fft(XM);
XF2=fftshift(XF2);
XF2=[XF2(:,Np/2+1:Np) XF2(:,1:Np/2)];
M=abs(XF2);
alphao=(-1:1/N:1)*fs;
fo=(-.5:1/Np:.5)*fs;
Sx=zeros(Np+1,2*N+1);
for k1=1:N
    for k2=1:Np
        alpha=(k1-1)/N+(k2-1)/Np-1;
        f=((k2-1)/Np-(k1-1)/N)/2;
        k=1+Np*(f+.5);
        l=1+N*(alpha+1);
        Sx(k,l)=M(k1,k2);
    end
end
```

APPENDIX D. FUNCTION CROSSFAM

```
function [Sxy,alphao,fo]=crossfam(x,y,fs,df,dalpha)
%       CROSSFAM(X,Y,FS,DF,DALPHA) computes the spectral cross-
%       correlation density function estimate of the signals X
%       and Y, by using the FFT Accumulation Method(FAM). Make
%       sure that DF is much bigger than DALPHA in order to have
%       a reliable estimate.
%
%       INPUTS:
%       X      - input column vector;
%       Y      - input column vector;
%       FS     - sampling rate;
%       DF     - desired frequency resolution; and
%       DALPHA - desired cyclic frequency resolution.
%
%       OUTPUTS:
%       SXY    - spectral cross-correlation density function estimate;
%       ALPHAO - cyclic frequency; and
%       FO     - spectrum frequency.
%
%       Author: E.L.Da Costa,9/28/95.

If nargin ~= 5
   error('Wrong number of arguments.');
end

%%%%%%%%%%%%%%%%%%%%%%%%%%%%
% Definition of Parameters %
%%%%%%%%%%%%%%%%%%%%%%%%%%%%
Np=pow2(nextpow2(fs/df));          % Number of input channels, defined
                                   % by the desired frequency
                                   % resolution(df) as follows:
                                   % Np=fs/df, where fs is the original
```

```
                                % data sampling rate. It must be a
                                % power of 2 to avoid truncation or
                                % zero-padding in the FFT routines;
L=Np/4;                         % Offset between points in the same
                                % column at consecutive rows in the
                                % same channelization matrix. It
                                % should be chosen to be less than
                                % or equal to Np/4;
P=pow2(nextpow2(fs/dalpha/L));  % Number of rows formed in the
                                % channelization matrix, defined by
                                % the desired cyclic frequency
                                % resolution(dalpha) as follows:
                                % P=fs/dalpha/L. It must be a power
                                % of 2;
N=P*L;                          % Total number of points in the
                                % input data.

%%%%%%%%%%%%%%%%%%%%%%%%
% Input Channelization %
%%%%%%%%%%%%%%%%%%%%%%%%
if length(x)<N
   x(N)=0;
elseif length(x)>N
   x=x(1:N);
end
if length(y)<N
   y(N)=0;
elseif length(y)>N
   y=y(1:N);
end
NN=(P-1)*L+Np;
xx=x;
yy=y;
xx(NN)=0;
yy(NN)=0;
```

```
xx=xx(:);
yy=yy(:);
X=zeros(Np,P);
Y=zeros(Np,P);
for k=0:P-1
    X(:,k+1)=xx(k*L+1:k*L+Np);
    Y(:,k+1)=yy(k*L+1:k*L+Np);
end

%%%%%%%%%%%%%
% Windowing %
%%%%%%%%%%%%%
a=hamming(Np);
XW=diag(a)*X;
YW=diag(a)*Y;

%%%%%%%%%%%%%
% First FFT %
%%%%%%%%%%%%%
XF1=fft(XW);
YF1=fft(YW);
XF1=fftshift(XF1);
YF1=fftshift(YF1);
XF1=[XF1(:,P/2+1:P) XF1(:,1:P/2)];
YF1=[YF1(:,P/2+1:P) YF1(:,1:P/2)];

%%%%%%%%%%%%%%%%%
% Downconversion %
%%%%%%%%%%%%%%%%%
E=zeros(Np,P);
for k=-Np/2+1:Np/2
    for m=0:P-1
        E(k+Np/2,m+1)=exp(-i*2*pi*k*m*L/Np);
    end
end
```

```
XD=XF1.*E;
YD=YF1.*E;
XD=conj(XD');
YD=conj(YD');


%%%%%%%%%%%%%%%%%%
% Multiplication %
%%%%%%%%%%%%%%%%%%
XYM=zeros(P,Np^2);
for k=1:Np
    for l=1:Np
        XYM(:,(k-1)*Np+l)=XD(:,k).*conj(YD(:,l));
    end
end

%%%%%%%%%%%%%%
% Second FFT %
%%%%%%%%%%%%%%
XYF2=fft(XYM);
XYF2=fftshift(XYF2);
XYF2=[XYF2(:,Np^2/2+1:Np^2) XYF2(:,1:Np^2/2)];
XYF2=XYF2(P/4:3*P/4,:);
M=abs(XYF2);
alphao=(-1:1/N:1)*fs;
fo=(-.5:1/Np:.5)*fs;
Sxy=zeros(Np+1,2*N+1);
for k1=1:P/2+1
    for k2=1:Np^2
        if rem(k2,Np)==0
           l=Np/2;
        else
           l=rem(k2,Np)-Np/2;
        end
        k=ceil(k2/Np)-Np/2;
```

```
            p=k1-P/4-1;
            alpha=(k-1)/Np+(p-1)/L/P;
            f=(k+1)/2/Np;
            if alpha<-1 | alpha>1
               k2=k2+1;
            elseif f<-.5 | f>.5
               k2=k2+1;
            else
               kk=1+Np*(f+.5);
               ll=1+N*(alpha+1);
               Sxy(kk,ll)=M(k1,k2);
            end
        end
    end
```

APPENDIX E. FUNCTION CROSSSSCA

```
function [Sxy,alphao,fo]=crossssca(x,y,fs,df,dalpha)
%       CROSSSSCA(X,Y,FS,DF,DALPHA) computes the spectral cross-
%       correlation density function estimate of the signals X
%       and Y, by using the Strip Spectral Correlation Algorithm
%       (SSCA). Make sure that DF is much bigger than DALPHA in order
%       to have a reliable estimate.
%
%       INPUTS:
%       X       - input column vector;
%       Y       - input column vector;
%       FS      - sampling rate;
%       DF      - desired frequency resolution; and
%       DALPHA - desired cyclic frequency resolution.
%
%       OUTPUTS:
%       SXY     - spectral cross-correlation density function estimate;
%       ALPHAO - cyclic frequency; and
%       FO      - spectrum frequency.
%
%       Author: E.L.Da Costa,9/28/95.

If nargin ~= 5
   error('Wrong number of arguments.');
end

%%%%%%%%%%%%%%%%%%%%%%%%%%%%
% Definition of Parameters %
%%%%%%%%%%%%%%%%%%%%%%%%%%%%
Np=pow2(nextpow2(fs/df));          % Number of input channels, defined
                                   % by the desired frequency
                                   % resolution(df) as follows:
                                   % Np=fs/df, where fs is the original
```

```
                                % data sampling rate. It must be a
                                % power of 2 to avoid truncation or
                                % zero-padding in the FFT routines;
L=Np/4;                         % Offset between points in the same
                                % column at consecutive rows in the
                                % same channelization matrix. It
                                % should be chosen to be less than
                                % or equal to Np/4;
P=pow2(nextpow2(fs/dalpha/L));  % Number of rows formed in the
                                % channelization matrix, defined by
                                % the desired cyclic frequency
                                % resolution(dalpha) as follows:
                                % P=fs/dalpha/L. It must be a power
                                % of 2;
N=P*L;                          % Total number of points in the
                                % input data.

%%%%%%%%%%%%%%%%%%%%%%%%
% Input Channelization %
%%%%%%%%%%%%%%%%%%%%%%%%
if length(x)<N
   x(N)=0;
elseif length(x)>N
   x=x(1:N);
end
if length(y)<N
   y(N)=0;
elseif length(y)>N
   y=y(1:N);
end
NN=(P-1)*L+Np;
xx=x;
xx(NN)=0;
xx=xx(:);
X=zeros(Np,P);
```

```
for k=0:P-1
    X(:,k+1)=xx(k*L+1:k*L+Np);
end


%%%%%%%%%%%%
% Windowing %
%%%%%%%%%%%%
a=hamming(Np);
XW=diag(a)*X;

%%%%%%%%%%%%
% First FFT %
%%%%%%%%%%%%
XF1=fft(XW);
XF1=fftshift(XF1);
XF1=[XF1(:,P/2+1:P) XF1(:,1:P/2)];

%%%%%%%%%%%%%%%%%
% Downconversion %
%%%%%%%%%%%%%%%%%
E=zeros(Np,P);
for k=-Np/2+1:Np/2
    for m=0:P-1
        E(k+Np/2,m+1)=exp(-i*2*pi*k*m*L/Np);
    end
end
XD=XF1.*E;
XD=conj(XD');

%%%%%%%%%%%%%%%
% Replication %
%%%%%%%%%%%%%%%
XR=zeros(Np,P*L);
for k=1:P
```

```
    XR(:,(k-1)*L+1:k*L)=XD(:,k)*ones(1,L);
end

%%%%%%%%%%%%%%%%%%
% Multiplication %
%%%%%%%%%%%%%%%%%%
yc=ones(Np,1)*y';
XYM=XR.*yc;
XYM=conj(XYM');

%%%%%%%%%%%%%%
% Second FFT %
%%%%%%%%%%%%%%
%%%%%%%%%%%%%%
% Second FFT %
%%%%%%%%%%%%%%
XYF2=fft(XYM);
XYF2=fftshift(XYF2);
XYF2=[XYF2(:,Np^2/2+1:Np^2) XYF2(:,1:Np^2/2)];
M=abs(XYF2);
alphao=(-1:1/N:1)*fs;
fo=(-.5:1/Np:.5)*fs;
Sxy=zeros(Np+1,2*N+1);
for k1=1:N
    for k2=1:Np
        alpha=(k1-1)/N+(k2-1)/Np-1;
        f=((k2-1)/Np-(k1-1)/N)/2;
        k=1+Np*(f+.5);
        l=1+N*(alpha+1);
        Sxy(k,l)=M(k1,k2);
    end
end
```

APPENDIX F. PLOTTING ROUTINES

```
%%%%%%%%%%%%%%
%Surface Plot%
%%%%%%%%%%%%%%
figure(1)
surfl(alphao,fo,Sx);
view(-37.5,60);
title('SCD estimate using FAM');
xlabel('alpha');
ylabel('f');
zlabel('Sx');

%%%%%%%%%%%%%%
%Contour Plot%
%%%%%%%%%%%%%%
figure(2)
contour(alphao,fo,Sx);
xlabel('alpha(Hz)');
ylabel('f(Hz)');

%%%%%%%%%%%%%%%%%%%%
%Cross-Section Plots%
%%%%%%%%%%%%%%%%%%%%
figure(3)
plot(fo,Sx(:,1+N*(alpha/fs+1)));   % alpha is the desired cyclic
                                   % frequency.
xlabel('f(Hz)');
ylabel('Sx(alpha)');
```

LIST OF REFERENCES

1. Gardner, W. A., *An Introduction to Cyclostationary Signals*, Chapter 1, Cyclostationarity in Communications and Signal Processing, IEEE Press, Piscataway, NJ, 1993.

2. Roberts, R. S., Brown, W. A., and Loomis, H. H., *Computationally Efficient Algorithms for Cyclic Spectral Analysis*, IEEE Signal Processing Magazine, April 1991.

3. The MathWorks, Inc., *MATLAB User's Guide*, August, 1992.

4. Carter, N. J., "Implementation of Cyclic Spectral Analysis Methods", Master's Thesis, Naval Postgraduate School, December, 1992.

5. Ross, D., *Mechanics of Underwater Noise*, Peninsula Publishing, Los Altos, CA, 1987.

6. Urick, R. J., *Ambient Noise in the Sea,* Peninsula Publishing, Los Altos, CA, 1986.

7. Kinsler, L. E., Frey, A. R., Coppens, A. B., and Sanders, J. V., *Fundamentals of Acoustics*, John Wiley & Sons, Inc., New York, NY, 1982.

8. Urick, R. J., *Principles of Underwater Sound*, McGraw-Hill, Inc., New York, NY, third edition.

9. Gardner, W. A., *Statistical Spectral Analysis*, Prentice Hall, Englewood Cliffs, NJ, 1988.

INITIAL DISTRIBUTION LIST

1. Defense Technical Information Center 2
   8725 John J. Kingman Rd., STE 0944
   Ft. Belvoir, VA 22060-6218

2. Library, Code 13 2
   Naval Postgraduate School
   Monterey, CA 93943-5101

3. Chairman, Code EC 1
   Department of Electrical and Computer Engineering
   Naval Postgraduate School
   Monterey, CA 93943-5121

4. Chairman, Code PH/Ay 1
   Engineering Acoustics Academic Committee
   Naval Postgraduate School
   Monterey, CA 93943-5117

5. Prof. H. H. Loomis, Jr., Code EC/Lm 1
   Department of Electrical and Computer Engineering
   Naval Postgraduate School
   Monterey, CA 93943-5121

6. Prof. Ralph Hippenstiel, Code EC/Hi 3
   Department of Electrical and Computer Engineering
   Naval Postgraduate School
   Monterey, CA 93943-5121

7. Prof. Roberto Cristi, Code EC/Cx 1
   Department of Electrical and Computer Engineering
   Naval Postgraduate School
   Monterey, CA 93943-5121

8. CC(EN) Evandro Luiz da Costa 2
   Instituto de Pesquisas da Marinha
   Rua Ipiru No. 2 - Jardim Guanabara - Ilha do Governador
   Rio de Janeiro, RJ - CEP. 21931-090
   BRAZIL